

University of Denver

Digital Commons @ DU

Electronic Theses and Dissertations

Graduate Studies

1-1-2016

A Reserve-Based Method for Mitigating the Impact of Renewable Energy

Ibrahim Krad
University of Denver

Follow this and additional works at: <https://digitalcommons.du.edu/etd>



Part of the [Electrical and Computer Engineering Commons](#)

Recommended Citation

Krad, Ibrahim, "A Reserve-Based Method for Mitigating the Impact of Renewable Energy" (2016).
Electronic Theses and Dissertations. 1118.
<https://digitalcommons.du.edu/etd/1118>

This Dissertation is brought to you for free and open access by the Graduate Studies at Digital Commons @ DU. It has been accepted for inclusion in Electronic Theses and Dissertations by an authorized administrator of Digital Commons @ DU. For more information, please contact jennifer.cox@du.edu, dig-commons@du.edu.

A Reserve-based Method for Mitigating the Impact of Renewable Energy

A Dissertation

Presented to

the Faculty of the Daniel Felix Ritchie School of Engineering and Computer Science

University of Denver

In Partial Fulfillment

of the Requirements for the Degree

Doctor of Philosophy

By

Ibrahim Krad

June 2016

Advisor: Dr. Wenzhong David Gao

Author: Ibrahim Krad
Title: A Reserve-based Method for Mitigating the Impact of Renewable Energy
Advisor: Dr. Wenzhong David Gao
Degree Date: June 2016

Abstract

The fundamental operating paradigm of today's power systems is undergoing a significant shift. This is partially motivated by the increased desire for incorporating variable renewable energy resources into generation portfolios. While these generating technologies offer clean energy at zero marginal cost, i.e. no fuel costs, they also offer unique operating challenges for system operators. Perhaps the biggest operating challenge these resources introduce is accommodating their intermittent fuel source availability. For this reason, these generators increase the system-wide variability and uncertainty. As a result, system operators are revisiting traditional operating strategies to more efficiently incorporate these generation resources to maximize the benefit they provide while minimizing the challenges they introduce.

One way system operators have accounted for system variability and uncertainty is through the use of operating reserves. Operating reserves can be simplified as excess capacity kept online during real time operations to help accommodate unforeseen fluctuations in demand. With new generation resources, a new class of operating reserves has emerged that is generally known as flexibility, or ramping, reserves. This new reserve class is meant to better position systems to mitigate severe ramping in the net load

profile. The best way to define this new requirement is still under investigation. Typical requirement definitions focus on the additional uncertainty introduced by variable generation and there is room for improvement regarding explicit consideration for the variability they introduce. An exogenous reserve modification method is introduced in this report that can improve system reliability with minimal impacts on total system wide production costs.

Another potential solution to this problem is to formulate the problem as a stochastic programming problem. The unit commitment and economic dispatch problems are typically formulated as deterministic problems due to fast solution times and the solutions being sufficient for operations. Improvements in technical computing hardware have reignited interest in stochastic modeling. The variability of wind and solar naturally lends itself to stochastic modeling. The use of explicit reserve requirements in stochastic models is an area of interest for power system researchers. This report introduces a new reserve modification implementation based on previous results to be used in a stochastic modeling framework.

With technological improvements in distributed generation technologies, microgrids are currently being researched and implemented. Microgrids are small power systems that have the ability to serve their demand with their own generation resources and may have a connection to a larger power system. As battery technologies improve, they are becoming a more viable option in these distributed power systems and research is necessary to determine the most efficient way to utilize them. This report will investigate several unique operating strategies for batteries in small power systems and

analyze their benefits. These new operating strategies will help reduce operating costs and improve system reliability.

Acknowledgements

I would like to extend my gratitude and appreciation to my academic advisor, Dr. Wenzhong Gao, for all of his help and guidance throughout the entirety of my doctoral candidacy. His inputs and ideas have helped me in creating this dissertation and for that I am truly grateful. His kind words and support have helped me through this trying time in my academic career. Under his tutelage, I have expanded my technical expertise and grown both scholastically and professionally and I would like to offer sincere a thank you for all of his effort.

I would like to also extend my appreciation to several colleagues for their support and advice. I would like to thank Dr. Erik Ela with the Electric Power Research Institute and Dr. Eduardo Ibanez with General Electric for all of their effort. Through their guidance, I have been able to produce research that is both of high academic standard and valuable to industry partners and researchers.

I would like to thank my classmates for their input and good wishes. I am truly grateful for all of their support.

I would like to thank my family and specifically my parents. Their love and support have helped motivate me and keep me on track to complete my studies. I am grateful to my brothers for their support as well. Finally, I would like to thank my wife for all of her patience, love, and support. I could not have finished this dissertation without her.

Table of Contents

Abstract	ii
Acknowledgements.....	v
List of Figures	vii
List of Tables	viii
List of Acronyms	ix
Chapter 1: Introduction.....	1
1.1 Motivation.....	1
1.2 Problem Statement	3
1.3 Theoretical background	5
1.4 My contributions to this research.....	22
Chapter 2: Description of simulation platform	25
Chapter 3: Improving Flexibility Reserves for System Operations	30
3.1 Advanced flexibility reserve techniques	30
3.2 Analysis of advanced flexibility reserve techniques	39
3.3 Three-Stage Reliability-Based Reserve Modifiers for Enhanced Operation	48
Chapter 4: Using Stochastic Modeling to Address System Uncertainty.....	58
4.1 Motivation.....	58
4.2 Stochastic Formulation	59
4.3 Analyzing the use of reserves in stochastic modeling	62
4.4 Three-Stage Stochastic Modifiers.....	73
Chapter 5: Future Roles of Emerging Technologies in Grid Operations.....	83
5.1 Utilizing PHEVs for Reserve Scheduling	83
5.2 Optimizing BESS for Ancillary Services in Microgrids.....	91
Chapter 6: Conclusion.....	103
6.1 Final Remarks	103
6.2 List of Publications	108
References.....	110
Appendix A: Additional Model Details	119
Appendix B: Extensive form of Stochastic RTSCED	133

List of Figures

Figure 1 – Sample flexible ramping demand curve	11
Figure 2 – Simulation platform flow chart.....	28
Figure 3 – Modified simulation workflow with 3-Stage modifiers	34
Figure 4 – Example FRDC curves	36
Figure 5 – FRDC maximum requirements for the month of October.....	38
Figure 6 – Unused thermal capacity in the month of April across all cases	41
Figure 7 – Number of thermal generators committed in April	42
Figure 8 – LMP duration curve for October across all cases.....	42
Figure 9 – Mean-absolute difference between day-ahead and real-time LMPs across all cases ...	44
Figure 10 – Accumulated ACE broken down by direction across all cases	45
Figure 11 – Distributions of raw ACE across all cases.....	46
Figure 12 – Distribution of ACE across all cases with the modifiers (right) and without (left)....	55
Figure 13 – Stochastic simulation workflow	63
Figure 14 – Scenarios set type 1 (top) and type 2 (bottom).....	64
Figure 15 – Number of thermal start-ups in January	66
Figure 16 - Distribution of ACE across all cases in April	67
Figure 17 - Comparison of net-load ramp tracking in Case 1 and Case 2	69
Figure 18 – Number of committed thermal units in each simulated month.....	72
Figure 19 – Direction of accumulated ACE for cases 7 and 8 in October.....	73
Figure 20 – Stochastic simulation workflow with modification stage.....	76
Figure 21 – Computation time (in minutes) across all cases	78
Figure 22 – Distribution of ACE in April.....	79
Figure 23 – Average unused thermal ramping capacity	80
Figure 24 – Number of committed thermal generators in January	81
Figure 25 – System LMPs with and without PHEVs providing energy and ancillary services.....	89
Figure 26 – Relationship between the number of PHEVs and depth of discharge	90
Figure 27 – Modified IEEE single-area reliability test system for microgrid applications	95
Figure 28 – Distribution of ACE in October for all microgrid operating scenarios	97
Figure 29 – SOC of the battery providing energy and regulation and regulation only.....	98
Figure 30 – Amount of load lost to multiple contingencies with and without the BESS	101

List of Tables

Table 1 – State RPS requirements as of September 2014.....	2
Table 2 – Summary of different forms of operating reserves	4
Table 3 - Modified IEEE 118 Bus Test System Characteristics	32
Table 4 – Breakpoints on the FRDC implementation.....	36
Table 5 – Summary of different flexibility reserve scenarios.....	39
Table 6 – Flexibility reserves simulation results	40
Table 7 – VG curtailment per case per month in GWh	43
Table 8 – Percentage of intervals with transmission congestion	47
Table 9 – Change in reliability and economic metrics due to three-stage reserve modification ...	52
Table 10 – Mean absolute difference between DA and RT LMPs in \$/MWh.....	54
Table 11 – Summary of reserve methods for each case.....	64
Table 12 – Summary of stochastic reserve results	65
Table 13 – Summary of sensitivity scenario reserve requirements.....	70
Table 14 – Summary of stochastic sensitivity scenario results.....	71
Table 15 – Three stage stochastic modifier simulation results	77
Table 16 – Summary of curtailed wind with stochastic modifiers.....	81
Table 17 – PHEV operational data used in simulations.....	86
Table 18 – Nine bus system line data	86
Table 19 – Nine bus system generator data	87
Table 20 – System production costs for three different reserve scenarios that both include and exclude PHEVs	88
Table 21 – Generator commitment schedules impact by PHEV scheduling	89
Table 22 – Numerical results from BESS analysis	96
Table 23 – Numerical results from contingency scenarios	100

List of Acronyms

AACEE: Absolute ACE in Energy
ACE: Area Control Error
AGC: Automatic Generation Control
APEC: Applied Power Electronics Conference
ARMA: Auto Regressive Moving Average
BA: Balancing Area
BESS: Battery Energy Storage System
CAISO: California Independent System Operator
CPS2: Control Performance Standard 2
DASCUC: Day-Ahead Security Constrained Unit Commitment
DOD: Depth Of Discharge
EENS: Expected Energy Not Served
EPEC: Electrical Power and Energy Conference
ERCOT: Electric Reliability Council of Texas
ESS: Energy Storage System
EV: Electric Vehicle
FRDC: Flexible Ramping Demand Curve
GAMS: General Algebraic Modeling System
HOMER: Hybrid Optimization of Multiple Energy Resources
IEEE: Institute of Electrical and Electronics Engineers
ITA: Information Theory and Applications
LMP: Locational Marginal Price
LOLP: Loss of Load Probability
LP: Linear Programming
MAACE: Mean Absolute ACE
MILP: Mixed-Integer Linear Program
MISO: MidContinent Independent System Operator
MPP: Maximum Power Point
MW: Megawatt
MWh: Megawatt hour
NERC: North America Electric Reliability Corporation
NREL: National Renewable Energy Laboratory
NSRS: Non-Spinning Reserve Service
PHEV: Plugin Hybrid Electric Car
PV: Photovoltaic
RPS: Renewable Portfolio Standard
RTSCUC: Real-Time Security Constrained Unit Commitment
RTSCED: Real-Time Security Constrained Economic Dispatch
SOC: State of Charge
TEPPC: Transmission Expansion Planning Policy Committee
VG: Variable Generation
WECC: Western Electricity Coordinating Council

Chapter 1: Introduction

1.1 Motivation

Since the creation of the electric power system, system operators have been tasked with the responsibility of ensuring that when a customer turns a light switch, the lights turn on. As the power system continuously evolves, this task is becoming more challenging. As utility footprints expand and total customer demand increases, power system operators must plan and operate the system in a preemptive manner to help avoid contingency-induced events, like blackouts. This task is further compounded by the composite nature of the emerging power system. With increasing societal pressure to curb the use of non-environmentally friendly fuels and to reduce our collective dependency on fossil fuels, utilities are trying to accommodate more and more renewable energy resources, such as generation from wind and solar power, in their generation portfolios. These renewable energy resources help reduce air, land, and water pollution caused by thermal generators. They help reduce sulfur dioxides, nitrogen oxides, and other disease causing bacteria found in generating plants [1]. States are individually responsible for utilizing renewable energy resources. In this regard, many states are

adopting renewable portfolio standards (RPS). An RPS is a policy that mandates a certain amount of demand served for customers must come from renewable energy resources.

Table 1 summarizes some RPS goals for several states [2].

State	RPS Goal Penetration	RPS Goal Date
Hawaii	40 %	2030
California	33 %	2020
Colorado	30 %	2020
New York	29 %	2015
Connecticut	27 %	2020
Minnesota	26.5 %	2025
Nevada	25 %	2025
Oregon	25 %	2025
Illinois	25 %	2026
West Virginia ¹	25 %	2025
Vermont ¹	20 %	2017

Table 1 – State RPS requirements as of September 2014

For example, California is planning and operating their electric system with the goal of providing 33 % of the electrical demand by renewable energy resources by 2020. Renewable energy resources present unique challenges for power system operators that are significantly different from traditional operating procedures. The most noteworthy of these challenges is their inherent intermittent nature. Traditionally, in a utility with an all fossil-fuel fired generation fleet, the operator has 100% control over generation variables (namely commitment and dispatch). However, renewable energy resources reverse this paradigm. They are available when nature says they are available and the system operator must plan accordingly. Predicting how much renewable energy will be available may or may not be a trivial task. Sources such as hydro and biogas can be fairly well predicted

¹ West Virginia and Vermont have renewable portfolio goals. This is similar to a renewable portfolio standard with the exception that it is not legally binding.

and operated. Solar generation, while the daily pattern can be fairly well forecasted, the actual power output of solar plants may be difficult to forecast due to the complicated nature of their dependencies (atmospheric conditions, cloud cover, etc.). Wind power is perhaps the most complicated to predict since wind power does not adhere to any binding patterns. It is not uncommon for wind power to be above/below forecasted values. These forecast errors effect how efficiently the wind power, and all renewable resources in general, are used.

The continual advancement of technologies has also led to small, independent power systems within larger power systems. These smaller systems go by many names, namely “micro-grids” and sometimes “smart grids.” These systems allow for more customer participation, more adoption of emerging technologies such as energy storage systems, new operating principles and strategies, higher power quality, and reliable power delivery [3]. Since these systems operate in both a grid connected mode (connected to the larger power system) and islanded mode (disconnected from the larger power system), careful consideration must be made regarding operating strategies and control techniques to ensure safe operation. One of the main operating challenges of these smaller systems is ensuring that there is always enough energy available to supply the entire load as well as any ancillary service requirements.

1.2 Problem Statement

The proliferation of wind and solar generation will change the way system operators have traditionally handled variability and uncertainty in power system operations. Historically, operating reserves are withheld in real-time via an arbitrary

requirement calculated offline before power system operations begin. Table xxx summarizes different forms of operating reserve products.

Type	Event Driven?	Online/ Offline	Deployment	Purpose
Regulation Reserves	No	Online	Automatic Generation Control	Used to correct the current unanticipated imbalance
Load Following Reserves	No	Online	Part of economic dispatch	Used to dispatch anticipated changes in the load
Spinning Contingency Reserves	Yes	Online	Operator driven in response to event	Used to restore system operations after an event from online generators
Non-spinning Contingency Reserves	Yes	Offline	Operator driven in response to event	Used to restore system operations after an event from offline generators
Flexibility Reserves	Yes	Online	Part of economic dispatch in response to events	Used to dispatch generation in response to uncertainty in the net-load profile

Table 2 – Summary of different forms of operating reserves

The unpredictability of wind and solar generation make this approach inefficient. Research must be done to find ways to optimize the operating reserve requirements. This paper will explore using an updated methodology to update the deterministic operating reserve requirements, explore the potential use of advanced modeling techniques in unison with operating reserve requirements to optimize system operations, and explore using advanced emerging technologies to provide ancillary services.

1.3 Theoretical background

It is natural for ideas and technologies to evolve over the course of time, and the electric power system is no different. In order to ensure reliable operation, system operators hold contingency reserves that could account for an outage of the largest power system component. Over time, as the size of the electric power system increased and electrification became more commonplace, additional ancillary services were developed in order to operate the power system more efficiently and reliably. The next step in the evolution of the power system is the incorporation of renewable energy resources in generation portfolios, namely wind and solar photovoltaic (PV). These variable generators (VG) provide particular operating challenges due to their intermittent nature. In order to accommodate these future changes, a number of new operating strategies are being researched. Among these strategies are flexibility reserves, stochastic programming, and the use of energy storage systems and other emerging technologies.

System operators require operating reserves in order to ensure reliable operation of the system. One class of these operating reserves is defined as contingency reserves,

also known as spinning and non-spinning reserves. These are used to return the system to normal operating conditions after an event, e.g. a generator outage. Primary contingency reserves are used to stabilize the system operating frequency. Secondary contingency reserves are used to return the frequency back to nominal. Tertiary contingency reserves are used to replace primary and secondary contingency reserves. This is done so primary and secondary reserves can go offline and prepare in case another event happens. Ramping reserves are similar to contingency reserves except they respond to slower events that occur in the system over several minutes up to an hour. Regulation reserves are used to maintain the balance of real time electricity generation and consumption that occurs at temporal resolutions that are typically finer than the temporal resolution of the economic dispatch solution. Generators that provide this type of ancillary serve typically must be equipped with communications that allow it to receive control signals from a centralized dispatch location. This type of control scheme is known as automatic generation control (AGC). Load following reserves are used to help track the changes in the electrical load in order to help maintain the real time balance of electrical generation and consumption in future time intervals. This type of reserve typically does not require AGC equipment since it is typically utilized at the same temporal resolution as the economic dispatch solution [4].

Variable generation will increase both the variability and uncertainty present in the system. Variability can be defined as the expected magnitude oscillations, in both the positive and negative direction, in power system variables. Uncertainty can be defined as the unexpected changes in power system variables in both the positive and negative

directions as well. Variability and uncertainty occur naturally in the power system, e.g. load forecast errors and power system component outages. Another type of power system event garnering more attention recently is the response of the system to unforeseen VG ramping events. This has led to the potential development of a new reserve product generally known as flexibility reserves. This type of reserve product aims to mitigate the additional uncertainty and variability introduced by increased levels of VG penetration [5]. This type of reserve product can be further generalized into variability based reserve products, load based reserve products, and net load based reserve products, and.

The variability based reserve methodologies are dependent on the intra-hour and inter-hour variability present in power system profiles such as load, wind speed, and solar irradiation. The authors of [6] present a flexibility reserve method that utilizes this type of calculation. The reserve requirement is dependent on the variability of wind and solar forecast errors. These forecast errors are then sorted according to the power associated with them. Then the flexibility requirement is calculated based on a 70% confidence interval, i.e. the reserve requirement must cover 70% of the forecast errors. This method is applied for wind profiles, and load profiles if the data is available. For solar forecasts, the solar generation output is forecasted by using a persistent cloud cover forecast [7]. This type of forecast can be modeled as follows:

$$P_F(t + \Delta t) = P(t) + SPI(t)[P_{CS}(t + \Delta t) - P_{CS}(t)]. \quad (1)$$

In (1), P_F is the forecasted power, P is the actual power at time t , SPI is the solar power index at time t , and P_{CS} is the clear-sky power at time t . The SPI can be calculated

in real-time based on historic clearsky data. The solar power index is the ratio of the actual power output of the solar generator to the clearsky output of the generator, or

$$SPI(t) = \min\left(\frac{P_{actual}}{P_{clearsky}}, 1\right) \quad (2)$$

Once the forecasts are calculated, a similar process as described above can be used to calculate the solar forecast errors and then subsequently to calculate the flexibility reserve requirement for solar power. The solar forecast errors can be calculated as follows:

$$P_{\varepsilon} = \Delta P(t) - P(t) - SPI(t) \cdot \Delta P_{CS}(t) \quad (3)$$

In (3), P_{ε} is the forecast error, P is the actual generation, and ΔP and ΔP_{CS} represent the change in actual power and clear-sky power, respectively, between the current time interval and the following time interval. A benefit of this methodology is it can be customized to particular systems by modifying the confidence intervals used in the calculations in order to find the reserve requirement that best fits certain applications.

There are a number of different variability based solutions being proposed in literature. The authors of [8] present a methodology where the reserve requirement is based on the variability of the load and wind profiles. The total amount of the reserve requirement is then calculated in such a way so as to maintain an acceptable level of operating risk. The goal is to maintain a constant risk of load shedding at every hourly time interval throughout the year. Simulations show that as the amount of wind generation present in the system increases, the amount of reserves needed to reliably operate the system (i.e. maintain a constant risk level of load shedding instances

throughout the year) will also moderately increase. The authors of [9] propose a reserve management tool (RMT) that defines the hourly operating reserve requirements based on different risk metrics including the loss of load probability (LOLP) and the expected energy not served (EENS). These metrics are calculated based on extracting the variability embedded in the load and wind forecast errors.

The authors of [10] propose a load based method that determines the optimal operating reserve requirement by simple market clearing mechanisms. A reserve capacity supply curve is plotted against a curve of system losses due to a service interruption. The intersection of these curves then sets the optimal reserve requirement. There are also load based methods that are typically used in large, interconnection-scale grid integration studies. These methods are often based on reliability standards put forth by the Western Electricity Coordinating Council (WECC). The requirement typically consists of a heuristically selected percentage of the changes in the load profile or with respect to the magnitude of the load profile. For example, operating reserve requirements can be approximated as 1% of the system peak load [11]. The WECC Transmission Expansion Planning Policy Committee (TEPPC) also suggest using 5% of the demand served by hydro and 7% of the demand served by thermal generators as the operating reserves requirement [12].

The authors of [13] propose a net load based method that determines the optimal spinning reserve requirement via stochastically optimizing the requirement. By minimizing the total cost of providing the reserve product (i.e. the cost of providing the reserve and the cost of the outages the reserve will be unable to prevent), the probability

distribution of the net load is divided into several intervals where the midpoint of each interval is the optimal reserve requirement for that interval. The overall requirement is then taken as the weighted sum of the requirement in each interval multiplied by the probability that the net load will occur in that interval. Monte Carlo simulations are then used to converge to a final solution. The Electric Reliability Council of Texas (ERCOT) has proposed a net load based ancillary service known as Non-Spinning Reserve Service (NSRS) that aims to protect the system against the variability and uncertainty in the net load profile [14]. ERCOT compares the actual historical net load forecast errors and schedules enough reserve such that the reserve scheduled, the responsive reserve service scheduled (500 MW as defined by ERCOT), and the average regulation reserve scheduled in the upward direction (Reg_{up}) will be greater than 95% of the uncertainties in the historical net load ($0.95\epsilon_{NL}$). This is shown in (4).

$$NSRS(t) + 500 + Reg_{up}(t) \geq 0.95\epsilon_{NL} \quad (4)$$

The California Independent System Operator (CAISO) has also presented a flexible ramping ancillary service that depends on the variations in the system net load [15]. The final requirement is calculated such that it covers 95% of the change in net load between model intervals (95% confidence interval between the 2.5% percentile and the 97.5% percentile). The requirement is also constrained to be in the same direction as the movement in net load, i.e. any negative requirement that is calculated as a result of the previous analysis is set to zero. The maximum and minimum values are connected via a series of gradually decreasing prices and quantity levels to construct a flexible ramping demand curve. The maximum values are set by the limits of the confidence intervals.

This demand curve is extended into advisory intervals although only the first interval is financially binding. A sample flexible ramping demand curve (FRDC) similar to the one used later in this report is shown in Figure 1.

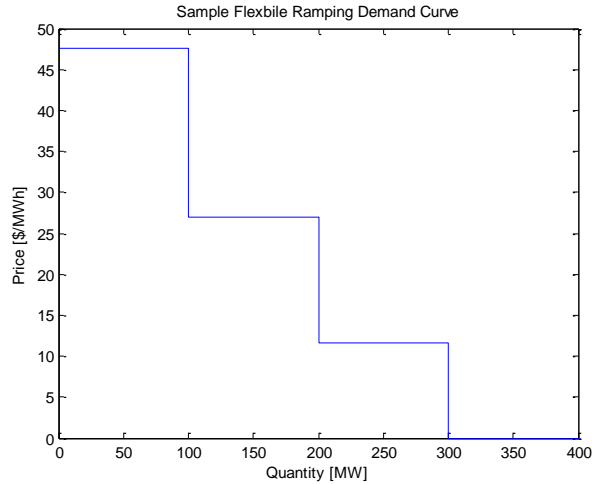


Figure 1 – Sample flexible ramping demand curve

The Midcontinent Independent System Operator (MISO) has proposed an ancillary service product designed to ensure that enough ramping flexibility is available in future time intervals. This method is calculated based on the changes in the net load profile (electrical demand – VG) and the observed historical uncertainty in the net load. The upward and downward requirements are calculated to ensure that the requirement covers the maximum change in net load plus the observed historical uncertainty occurring at the same temporal resolution as the reserve product. The scheduling of these reserves is done carefully to ensure that in the case of a net load event, this ramping capacity is deliverable by the generators scheduled to provide it [16]. The CAISO and MISO are also considering modifying their market clearing algorithms to incorporate additional constraints to facilitate the scheduling and deployment of these flexibility reserve products [17][18]. This modification should help reduce price spikes and help to better

position the system for the additional uncertainty and variability introduced by increased VG penetration levels.

Due to the inherent uncertainty surrounding variable generation, these types of problems naturally lend themselves to stochastic formulations. Stochastic modeling attempts to capture the variability and uncertainty found in power system variables by simulating many possible scenarios. The authors [19] of present a stochastic formulation for long term security constrained unit commitment problems. Essentially, the traditional objective function must be modified to link the multiple scenarios together. This can be accomplished with the following additional term:

$$\sum_s \sum_t \sum_i \mu_{i,t}^s (I_{i,t}^s - c_{i,t}) \quad (5)$$

In (5), μ is the Lagrangian multiplier penalty factor, I is the unit status variable (or the first stage decision variable), and c is the weighted average of the decision variables across scenarios and it is assumed to be the optimal solution. This solution is calculated as:

$$c_{i,t} = \sum_s \frac{P_s \cdot I_{i,t}^s}{P_s} \quad (6)$$

In (6), I is the first stage decision variable and P is the weighted average of scenario s . By iteratively solving the optimization and updating the implementable as shown in (6), eventually, the first stage decision variable will converge across all scenarios. However, since the unit commitment problem is not convex, the problem may not absolutely converge. As a result, a stopping criterion can be defined to signal the most feasible optimal solution has been found. The large stochastic problem is

decomposed into smaller, deterministic sub-problems via Lagrangian Relaxation. This is a scenario based model that embeds the uncertainty of state variables within different scenario outcomes. These scenarios are generated via Monte Carlo simulations. This technique can be used to capture the uncertainty in generator outages as well as load and renewable energy generation forecast errors.

The authors of [20] present a two stage stochastic unit commitment model that also includes integer variables in the second stage. Typically two-stage formulations solve linear programs in the second stage. The inclusion of integer variables in the second stage (e.g. quick start generation statuses) results in a problem that is not convex and requires more sophisticated solution techniques to solve. A modified Benders' Decomposition technique that employs L-shaped cuts is utilized to solve the problem where iterations control the upper and lower bounds of the solution space until the bounds converge. The authors [21] propose a two-stage stochastic unit commitment methodology that includes both demand response resources as well as energy storage systems. The second stage optimization includes reliability constraints in the form of transmission and risk constraints in order to control the loss of load probability. The risk constraints are functions of the conditional value-at-risk in order to maintain the linearity of the optimization problem. The complete problem is then solved via a modified Benders' Decomposition technique. Experiments show that more conservative reliability requirements typically results with higher production costs.

The authors of [22] present a stochastic formulation that incorporates uncertain demand side behavior. The reliability of the system is ensured by maintaining the loss of

load probability above a predetermined risk value. The model is solved using a sample average approximation method. Preliminary results show that employing a stochastic model for demand side participation can result with an increased amount of available generation capacity when compared to a deterministic representation. The authors of [23] developed a unified, two-stage stochastic and robust optimization model for solving the unit commitment problem. This problem is formulated as a dual objective problem where one half of the objective minimizes the total production cost and the second half of the objective function minimizes the cost of the worst case scenario. These dual objectives are mutually weighted such that the sum of both weights equals one. In this way, the system operator can control the main objective and can thus control the solution time. This allows for a balance between the solution time and solution robustness depending on the problem being solved. This model is solved using Benders' Decomposition by producing both feasibility and optimality cuts for both the stochastic and robust objectives separately. A comprehensive review of stochastic modeling applications for unit commitment can be found in [24].

In order to solve stochastic models, there are generally two approaches. The first approach models all scenarios at the same time and produces a final solution after one iteration. This approach is useful for academic demonstrations on small problems but becomes technically infeasible for larger systems. The second approach decomposes the stochastic problem in many deterministic sub-problems. This technique is easily scalable to large problems while maintaining feasible solution times. This method requires an iterative solution process to solve the sub-problems and check for optimality. One

method to accomplish this is through the use of progressive hedging. Using this method, a variable defined as the implementable is calculated as the average solution across all scenarios. Then, this average solution is included into the objective function of the sub-problems along with a penalty factor. This is to penalize the solutions that deviate from the optimal average solution. Once the deviation is below a predefined threshold, ε , the solution is considered to have converged and the optimal solution has been found [25][26]. The steps for this algorithm are given below.

1. Solve all deterministic sub-problems, one per scenario
2. Calculate the average solution across all scenarios, \bar{x}
3. Update penalty factor, ρ
4. Modify the objective function of sub-problems to include the following term:

$$\rho \cdot (x - \bar{x}) \tag{7}$$

5. Recalculate the average solution across all scenarios
6. Check for solution convergence using the following criteria:

$$\sum_s prob(s) \cdot \|x - \bar{x}\| < \varepsilon \tag{8}$$

- a. If solution has converged, a solution has been found, exit the algorithm
- b. If solution has not converged, go back to step 3

There has been some research regarding the use of stochastic modeling and the determination of operating reserves. The authors of [27] compare the differences in generation dispatch decisions between using a flexible ramping product explicitly modeled in a deterministic market clearing algorithm versus a stochastic market clearing algorithm without this product. They have found that the dispatch decisions between deterministic and stochastic models can be quite similar if the flexible ramping product is appropriately modeled for the system. The deterministic model may not always produce the least cost solution if more expensive generators with desirable flexibility are included in the generation fleet. This is because the deterministic model will try to schedule the flexible capacity from the expensive generators without necessarily considering the fact this excess capacity may physically be delivered in the future. This problem can be mitigated to an extent by using penalty factors in the market clearing algorithm's objective function but will still yield a solution that is less efficient, in terms of production costs, than the stochastic solution.

The authors of [28] explore the differences between scheduling reserves in a deterministic and stochastic market clearing model. This model solves the daily commitment and dispatch problems at hourly temporal resolutions with extended look-ahead horizons. They examined the differences in explicitly modeling a reserve requirement versus not including an explicit requirement. Simulations showed that not including the reserve requirements reduces production costs. They also conclude that the benefit of including an explicit reserve requirement is more pronounced for deterministic models rather than stochastic models. This is due to the inherent nature of stochastic

models to consider the variability and uncertainty in power system variables. They also found that the value of different reserve requirements (in terms of security and production costs) may not be consistent across methods, i.e. a reserve requirement that improves the reliability in one case may not have the same behavior in another case. The authors of [29] explore the modeling of reserves in systems with large amounts of wind penetration. The variability and uncertainty of the wind power is captured through a stochastic day-ahead unit commitment problem and by Monte Carlo simulations for the economic dispatch problem. Their analysis is performed on eight representative days throughout the year and do not consider transmission constraints. The stochastic reserves implementation reduced the total production costs compared to the deterministic reserve implementations.

The inclusion of renewable energy resources as well as other emerging technologies, such as battery energy storage systems (BESS), will change the way power systems are operated and controlled. One significant change that has recently gained significant research interest is the development of microgrids. These are small, self-sufficient power systems that are capable of supplying the entire load within their geographical footprint without assistance from the main power system. These types of systems typically utilize renewable energy resources to provide cheap, clean energy as well as some form of dispatchable energy. They are capable of operating with a live connection to the main power system, i.e. grid-connected mode, as well as completely isolated from the main power system, i.e. islanded mode. Due to the small nature of these power systems, it is critical to optimize the dispatch of the generation fleet to minimize

the operating costs and ensure that the system is operated reliably, namely there is sufficient capacity to supply the entire load. The authors of [30] present a distributed form of economic dispatch suitable for small, distributed power systems that can be solved iteratively to produce a least cost dispatch solution with minimum knowledge of the system. Each generator in this algorithm measures the system imbalance at its point of connection via measuring the frequency offset from nominal. Using this information, generators iteratively adjust their outputs to eliminate the frequency offset while maintaining the minimum dispatch cost, the cost of dispatching the generators to meet the total demand. One drawback for this algorithm is the number of iterations required to achieve the optimal dispatch may be considered technically infeasible based on the application. The authors of [31] present a day-ahead unit commitment formulation for a microgrid in both grid connected and islanding modes of operation. This formulation takes into account the ability of the grid to provide energy and reserves as well the uncertainty in power system variables such as load, wind, and solar generation. Results show that load shedding may be necessary to provide sufficient reserve capacity, especially for critical loads, during islanded operation. The amount of committed, dispatchable capacity will also increase as the uncertainty in the power system variables increase. This is due to the fact that larger generators need to be committed in order to cover a larger uncertainty space.

The authors of [32] present an economic dispatch formulation for determining the optimum generator dispatch set-points for a microgrid in both grid-connected and islanded modes. The economic dispatch problem considers the modification of the line

flow capacities in order to obtain a solution that takes into account the additional line flows due to connecting the microgrid with the main power grid and with modifying the operational reserve requirements. This modification of line flow limits is necessary during islanding operation in order to further improve the stability of the islanded microgrid. This formulation also takes into account the power sharing control techniques popular in the design of today's microgrids, namely fixed-droop power sharing and adjustable-droop power sharing. In the first technique, the power balance is distributed based on generator nameplate capacities. In the second technique, the power balance is distributed based on the generator reserve schedules, a quantity that changes throughout the operation process. The economic dispatch problem is solved using a direct search method because it is simple to implement, has a robust formulation, and there is research being conducted in enhancing the algorithm's performance. The authors of [33] proposed a microgrid scheduling algorithm that optimizes the energy and reserve schedules of all generators in the microgrid to minimize both the total production cost and the generated emissions. This model solves the daily operating plan for the microgrid operator at an hourly temporal resolution. While the model of the microgrid's operation is simple, it does include a formulation to allow demand response as a resource to participate in both energy and reserve scheduling. The dual objective optimization problem is formulated as an augmented ϵ -constraint problem. Essentially, the emissions reduction problem is broken into several smaller optimization problems covering different portions of the potential solution space. Once the sub-problems are solved, a single pareto-optimal solution can be defined via Fuzzy sets. Results from this analysis show that these

objectives are conversely related, i.e. improving one objective will deteriorate the other. For example, reducing the total emissions in the microgrid may result in increasing costs.

The authors of [34] propose a dual layer microgrid control scheme that considers the integrity of system voltages throughout the microgrid. The schedule layer provides the layout of connected generators, similar to the unit commitment problem. The dispatch layer provides the real time control of the generators within the microgrid, similar to the economic dispatch problem. One of the main benefits of this type of control scheme is that proper communication between layers can help mitigate real time control issues that arise due to imperfect forecasts of power system variables. The formulation utilizes power reserves to help compensate for forecast errors. The utilization of this control scheme along with energy storage systems and demand response allows the microgrid to operate economically in grid-connected mode and reliably in islanded mode. The authors of [35] present a hierarchical control scheme for a microgrid with the objectives of reducing the microgrid operating cost and improving the microgrid reliability. This control scheme utilizes a stochastic security constrained unit commitment and dispatch model formulated as a mixed-integer program (MIP). The control will determine the optimal control of microgrid energy components including distributed generators, renewable generators including wind and solar, an energy storage system, and the loads participating in demand response. One of the main design features of the microgrid is the redundant nature of the network that is designed to minimize the amount of unserved loads when there are power system component outages and the controlling of these lines via advanced switchgear. The controller operates the microgrid components at an hourly

resolution for the entire year. Results show that the use of this type of control scheme can reduce costs in terms of minimizing the amount of penalty incurred due to not serving load, energy arbitrage with the main grid, and optimally dispatching generating units. The reliability of the microgrid also improves in terms of the frequency of service interruptions and the duration of these interruptions.

The authors of [36] present an analysis performed in order to determine the optimal design configuration of a microgrid with the goals of providing energy and reducing carbon emissions. The analysis was performed using the Hybrid Optimization of Multiple Energy Resources (HOMER) developed by the National Renewable Energy Laboratory (NREL). A microgrid with a live connection to a larger power system provides the cheapest solution due to the lowest required capital costs. However, in a system that cannot rely only on a larger power system, a hybrid diesel-renewable energy microgrid provides the best tradeoff between reducing the net present cost, the levelized cost of energy, and carbon emissions. The analysis showed that the inclusion of the diesel-fired distributed generators is necessary to minimize the amount of unserved energy. There has also been some research in determining not only the most optimal mix of generation resources, but also in how to get the most benefit from those resources. The authors of [37] explore a solar panel control scheme that will allow the solar panel to provide frequency regulation on a microgrid. This control scheme tracks a portion of the maximum power point (MPP) of the solar panel, leaving a certain amount uncommitted. This uncommitted capacity can then be used as frequency regulation reserve. As frequency begins to decrease and the solar panel is engaged for frequency regulation, the

MPP tracker will move closer to the actual MPP of the solar panel, increasing the amount of energy provided to the microgrid, thereby helping to correct the frequency deviations. This type of control is similar to the control described in [38] for wind plants in that in order for the solar to provide regulation, it must withhold some of its potential energy capacity. The authors of [38] examine the potential usage of wind plants in providing ancillary services, namely regulation, in market environments. The analysis shows that wind turbines possess the necessary hardware to provide regulation. As long as the market properly incentivizes the wind turbine to provide regulation, i.e. the price of providing regulation exceeds the price of providing energy, the wind turbine can feasibly provide regulation. However, there are potential technical drawbacks since wind generators provide up regulation by operating below their actual capacities and provide down regulation by curtailing their output.

1.4 My contributions to this research

The future of power systems will undoubtedly include more renewable energy generation resources as well as other emerging technologies such as energy storage systems. In this environment, it will be important to ensure that the power system, regardless of its size, continues to operate in an efficient and reliable manner. Successful adoption of these technologies will depend on maximizing the benefits they can provide while mitigating the challenges they introduce in daily operation.

Operating reserves are one tool system operators use to efficiently operate the power system. Future power systems with high penetrations of wind and solar generation

will necessitate changes to the ways operators have historically defined operating reserves. This report will demonstrate an updated modification algorithm to better position the power system to absorb high renewable energy penetration scenarios. This is accomplished by explicitly taking into account the variability of wind and solar generators in the reserve requirement calculation algorithm. This is achieved by examining the actual imbalance occurring in the system due to the variability of wind and solar generation.

Stochastic models still have some major barriers preventing them from becoming major players in industry. Perhaps the biggest barrier is the long computation times needed to arrive at an optimal solution. This is directly related to the number of scenarios and the structure of the scenarios being considered. This report will demonstrate the benefit of augmenting the stochastic model with explicit operating reserve requirements for optimal performance. In addition to this analysis, a three stage stochastic modification procedure will be presented that controls the structure of the stochastic model in real-time based on the realized variability and uncertainty in the system to optimize performance while maintaining solution integrity.

Smaller power systems will arguably face more significant challenges due to their physical limitations. Larger power systems have implicit operating advantages such as thousands of synchronous generators all rotating at the same speed. Small disturbances have negligible impact because they cannot affect the entire system. Microgrids do not have this characteristic and special care must be given to the control techniques used to operate them. This report will demonstrate new control techniques of emerging

technologies, such as electric cars and energy storage systems, to better operate microgrids. These technologies can be used to participate in reserve scheduling for microgrids that can improve system operation in terms of costs and sometimes reliability. By controlling the ways these technologies participate in this reserve scheduling, the microgrid can also handle additional variable generation penetrations, as will be demonstrated in this report.

Chapter 2: Description of simulation platform

In order to perform this analysis, a power system operations tool, known as the Flexible Energy Scheduling Tool for Integrating Variable generation (FESTIV), is used to simulate the scheduling and deployment of these operating reserves. This tool is developed by the National Renewable Energy Laboratory (NREL). This operation tool simulates all temporal resolutions of the scheduling process starting from day-ahead unit commitment all the way through automatic generation control (AGC). The first stage is the security-constrained day-ahead unit-commitment (DASCUC). During this stage, long start generation commitment decisions are made. This optimization is performed once before the operating day with hourly interval resolution. The second stage is the security-constrained real-time unit-commitment (RTSCUC). During this stage, the commitment decisions for all generation resources are decided. This optimization is performed three hours in advance (sometimes referred to as the hour-ahead commitment step) with a 15 minute interval resolution. The third stage is the security-constrained real-time economic dispatch (RTSCED). During this stage, the energy and ancillary service schedules for all generation resources is allocated. This optimization solves every five minutes while looking ahead for the next hour. The final stage is the AGC algorithm where generator

resource setpoints are adjusted to perform the real-time balance of generation and demand. This stage occurs every four seconds. Figure 2 shows the simulation flow chart. The unit commitment problems are formulated as mixed-integer linear programming (MILP) optimization problems. The economic dispatch problem is formulated as a linear programming (LP) optimization problem. All optimizations are formulated in the General Algebraic Modeling System (GAMS) and are solved using CPLEX [39]. The objective of all models is to minimize the production cost shown in (9).

$$\min \sum_i \sum_t C_G(P_{it}) + C_{SU}(P_{it}) + C_{NL}(P_{it}) + \gamma\sigma_t + \delta\rho_t \quad (9)$$

In (5), C_G is the marginal cost of generation, C_{SU} is the startup cost, C_{NL} is the no load cost, σ_t is the amount load lost at time t , ρ_t is the amount of insufficient reserves scheduled, γ and δ are penalty factors.

The AGC is a rule based algorithm that allocates regulation requirements based on regulation schedules. In order to perform the regulation, the area control error (ACE) is calculated as shown in equation 5.

$$ACE(t) = \sum_i P_i(t) - \sum_j D_j(t) \quad \forall i \in \{G\}, \forall j \in \{L\} \quad (10)$$

In (10), G is the set of all generation resources, L is set of electrical demands, P_i is the generation level of generator i and D_j is the electrical demand of resource j . The ACE is taken directly as the mismatch between generation and consumption. This formulation assumes perfect interchange knowledge between operating areas. The AGC algorithm then assigns regulation duties to all resources proportionally according to their regulation schedules to correct this ACE. The AGC module is typically executed every 4 seconds,

similar to the standard in the United States of performing AGC every 4-6 seconds. Figure 2 shows the solution flow chart of this simulation platform.

Reliability, as referred to in the rest of this report, is defined as the measure of the ACE accrued in the system. Systems experiences high values of ACE are said to be experiencing low reliability and vice versa for systems with low values of ACE. These ACE metrics can be used to measure system reliability performance with respect to satisfying NERC control performance standards.

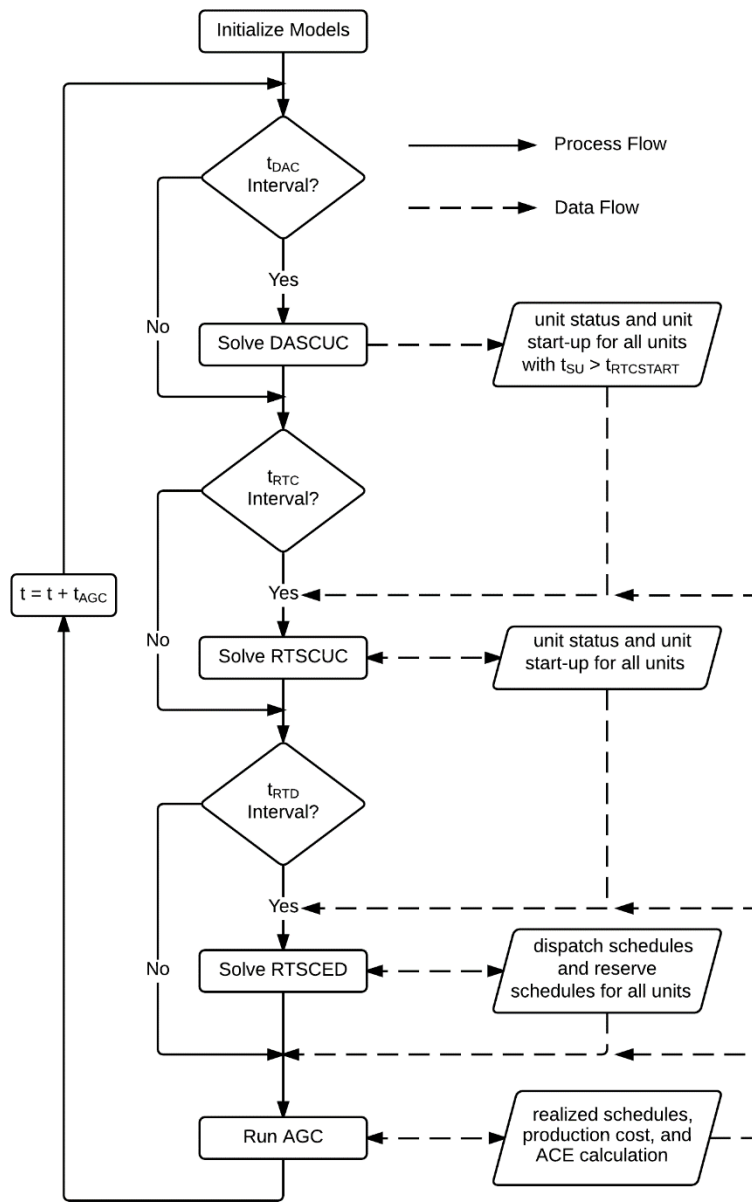


Figure 2 – Simulation platform flow chart

The previous models all leverage a DC optimal power flow formulation, common among similar models proposed in literature and industry. It should be noted that these models do not contain any information regarding the reactive components in the power systems, e.g. reactive power and voltages. As a result, in order to ensure a feasible

solution, some form of security-check should be performed after the optimal power flow is solved. This can be accomplished via a security constrained optimal power, or AC optimal power flow. Another method could be to solve an AC power flow iteratively with the DC optimal power flow until a feasible solution is found.

The previous models are by default linear programs (LP) and mixed-integer linear programs (MILP). While other solution methods have been proposed, such as evolutionary programming, particle swarm optimization, Lagrangian Relaxation, and dynamic programming, LP and MILP problems have become industry standards due to recent developments in computational science and their ability to find optimal solutions. CPLEX utilizes the dual problem formulated from the primal optimizations to gauge the maximum and minimum value of the objective function. When the gap between these separate bounds are within some predefined epsilon of each other, the simulation is completed and the optimal solution has been found.

Chapter 3: Improving Flexibility Reserves for System Operations

3.1 Advanced flexibility reserve techniques

Power system operators have historically withheld generator capacity to be deployed in response to system events. These operating reserves have been typically utilized to address unforeseen events, e.g. generator and transmission line outages, and small expected events, e.g. load following and regulation reserves. With the emergence of renewable energy generation that is dependent on intermittent fuel resources, i.e. wind speed and solar irradiance, a new class of operating reserves is being studied. These operating reserves are meant to help system operators ride through potentially severe ramping events from wind and solar generation as well as balance the sub-minute variability of these resources.

The first step in this analysis was to perform a direct comparison of the different flexibility reserve requirements proposed in literature discussed in section 1.2. The following equations are used to capture the scheduling of operating reserves. Equation (11) represents the reserve balance constraint. This constraint ensures that the amount of reserve scheduled is at least enough to fulfil the current requirement.

$$\sum_t \sum_i R_{i,t,\tau} \geq \Gamma_{t,\tau} \quad (11)$$

In (11), $R_{i,t,\tau}$ is the generator reserve schedule for generator i at time t for reserve type τ , and $\Gamma_{t,\tau}$ is the reserve requirement for reserve type τ at time t . Equations (12) and (13) are used to set the maximum and minimum capability of a generator to provide reserves, respectively.

$$P_{i,t} + R_{i,t,\tau} \leq P_{max,i} \cdot I_{i,t} \quad (12)$$

$$P_{i,t} - R_{i,t,\tau} \geq P_{min,i} \cdot I_{i,t} \quad (13)$$

In (12) and (13), $P_{i,t}$ is the generation scheduled for generator i at time t , $P_{max,i}$ is the maximum capacity of generator i , $P_{min,i}$ is the minimum capacity of generator i , and $I_{i,t}$ is the binary commitment variable of generator i at time t . Equation (12) is binding for all reserve types that are in the upward direction and require the generator to be online. Equation (13) is binding for all reserve types that are in the downward direction and require the generator to be online. The commitment variable is binary, in which a value of 1 indicates that the generator is online and a value of 0 indicates that the generator is offline. Equation (14) prohibits generators from providing reserves if the generator is currently within the start-up or shutdown trajectory.

$$R_{i,t,\tau} \leq P_{max,i} \cdot (1 - y_{i,t} - z_{i,t}) \quad (14)$$

In (14), $y_{i,t}$ is a binary variable indicating whether a generator is being turned on, and $z_{i,t}$ is a binary variable indicating whether a generator is being turned off. The start-up and shutdown indicators are mutually exclusive—i.e., a generator cannot be experiencing both a shutdown and a start-up during the same interval. The start-up and shut-down indicators are related by equations (15) and (16).

$$y_{i,t} - z_{i,t} = I_{i,t} - I_{i,t-1} \quad (15)$$

$$y_{i,t} + z_{i,t} \leq 1 \quad (16)$$

Equation (17) is used to determine the amount of available capacity a generator has that can participate in reserve scheduling.

$$R_{i,t,\tau} \leq I_{i,t} \cdot RR_i \cdot RT_\tau + (1 - I_{i,t}) \cdot QSC_i \quad (17)$$

In (17), $I_{i,t}$ is the binary commitment variable of generator i at time t , RR_i is the megawatt-per-minute ramp rate of generator i , RT_τ is the response time of reserve product τ , and QSC_i is the amount of megawatts generator i can quickly provide if it is turned on. The response time is time requirement of how quickly generators must provide the reserve. In this study, the quick-start capability of each generator is equal to its minimum generation capacity if it can reach that level within 30 minutes. Otherwise, the quick-start capacity is set to zero.

With the model prepared, a test system needed to be designed. A modified version of the IEEE 118 bus test system is used in this analysis. The generation data was updated according to [40] to better capture available operation cost data. Wind and solar generation was added to reflect high penetration scenarios. Table 3 summarizes the generation mixes of the new system.

System Characteristics	
Coal Capacity [TW]	2.3
Combined Cycle Capacity [TW]	2.76
Combustion Turbine Capacity [TW]	2.52
Peak Load [TW]	6.9
Average Annual Solar Energy Penetration [%]	17.45
Average Annual Wind Energy Penetration [%]	16.98

Table 3 - Modified IEEE 118 Bus Test System Characteristics

The penetration levels in Table 3 are with respect to actual load. The wind and solar data is taken from available data sets for northern California provided by the National Renewable Energy Laboratory [41]. Since the purpose of this report is not to optimize the locations of VG resources, the wind and solar plants were sited to maximize access to transmission capacity and thereby minimize potential curtailment. The system is then prepared to simulate an entire week's operation for four separate months, namely January, April, July, and October. This is done to capture the season trends in the load, wind, and solar profiles.

The simulation workflow is adjusted to perform the three stage modification process. The modification occurs before every optimization problem is solved. The modified simulation workflow is shown in Figure 3.

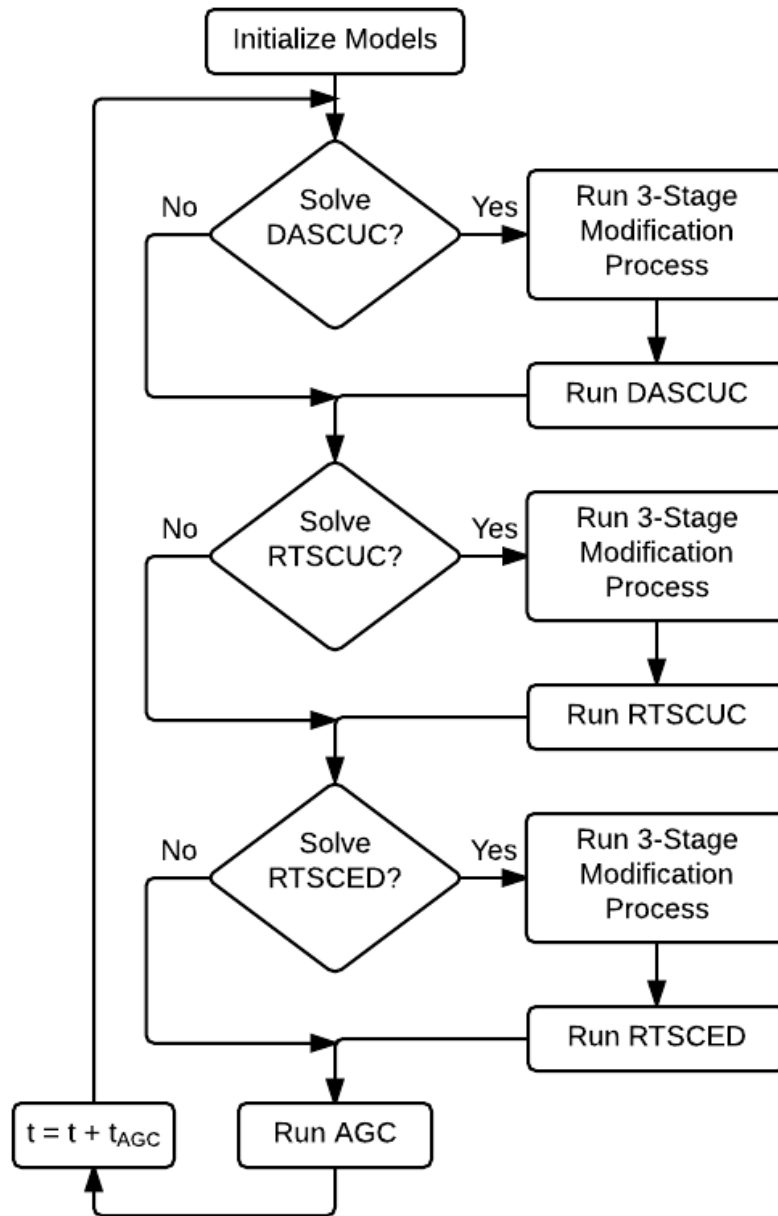


Figure 3 – Modified simulation workflow with 3-Stage modifiers

With the system prepared, the flexibility reserves need to be determined. In this report, several different reserve requirement methodologies are considered based on

techniques available in literature to get an idea of available flexibility reserve methodologies. These flexibility reserves are considered as excess capacity withheld during the scheduling process to account for unforeseen ramping events during real time operations. The first three reserve methods considered are based strictly on available load data. The method determines the flexibility reserve requirement as the megawatt (MW) requirement necessary to cover 70% of hour-ahead load forecast errors. In order to gain insight into the sensitivity of this number, a second reserve requirement is used that only covers 50% of the hour-ahead load forecast errors. In order to investigate the benefit of a dynamic requirement versus a static requirement, a third reserve requirement was implemented as the mean of the 70% requirement, constant for all time. These three methods can be generally categorized as load-based flexibility reserve requirements.

A fourth reserve requirement is calculated based on [7] as mentioned in section 1.2. For this method, the wind, solar, and load forecasts are treated independently. The contribution to the total requirement from each data set is the MW requirement needed to cover 70% of the hour-ahead forecast errors. Then the final requirement is taken as the geometric sum of each individual contribution. To gain insight into the sensitivity of this requirement, a fifth requirement is used that covers only 50% of the individual forecast errors. These two requirements can be generally classified as variability-based flexibility reserve requirements since each data set is treated separately and their individual contributions are calculated separately.

A sixth reserve requirement that is inspired by [14] and [18] is also considered. This requirement calculates the MW requirement needed to cover 95% of the day-ahead

net-load forecast errors. The net load is defined as the actual load profile minus the contributions by wind and solar generators. This method caps the maximum requirement as the size of the largest generation asset, in this case 700 MW. In order to gain some insight into this sensitivity of this method, a seventh reserve requirement that covers 90% of the day-ahead net-load forecast errors was also used. These two reserve methods can be generally classified as net-load based flexibility reserve requirements.

An eighth reserve requirement inspired by [15] is used to compare against a more sophisticated reserve requirement methodology. This method implements the flexibility reserve demand curve (FRDC). The shape of the demand curve is summarized in Table 4.

	DASCUC	RTSCUC	RTSCED
Step Width [MW]	250	50	50
Penalty Costs, Up Direction [\$/MW]	250, 24, 15, 8, 2.5		
Penalty Costs, Down Direction [\$/MW]	250, 3.6, 2.25, 1.2, 0.375		

Table 4 – Breakpoints on the FRDC implementation

Due to insufficient available data, historical data for a single year was used for northern California to determine the FRDC breakpoints. These breakpoints are functions of net-load forecast errors and will be detailed later. Another sample FRDC is shown in Figure 4 for convenience.

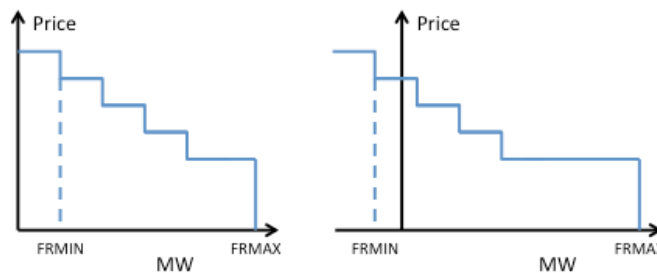


Figure 4 – Example FRDC curves

The left FRDC in Figure 4 shows a basic FRDC under normal operating conditions. The breakpoints on the FRDC are dynamically set for each optimization step. FRMIN and FRMAX are the minimum and maximum flexibility reserve requirements respectively. Each step in the FRDC has an associated penalty cost for insufficient reserve. The purpose of the FRDC is so that the system will schedule additional flexibility reserves when economically feasible to do so, namely when the marginal cost of providing the flexibility reserve is less than associated penalty cost. These requirements are set in both the upward and downward directions. If FRMIN is negative, the FRDC is shifted to the first nonnegative step (Figure 4, right). The calculation of the minimum and maximum breakpoints are outlined below for each model:

- **DASCUC**: Day-ahead flexibility requirements are calculated based on the hourly difference in net load. FRMIN is calculated based on the difference in day-ahead forecasts for each hour. FRMAX is calculated as the 97.5th and 2.5th percentiles for historic net load hourly ramps for each month and hour of the day for the upward and downward directions, respectively. It is a 60-minute product.
- **RTSCUC**: Intra-day unit commitment happens with a frequency of 15 minutes in the simulations. FRMIN is calculated as the difference between the forecast for each of the 5-minute RTSCED steps that correspond to each RTSCUC solution. FRMAX is calculated as the 95% confidence interval for historic FRMIN for each hour of the day within a month. Requirements are calculated for the binding and advisory intervals. It is a 5-min product.

- **RTSCED**: Real-time economic dispatch flexibility reserve requirements are based on the difference of each consecutive 5-minute forecasts for net load, both for the binding and advisory intervals. FRMIN values are calculated as the expected 5-minute ramps in the net load forecasts. Up and down FRMAX values are calculated to cover 95% of the historic net load differences. It is a 5-min product.

The maximum FRDC requirements for each of the three submodels for the month of October in both the upward and downward directions is shown in Figure 5.

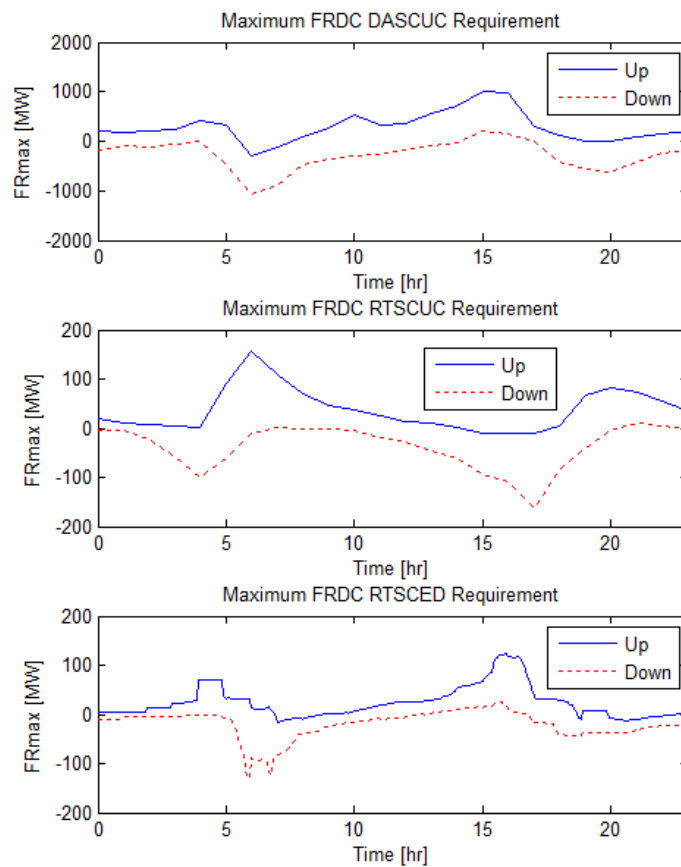


Figure 5 – FRDC maximum requirements for the month of October

A summary of all the different flexibility reserve techniques considered in this report is shown in Table 5. These requirements will be used to gain insight into the

operational implications of flexibility reserve to develop a more efficient means of setting the requirements.

Name	Flexibility Reserve Calculation
Base	No flexibility reserve
Case 0	Static , based on Case 1 average
Case 1	Based on 70% of load forecast error
Case 2	Based on 50% of load forecast error
Case 3	Based on 70% of VG and load forecast error
Case 4	Based on 50% of VG and load forecast error
Case 5	Based on 95% of net load forecast error
Case 6	Based on 90% of net load forecast error
Case 7	Based on dynamic FRDC net-load calculations

Table 5 – Summary of different flexibility reserve scenarios

3.2 Analysis of advanced flexibility reserve techniques

All the cases summarized in Table 5 were simulated and the results are shown in Table 6. The column labeled cost is the total system-wide production cost. The production cost per generator is defined as the product of the energy produced by that generator and the marginal cost of generation for that generator including start-up and no-load costs. The second column is the number of spikes in the real-time price of energy, or locational marginal price (LMP). This column indicates the number of real-time market infeasibilities. This metric is useful because one of the potential benefits of flexibility reserves mentioned throughout literature is the potential of flexibility reserves to reduce the number of real-time price spikes. The third column is the absolute ACE in energy (AACEE). This metric is the integral of the absolute value of ACE over the entire study period. This metric provides some insight into how well the system was balanced. The fourth column is the standard deviation of the ACE.

Case	Cost [\$M]	Δ Cost	Number Of Price Spikes	Δ Number of Price Spikes	AACEE [MWh]	Δ AACEE	σ_{ACE} [MW]	$\Delta \sigma_{ACE}$	
January	Base	12.44	–	226	–	2,201	–	25.3	–
	Case 0	12.49	0.3%	160	-29.2%	2,379	8.08%	28.6	13.0%
	Case 1	12.42	-0.2%	176	-22.1%	2,145	-2.52%	24.8	-2.0%
	Case 2	12.40	-0.3%	179	-20.8%	2,160	-1.85%	25.0	-1.1%
	Case 3	12.17	-2.2%	104	-54.0%	2,070	-5.92%	23.2	-8.0%
	Case 4	12.53	0.7%	118	-47.8%	2,023	-8.06%	23.4	-7.4%
	Case 5	13.09	5.2%	0	-100%	1,903	-13.52%	22.6	-10.8%
	Case 6	12.95	4.1%	0	-100%	1,883	-14.44%	21.6	-14.6%
	Case 7	12.11	-2.7%	6	-97.4%	2,231	1.36%	24.5	-3.2%
April	Base	7.83	–	219	–	3,044	–	39.4	–
	Case 0	7.85	0.2%	206	-5.9%	3,184	4.58%	44.5	13.0%
	Case 1	7.92	1.0%	199	-9.1%	2,993	-1.70%	40.4	2.5%
	Case 2	7.87	0.5%	192	-12.3%	2,815	-7.53%	37.6	-4.6%
	Case 3	8.018	2.4%	161	-26.5%	2,880	-5.39%	39.1	-0.8%
	Case 4	7.987	2.0%	166	-24.2%	3,026	-0.60%	40.7	3.1%
	Case 5	9.279	18.4%	0	-100%	3,341	9.73%	50.9	29.0%
	Case 6	8.982	14.7%	3	-98.6%	3,061	0.54%	44.8	13.7%
	Case 7	8.22	5.0%	25	-88.6%	2,917	4.17%	35.3	-10.4%
July	Base	17.74	–	459	–	5,522	–	94.4	–
	Case 0	17.92	1.1%	425	-7.4%	4,264	-22.78%	70.0	-25.8%
	Case 1	17.93	1.1%	425	-7.4%	4,959	-10.19%	87.0	-7.8%
	Case 2	17.90	0.91%	448	-2.4%	4,887	-11.50%	83.3	-11.7%
	Case 3	17.56	-0.98%	366	-20.3%	2,675	-51.55%	51.0	-45.9%
	Case 4	18.12	2.2%	412	-10.2%	3,960	-28.28%	66.1	-30.0%
	Case 5	18.27	3.0%	31	-93.3%	1,063	-80.74%	11.9	-87.4%
	Case 6	18.46	4.1%	53	-88.5%	1,060	-80.81%	11.8	-87.5%
	Case 7	17.66	-0.45%	101	-78.0%	1,388	-74.86%	16.0	-83.1%
October	Base	9.09	–	130	–	2,117	–	27.6	–
	Case 0	9.09	0.1%	91	-30.0%	2,151	1.64%	29.0	4.8%
	Case 1	9.11	0.2%	99	-23.9%	2,101	-0.72%	27.6	0.01%
	Case 2	9.16	0.8%	116	-10.8%	2,264	6.96%	30.7	11.3%
	Case 3	9.12	0.4%	59	-54.6%	2,135	0.86%	30.5	10.6%
	Case 4	9.12	0.4%	79	-39.2%	2,044	-3.44%	26.9	-2.7%
	Case 5	10.16	11.8%	1	-99.2%	2,223	5.02%	33.5	21.4%
	Case 6	9.94	9.4%	2	-98.5%	2,187	3.35%	31.6	14.5%
	Case 7	9.31	2.4%	8	-93.9%	2,172	2.60%	26.8	-2.9%

Table 6 – Flexibility reserves simulation results

The production costs in general are not changed very much. However, for cases 5 and 6, the production costs are notably increased. These cases are overly conservative in their attempt to cover 95% and 90% of day-ahead net-load forecast errors. This results in the over commitment of generators. All cases exhibit this behavior; however, it is magnified in cases 5 and 6. Figure 6 shows the amount of excess capacity in all cases for the April simulations.

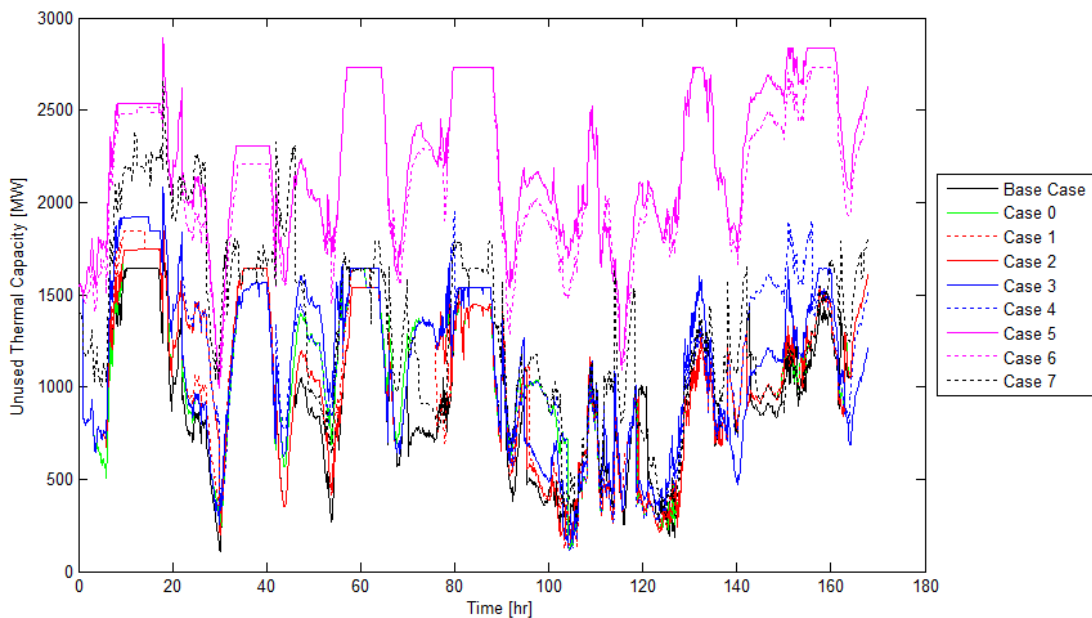


Figure 6 – Unused thermal capacity in the month of April across all cases

This excess capacity is directly related to the number of committed thermal generators (maximum of 74 generators). The flexibility reserve requirement results in the commitment of additional thermal generators in order to meet the additional flexibility requirements (Figure 7). These additional commitments resulted in slightly higher production costs, as shown in Table 6.

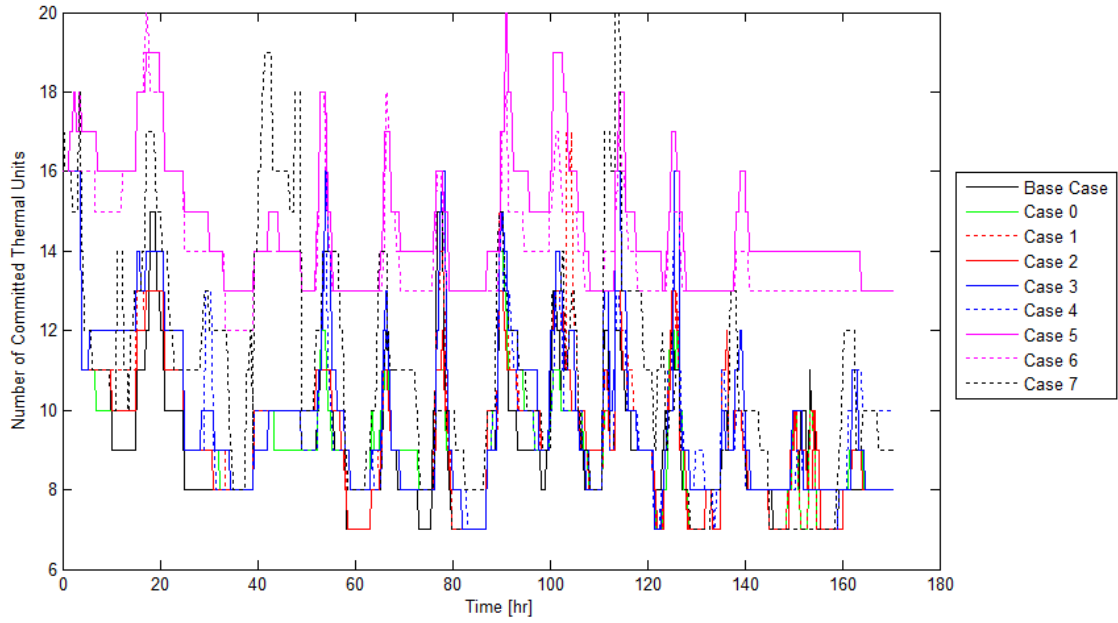


Figure 7 – Number of thermal generators committed in April

The flexibility reserves also have implications on economic metrics as well.

Figure 8 shows an LMP duration curve for the month of October across all cases.

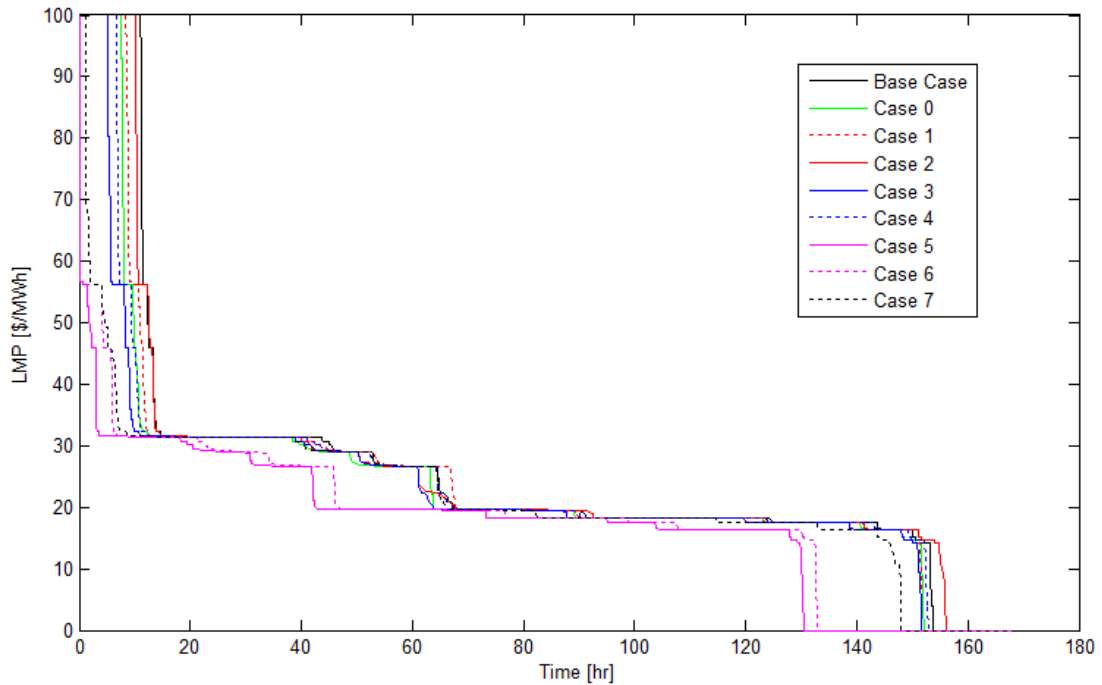


Figure 8 – LMP duration curve for October across all cases

The additional thermal generators provide an interesting result with respect to VG penetration and ultimately LMPs. The excess capacity results in times where all online generators are operating at or near their minimum generation levels and as a result cannot be backed down any further. Coincidentally when wind and solar generator outputs are increasing, the only available mechanism for the system operator to maintain reliability, i.e. minimize ACE, is to curtail the VG output. The curtailment of VG output, the marginal units of energy in the system, result with significant times where the price of energy is 0 \$/MWh. Notice, in Table 7, as the requirement becomes more conservative, the amount of curtailed VG also increases. This is because more generators are committed for the more conservative requirements and this magnifies the minimum generation problem mentioned earlier.

	January	April	July	October
Base Case	11.83	28.34	11.42	20.48
Case 0	12.04	29.51	12.09	19.65
Case 1	11.92	30.24	12.12	20.62
Case 2	11.81	29.31	11.42	19.63
Case 3	11.93	31.01	11.97	20.65
Case 4	13.13	30.51	12.09	20.53
Case 5	19.64	43.36	19.67	30.65
Case 6	18.60	41.97	19.68	29.41
Case 7	15.02	32.38	11.35	25.44

Table 7 – VG curtailment per case per month in GWh

Another benefit of the flexibility reserves mentioned in literature is the potential for converging day-ahead and real-time prices. The analysis performed in this study confirm this behavior. Figure 9 shows the mean-absolute difference between day-ahead and real-time LMPs.

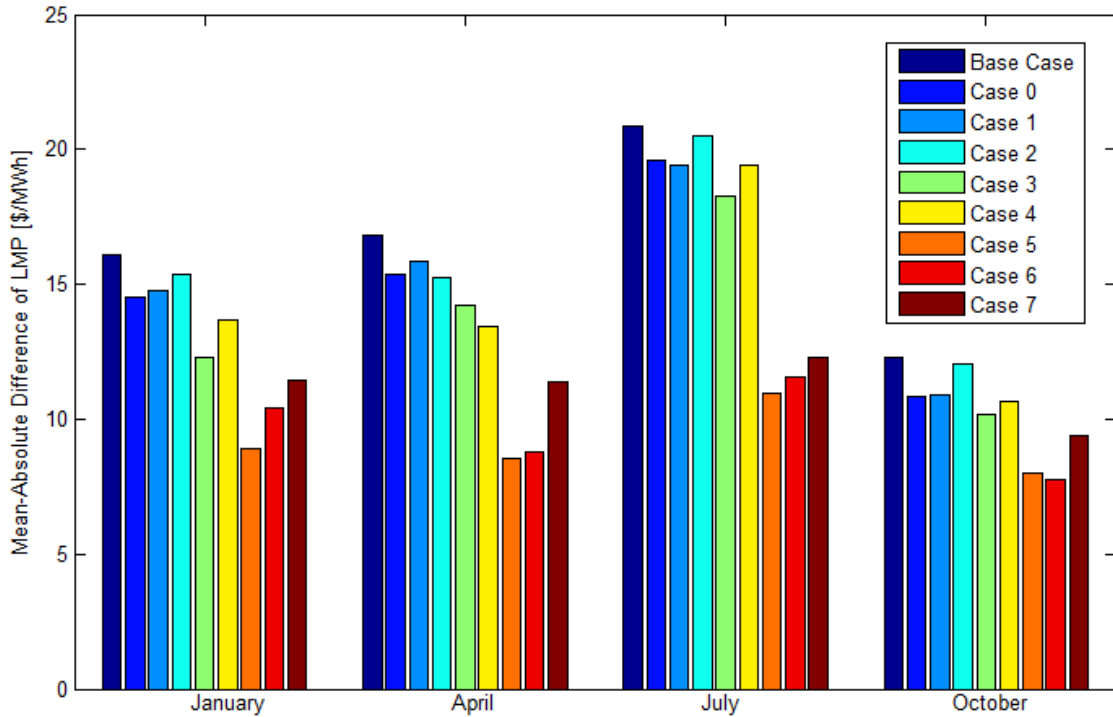


Figure 9 – Mean-absolute difference between day-ahead and real-time LMPs across all cases

There are also noticeable implications on reliability metrics. Figure 10 shows the accumulated ACE broken down by direction. Notice in July that the amount ACE accumulated in the positive direction, i.e. as a result of over-generation, is relatively flat across all cases. This means that under peak loading conditions, the system is more susceptible to under-generation and can benefit greatly from additional upward ramping capacity. Outside of the peak loading condition, the system mostly incurs positive ACE during the valleys of net-load profile. This implies that there are significant times where the net-load is decreasing and online thermal generators cannot ramp down quick enough to accommodate the wind and solar generation ramping up. This implies that the system could benefit from additional downward ramping capacity.

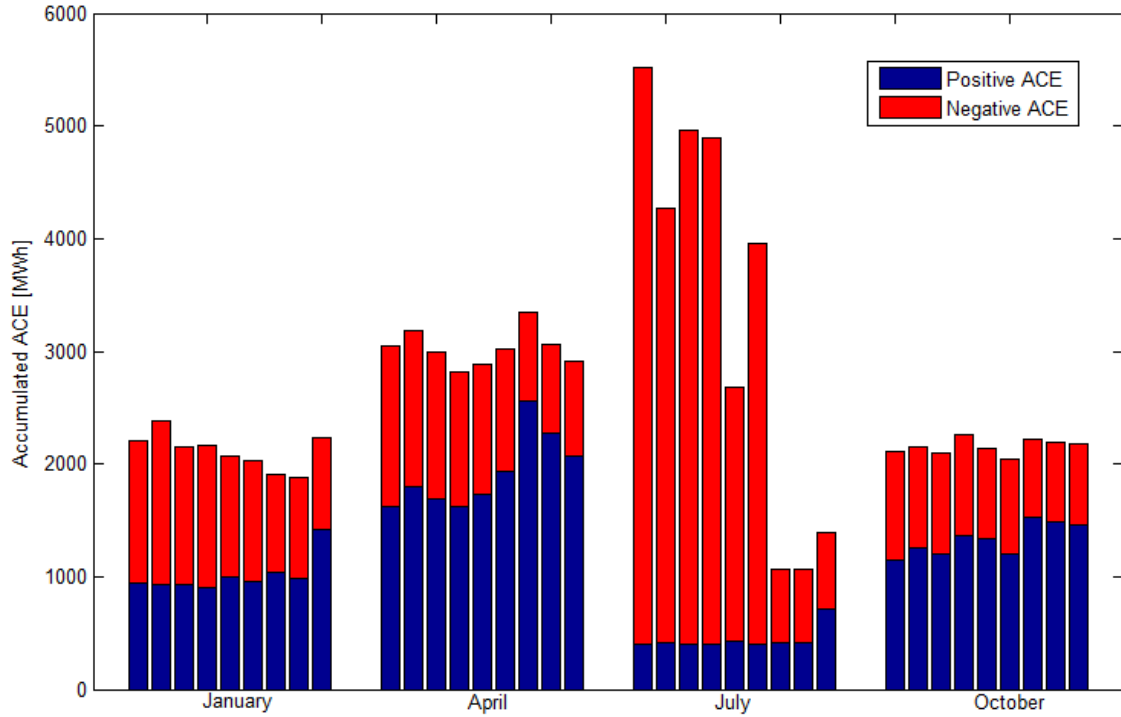


Figure 10 – Accumulated ACE broken down by direction across all cases

Figure 11 shows the distribution of ACE across all cases for all months. From these distributions, it can be seen that the majority of the ACE being realized in the system occurs between positive and negative 20 MW. This is important because in order to substantially improve reliability metrics, reserve methodologies should focus mainly on reducing the tails of these distributions and a secondary objective should be tightening the distribution around zero. Another interesting deduction from these distributions is that the majority of flexibility requirements have similar distributions, i.e. the distributions overlap, regardless of the complexity of the reserve determination method. This implies that there is a capacity threshold that once exceeded, results in similar commitment decisions by the optimization.

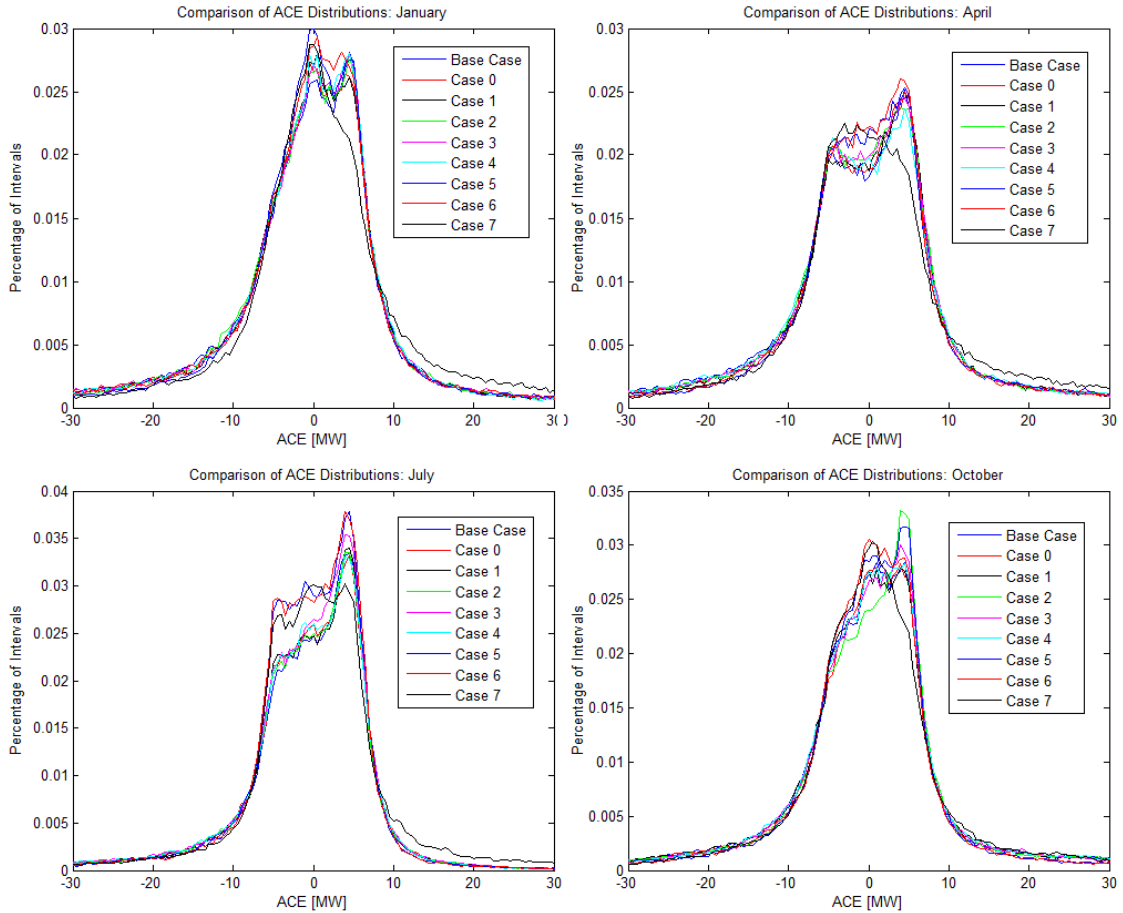


Figure 11 – Distributions of raw ACE across all cases

The inclusion of the flexibility reserve requirement has minimal implications on transmission congestion as well. In general, all the different flexibility reserve requirements studied in this report reduced the number of intervals exhibiting transmission congestion, shown in Table 8. Transmission congestion is defined as any interval where the flow on a transmission line exceeds 95% of its rated capacity. However, there are some cases where the number of congested intervals increased. The congestion in this system is highly dependent on the commitment decisions being made

and since the flexibility reserve requirements do not drastically change the commitment decisions, the congestion is minimally impacted.

	January	April	July	October
Base Case	1.51 %	1.47 %	1.87 %	1.28 %
Case 0	1.55 %	1.44 %	1.81 %	1.29 %
Case 1	1.55 %	1.51 %	1.83 %	1.25 %
Case 2	1.60 %	1.46 %	1.85 %	1.32 %
Case 3	1.54 %	1.38 %	1.87 %	1.22 %
Case 4	1.59 %	1.39 %	1.77 %	1.23 %
Case 5	1.35 %	1.10 %	1.68 %	1.20 %
Case 6	1.45 %	1.16 %	1.72 %	1.19 %
Case 7	1.52 %	1.39 %	1.70 %	1.23 %

Table 8 – Percentage of intervals with transmission congestion

The previous analysis provides significant insight into the operational implications of flexibility reserves. These insights can be used to develop a modified flexibility reserve requirement that can better position the system to handle the additional variability and uncertainty introduced by VG resources. The following conclusions can be made:

1. All of the flexibility reserve requirement methodologies do not explicitly consider the variability of wind and solar generation. Uncertainty is accounted for via some form of consideration of the forecast errors.
2. When the system is operating in the valleys of the net-profile, the system has a tendency to accumulate ACE is in the positive direction.
3. Due to the commitment of additional thermal generation, there are times when these generators are operating at their minimum generation levels and zero-cost wind and solar generation must be curtailed to accommodate unexpected ramps in the net-load profile.

4. The excess thermal capacity committed does provide additional ramping capacity. However, if this extra requirement results in the commitment of larger, slower generators rather than several smaller, faster generators, this may have an adverse effect on the system imbalance.
5. Flexibility reserves have been found, both in literature and this analysis, to reduce the total number of real-time price spikes.
6. Flexibility reserves also help reduce the divergence between day-ahead and real-time energy prices.

3.3 Three-Stage Reliability-Based Reserve Modifiers for Enhanced Operation

Based on the analysis and conclusions discussed in section 2.4, a new reserve modification algorithm is proposed. This new reserve modification technique overcomes the shortcoming of traditional flexibility reserve techniques that do not explicitly consider the additional variability introduced by VG resources. This section will detail an ex post facto addendum to any reserve requirement methodology that explicitly accounts for additional variability introduced by VG resources. This three-stage process is designed to improve reliability metrics with minimal impacts on economic metrics. This new three-stage process is outlined below:

Step 1. Calculate modifier α_1 .

$$\alpha_1 = 1 - \frac{\text{Net Load}}{\text{Actual Load}} \quad (18)$$

Step 2. If $\alpha_1 \geq 0.70$, then increase the downward reserve requirement by one percent.

If $\alpha_1 < 0.70$, then increase the upward reserve requirement by one percent.

Step 3. Calculate modifier α_2 .

$$\alpha_2 = 1 - \frac{\text{Actual VG Output}}{\text{Maximum Possible VG Output}} \quad (19)$$

Step 4. If $\alpha_2 \leq 0.40$, then increase the downward reserve requirement by one percent.

If $\alpha_2 > 0.40$, then increase the upward reserve requirement by one percent.

Step 5. Calculate modifier α_3 .

$$\alpha_3 = \frac{\frac{1}{T} \int_T ACE(\tau) d\tau}{L_{10}} \quad (20)$$

Step 6. If $\alpha_3 > 0$, then increase the downward reserve requirement by one percent.

If $\alpha_3 < 0$, then increase the upward reserve requirement by one percent.

The first stage of this process looks to determine whether or not the system is operating in the valleys of the net load profile. During these times, reserves in the downward direction are more valuable than upward reserves since upward generation can be obtained via VG curtailment. The second stage looks at the actual curtailment of VG power output. If the curtailment is exceeding some predefined threshold, in this case 40%, then the downward reserves are increased. This is intended to help mitigate

curtailment occurring due to inflexible online capacity. The first two stages are based on the actual uncertainty in the system occurring in real time. The final stage takes into account the actual variability occurring in the system. This is captured via consideration of the actual ACE. This stage looks into the actual ACE being realized in the system in real time. The numerator is the average of the last T minutes, in this case 5 minutes. The denominator is the L_{10} threshold from the NERC Compliance Performance Standard 2 (CPS2) for the balancing area being studied. If this modifier is positive, positive ACE is being accumulated, and the downward reserve requirement should be increased, and similarly if the average ACE is negative. The modified reserve requirement is capped so as not to exceed 2% of the actual load at the same time. While in theory, increasing reserves will result in approaching a perfectly reliable system, in practice, this is not economically feasible. Thus it is important to ensure that the reserve requirement improves the reliability metrics while, at worst, maintaining the same total system-wide cost. The cap of 2% is double the standard integration study practice by the WECC TEPPC of 1% of the current load. The threshold values associated with each stage are determined empirically using an iterative trial-and-compare technique until a sufficient optimal solution was obtained. While this reserve modification algorithm is reliability-based and designed to improve reliability metrics in terms of ACE, it could potentially yield economic savings if this improvement results in avoiding potential NERC sanctions as a result of violating CPS2 requirements which can be greater than \$300,000 per violation [42].

The analysis performed in section 2.4 is repeated with the three-stage reserve modification algorithm included in the optimizations. All operating assumptions and system characteristics are kept constant. This allows for the implications of the three-stage reserve modification algorithm to be extracted. Table 9 summarizes the difference in the results from section 2.4 by including the three-stage reserve modification algorithm. The columns in Table 9 from left to right correspond to the change in total system wide production cost, the change in AACEE, the change in the standard deviation of the ACE, the change in the number of real time price spikes, and the change in number of real time market infeasibilities.

Case	Δ COST	Δ AACEE	$\Delta \sigma_{ACE}$	Δ Number of Price Spikes	Δ RT Inf.	
January	Case 0	-4.0%	-21.2%	-22.6%	-50.0%	-91.5%
	Case 1	-0.4%	-13.4%	-11.3%	-51.1%	-79.8%
	Case 2	-0.2%	-14.9%	-14.7%	-52.0%	-88.7%
	Case 3	2.1%	-11.0%	-8.3%	-57.7%	-78.7%
	Case 4	-0.8%	-8.4%	-6.9%	-39.8%	-68.3%
	Case 5	-1.3%	0.3%	7.6%	-	-
	Case 6	-0.2%	-1.3%	5.7%	-	-
	Case 7	-0.3%	2.4%	3.5%	11%	190%
April	Case 0	2.7%	-16.3%	-10.3%	-45.6%	-74.6%
	Case 1	1.5%	-14.5%	-17.7%	-42.2%	-68.4%
	Case 2	1.5%	-6.0%	0.4%	-27.1%	-55.7%
	Case 3	1.9%	-13.9%	-10.8%	-55.9%	-55.3%
	Case 4	1.9%	-16.3%	-11.0%	-50.0%	-51.0%
	Case 5	-1.0%	-5.1%	-6.0%	-	-
	Case 6	0.6%	-1.4%	1.6%	-100.0%	-100%
	Case 7	0.7%	6.3%	7.9%	-20%	-35.4%
July	Case 0	-1.1%	-13.7%	-7.8%	-9.6%	-16.8%
	Case 1	-1.0%	-19.6%	-19.7%	-11.5%	-23.9%
	Case 2	-0.8%	-24.0%	-15.4%	-18.8%	-29.2%
	Case 3	-1.3%	-16.0%	-2.3%	-28.1%	-25.0%
	Case 4	-2.0%	-9.0%	-6.3%	-7.8%	-11.1%
	Case 5	1.9%	-6.4%	-6.5%	-48.4%	168.9%
	Case 6	-0.4%	-8.5%	-8.0%	-24.5%	-65.3%
	Case 7	-0.0%	-0.2%	-0.7%	-2.0%	23.1%
October	Case 0	0.7%	-14.7%	-16.1%	3.3%	-34.2%
	Case 1	1.0%	-13.0%	-13.36%	-17.2%	-20.6%
	Case 2	0.0%	-20.3%	-23.3%	-28.4%	-44.2%
	Case 3	0.0%	-9.3%	-11.9%	0.0%	-6.9%
	Case 4	0.6%	-10.1%	-10.1%	-27.8%	-19.7%
	Case 5	-1.4%	-2.2%	-1.9%	100.0%	2.5%
	Case 6	0.0%	3.7%	7.4%	0.0%	-57.8%
	Case 7	-0.1%	-0.8%	-0.7%	20%	57.1%
Average	0.03%	-9.34%	-7.17%	-23.50%	-33.9%	

Table 9 – Change in reliability and economic metrics due to three-stage reserve modification

The results in Table 9 show an important result summarized in the final row. The average impact across all cases with the three-stage reserve modification algorithm is able to improve all of the reliability metrics across the board while minimally impacting the total system production cost. There are some blank entries in this table and that is because the three-stage reserve modification process did not impact the result.

One of the benefits of the three-stage reserve modification algorithm is its impact on the ACE occurring in the system. Figure 12 shows the distributions of the ACE across all scenarios for all months. The plots on the left correspond to the scenarios without the three-stage reserve modifiers starting from January (top) through October (bottom). The plots on the right correspond to the same scenarios re-run with the three-stage reserve modifiers. The modifiers help converge the distributions across cases implying the modifiers allow the generators to reach a more optimal dispatch solution. In general, the distributions with the modifiers are also more symmetric around zero which is desirable to help mitigate generator wear in a single direction and removes any undesirable bias in the imbalance.

The modifiers, while designed around reliability metrics, also have implications on economic metrics as well. As was mentioned before, the three-stage reserve modification process is able to further reduce the number of real-time price spikes. This is desirable because it helps minimize the volatility of the real-time electricity market. Another benefit in this regard is the ability of the modifiers to further converge the day-ahead and real-time energy prices. Table 10 shows the change in the difference between the mean-absolute day-ahead LMP and real-time LMP by including the three-stage

modifiers. This metric essentially reflects the convergence of the electricity markets, a value of zero implying that the day-ahead and real-time markets have the same LMP. A negative value in Table 10 implies that the case with the modifiers was able to further converge the prices by the magnitude of the value. For example, including the modifiers further converges the day-ahead and real-time LMPs in July Case 2 by 3.36 \$/MWh.

	January	April	July	October
Case 0	-0.27	-1.68	-2.56	-0.40
Case 1	0.31	-0.09	-2.19	-0.35
Case 2	-0.98	0.82	-3.36	-1.37
Case 3	0.79	-1.22	-3.40	-0.37
Case 4	-0.61	-1.16	-3.65	-0.93
Case 5	0.99	-0.42	0.51	0.02
Case 6	-0.65	-1.32	-1.55	0.19
Case 7	-0.01	-0.43	-0.14	-0.02
Average	-0.05	-0.69	-2.04	-0.40

Table 10 – Mean absolute difference between DA and RT LMPs in \$/MWh

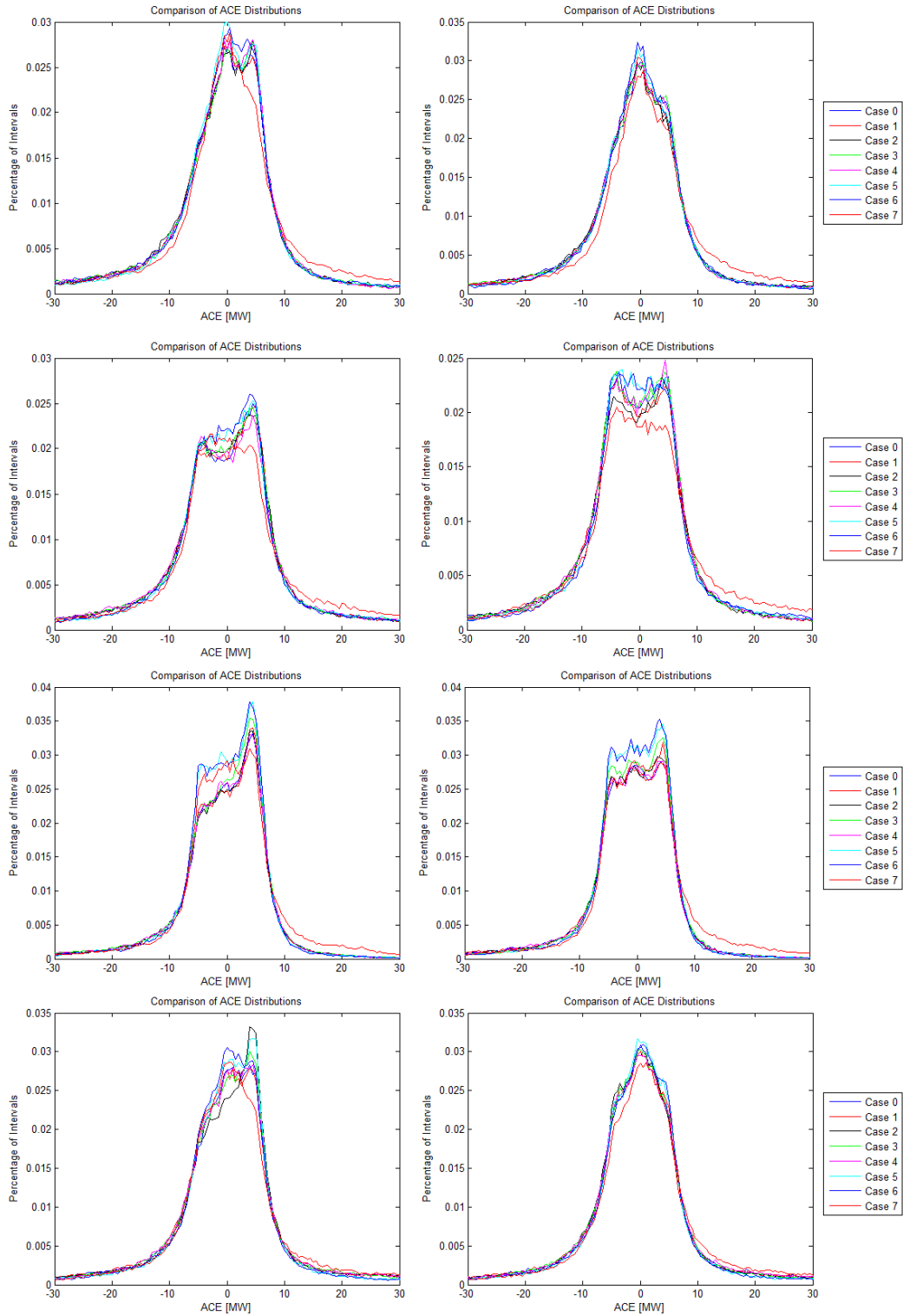


Figure 12 – Distribution of ACE across all cases with the modifiers (right) and without (left)

As the landscape of electric power systems continues to evolve, the operating strategies with which system operators have historically relied on will need to change. This is especially true of operating reserves. Due to the inherent individuality of power systems, there is no clear cut operating strategies enforced across all systems. Rather, each operator operates their own system according to its own best interest since each power system can significantly vary due to demand profiles, geographical footprints, social pressures, political agendas, etc. Therefore, in order to maximize positive impacts, it is important to improve operational guidelines rather than specific operational strategies.

With this in mind, this report proposed a three-stage reserve modification process that was designed with the goal of improving reliability metrics with minimal impacts on economic metrics. This process addresses several shortcomings of different operational flexibility reserve methodologies proposed in literature by industrial and academic professionals. Firstly, this process explicitly captures the variability of wind and solar generation in determining the final reserve requirement. Secondly, the proposed three-stage modification process is dynamic and takes into account the current operating state of the system as opposed to the static reserve calculation methods proposed in literature. Thirdly, this process is also independent of individual operating reserve calculation methodologies. That means that this process can be applied to any operating reserve methodology.

This three-stage reserve modification process was shown to on average, improve the reliability metrics across the board and across all cases simulated. While designed

with the intention of improving reliability metrics, it also provided economic benefits. The three-stage process is able to further reduce the number of real-time prices spikes and it also further converges the day-ahead and real-time energy prices. Because this three-stage process happens just before the optimization and is a strict calculation, it can be easily implemented in any market clearing algorithm with minimal impact on hardware execution time, which is desirable especially for large power systems. While not perfect, this proposed algorithm should help system operators more accurately account for the increased variability and uncertainty introduced by wind and solar generation under high penetration scenarios.

Chapter 4: Using Stochastic Modeling to Address System Uncertainty

4.1 Motivation

As renewable energy resources become more ubiquitous in tomorrow's power systems, the way system operators treat them will have to adapt. Typically, wind and solar generation are treated as price-takers. This means that they generate what they are physically capable of and the power system operator must adjust the remaining online generation to accommodate them. While this may be feasible under low penetrations, this paradigm will offer significant challenges under high penetration scenarios. System operators will have to find ways to include these resources in market clearing models so that they become fully integrated into power system operations. One of the major challenges in this regard is the additional variability and uncertainty that they introduce into the system.

Since these resources are naturally uncertain, it is natural to extend their representations into the stochastic modeling space. With unlimited time and computational power, it is not unreasonable to assume that power system operators could solve a stochastic representation of the energy scheduling problem to an optimal solution that guarantees security without the need to withhold capacity in the form of operating

reserves. However, due to computational limits, the amount of uncertainty scenarios that can be considered must be reduced. Reducing the number of scenarios results in increasing the uncertainty in the solution. One way to accommodate this shortcoming is by introducing an explicit operating reserve requirement, similar to those described in Chapter 3, which can be used to address this uncertainty. This report will explore the benefits of using an explicit operating reserve requirement in a stochastic modeling formulation and improve on this formulation by adapting to realized variability and uncertainty occurring in real time in the power system.

4.2 Stochastic Formulation

The base simulation platform described in Chapter 2 is modified to expand its capability into the stochastic modeling domain. The unit commitment problems (DASCUC and RTSCUC) utilize a progressive hedging algorithm to help solve the multiple scenarios to a good enough solution as outlined in Chapter 1. This is an iterative process that solves each scenario separately, as a single deterministic sub-problem, and compares the optimal solution of all scenarios against each other. If the difference between solutions is too great, the optimization is updated with a penalty factor and solved again. This process continues until a final solution is found. The solution process is outlined below.

1. Modify the objective function of sub-problems with relaxed term:

$$\rho \cdot (x - \bar{x}) \tag{21}$$

2. Solve all deterministic sub-problems, one per scenario, x

3. Calculate the average solution across all scenarios, \bar{x}
4. Check for solution convergence using the following criteria:

$$\sum_i \sum_t \sum_s \lambda_{its} < \varepsilon \quad (22)$$

5. If solution has converged, solution found, end of search. If solution has not converged, continue to step 5.
6. Update penalty factor, ρ
7. Go back to step 3

The previous steps give some high level insight into the solution process. The use of the progressive hedging algorithm helps enforce the non-anticipativity across all scenarios. The sub-problems utilize Lagrangian Relaxation in order to facilitate the iterative solution process. The relaxed objective function is given in (37).

$$\min \sum_i \sum_t C_G(P_{it}) + C_{SU}(P_{it}) + C_{NL}(P_{it}) + \gamma \sigma_t + \delta \rho_t + \rho \cdot (x - \bar{x}) + w \cdot (|C_{it} - I_{it}| - \lambda_{it}) \quad (23)$$

This additional terms in the objective function help converge the solutions, i.e. enforce non-anticipativity across scenarios via progressive hedging, and move the solution towards the optimal solution via updates to the updated Lagrangian multiplier, w . The process of updating the Lagrangian multiplier w is outlined below.

1. Solve for the sub-gradient of each individual scenario

$$\sigma_{its} = c_{its} - I_{its} \quad (24)$$

2. Determine the step size to approach the optimal solution

$$N_t = \sqrt{\sum_i \sum_t \sum_s (c_{its} - I_{its})^2} \quad (25)$$

$$\text{if } \frac{N_{t-1}}{N_t} \leq 1, \text{ then } \tau_t = \left(\frac{N_{t-1}}{N_t}\right)^3 \cdot 0.75 \cdot \tau_{t-1} \cdot \frac{N_t}{(N_{t-1} + 0.001N_t)} \quad (26)$$

$$\text{if } \frac{N_{t-1}}{N_t} > 1, \text{ then } \tau_t = \left(\frac{N_{t-1}}{N_t}\right)^2 \cdot 0.75 \cdot \tau_{t-1} \cdot \frac{N_t}{(N_{t-1} + 1.001N_t)} \quad (27)$$

3. Update the Langrangian multiplier, λ

$$\lambda_{its} = \tau_t \cdot \sigma_{its} \quad (28)$$

This process utilizes an adaptive step size to adjust the solution step (step 2 above) to control the convergence speed of the problem [43]. The final solution is a near-optimal solution relative to all scenarios. In order to adjust the penalty factor ρ , a cost-proportional strategy is used the updates the penalty factor based on difference between the scenario solutions, i.e. the sub-gradient from step 1 above [44]. The scenario solutions are linked via the linking variable, c , through all cases and is defined as follows.

$$c_{i,t} = \sum_s \frac{P_s \cdot I_{i,t}^s}{P_s} \quad (29)$$

In the above equations, the variable ‘ I ’ is the thermal generator commitment status. A value of one signifies that the unit is online, and conversely, a value of zero signifies that the unit is offline.

The previous discussion describes a stochastic unit commitment problem in the decomposed form. This decomposition is separates the master stochastic problem into a subset of deterministic sub-problems to be solved separately using a progressive hedging

algorithm to enforce non-anticipativity and a Lagrangian subgradient based method to determine solution optimality. Another stochastic formulation involves extending the traditional optimization problem into the scenario domain. This type of formulation is called the extensive form. This type of formulation is not practical for the unit commitment problem. This is because the extension of the mixed-integer problem into an additional third dimension exponentially increases the solution time. However, for the economic dispatch problem, it is computationally feasible to extend the problem into an additional domain. This is simply done by extending the formulation to include a third dimension for scenarios. The economic dispatch formulation in the extensive form is given in Appendix B.

4.3 Analyzing the use of reserves in stochastic modeling

The analysis is performed on a modified IEEE 118 bus system described in Chapter 3. Wind generation was added to this system in order to simulate high penetration scenarios. Particularly, renewable energy generation was added to have an average energy penetration level of 33%. Renewable energy sites were selected to maximize access to transmission capacity in order to minimize the amount of curtailment occurring due to congestion. The flexibility reserves modeled in this analysis are based on non-spinning reserve service developed by the Electric Reliability Council of Texas. This product is meant to cover 95% of net-load forecast errors from the previous month and the same month from the previous year. The scenario data was simulated using an

auto regressive moving average (ARMA) technique [45][46]. This method modified the forecast by introducing normally distributed errors. This modification is performed as:

$$X_t = \alpha \cdot X_{t-1} + \beta \cdot Z_{t-1} + Z_t \quad (30)$$

For the analysis in this paper, the α and β constants are defined as 0.98 and -0.7 respectively. The standard deviation of the sampled normal distribution, Z_t , is 3% for the load and reserve requirement profiles and 6% for the wind profile. The stochastic simulation workflow is shown in Figure 13.

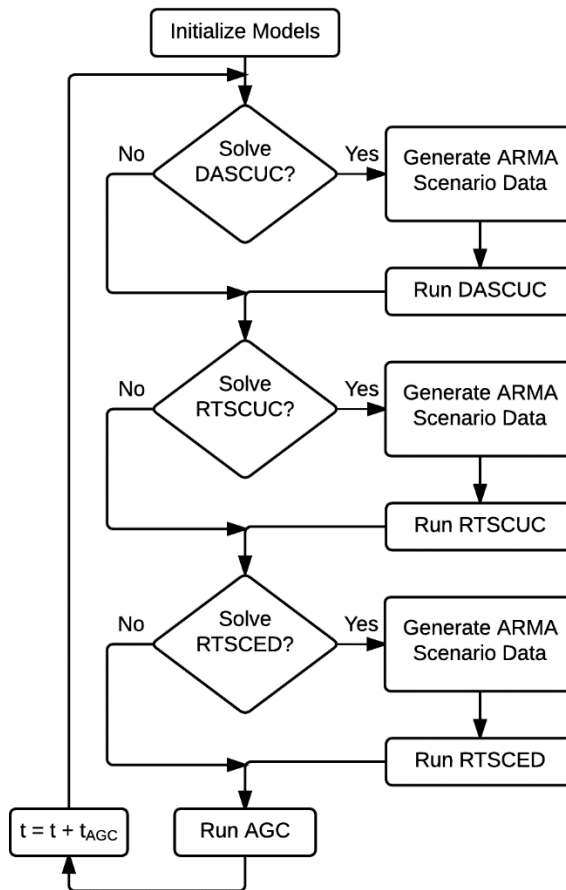


Figure 13 – Stochastic simulation workflow

There are two types of scenario sets created for this study. The first type considers a fully stochastic scenario set, including the first interval of the optimization. The second type considers a deterministic binding interval, i.e. the first interval of the optimization, and the scenarios deviate starting from the second interval. These different types are illustrated in Figure 14.

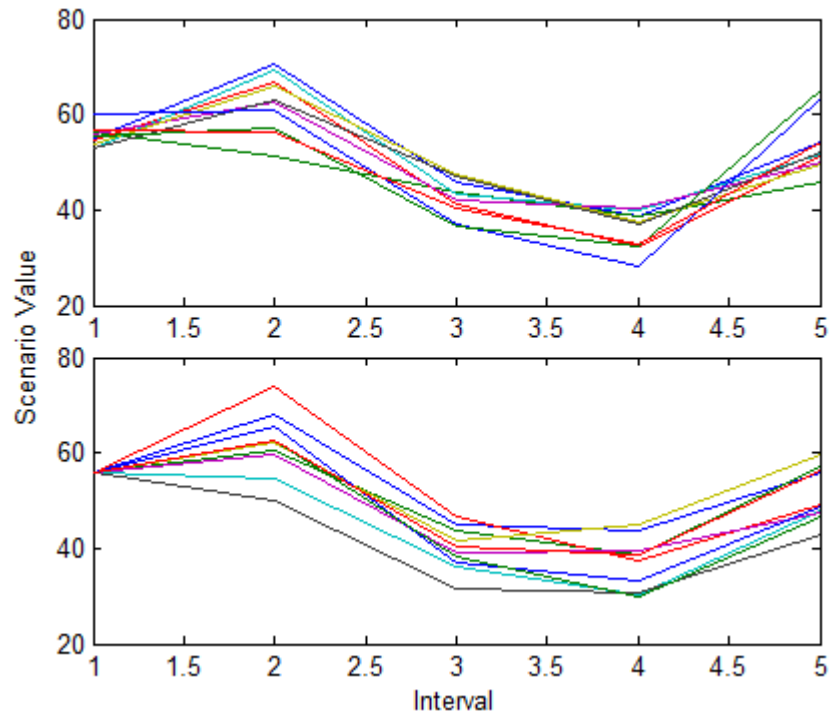


Figure 14 – Scenarios set type 1 (top) and type 2 (bottom)

The following cases were developed in order to study the impact of using an explicit operating reserve requirement in a stochastic modelling framework.

	Model Type	No Reserves	Deterministic Reserves	Stochastic Reserves
Case 1	Det		X	
Case 2	Sto	X		
Case 3	Sto		X	
Case 4	Sto			X

Table 11 – Summary of reserve methods for each case

Case 1 is a fully deterministic model. This case is used as a baseline solution. Case 2 is a fully stochastic model that does not include any flexibility reserves. Case 3 is a fully stochastic model with a deterministic flexibility reserve requirement. Case 4 is a fully stochastic model. Table 12 summarizes the economic and reliability results from studying cases 1-4.

		Cost	Δ Cost	AACEE	Δ AACEE
		[\$M]	[%]	[MWh]	[%]
January	Case 1	16.29	—	617.6	—
	Case 2	16.96	+4.1	781.3	+26.5
	Case 3	18.27	+12.2	632.8	+2.5
	Case 4	18.35	+12.7	614.4	-0.5
April	Case 1	13.05	—	667.9	—
	Case 2	13.54	+3.7	811.3	+21.5
	Case 3	13.40	+2.7	606.8	-9.1
	Case 4	13.63	+4.5	605.3	-9.4
July	Case 1	22.64	—	616.9	—
	Case 2	21.99	-2.9	1388.0	+125
	Case 3	22.77	+0.6	864.5	+40.2
	Case 4	24.16	+6.7	817.8	+32.6
October	Case 1	13.79	—	622.4	—
	Case 2	14.22	+3.1	927.9	+49.1
	Case 3	14.14	+2.5	602.8	-3.1
	Case 4	14.09	+2.2	580.5	-6.7

Table 12 – Summary of stochastic reserve results

From Table 12, in general, stochastic modeling increases the system production cost. This is expected since stochastic models can result in committing additional thermal generators than a comparable deterministic model. Figure 15 shows the total number of thermal generator start-ups split between “small” generators, i.e. less than 150 MW, and “large” generators, i.e. greater than 150 MW for the January simulation. While this only shows the number of start-ups for January, other weeks display similar results.

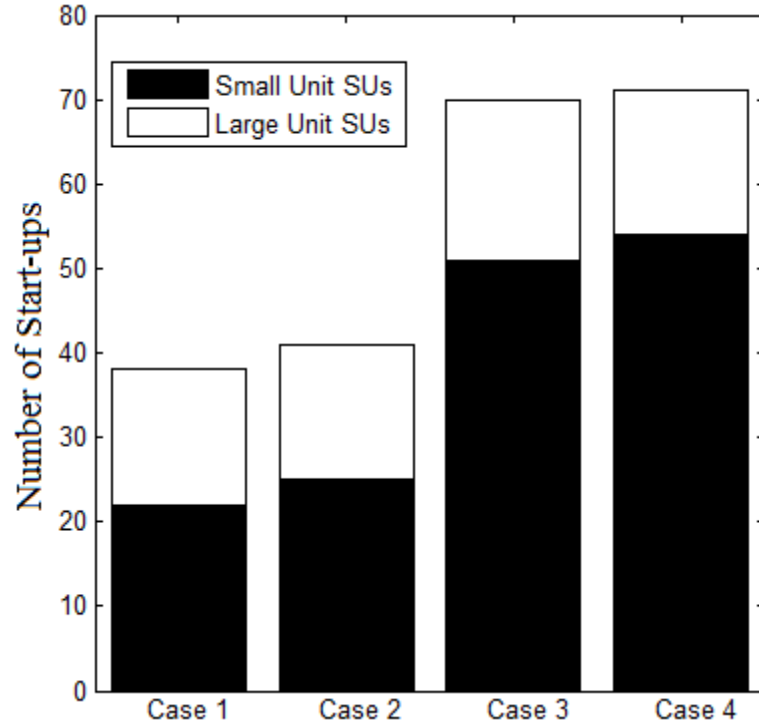


Figure 15 – Number of thermal start-ups in January

Investigating the reliability ACE results exposes an interesting result. Figure 16 shows a distribution of the ACE for all the cases (the outliers have been excluded in order to improve readability of the plots) for the April simulations.

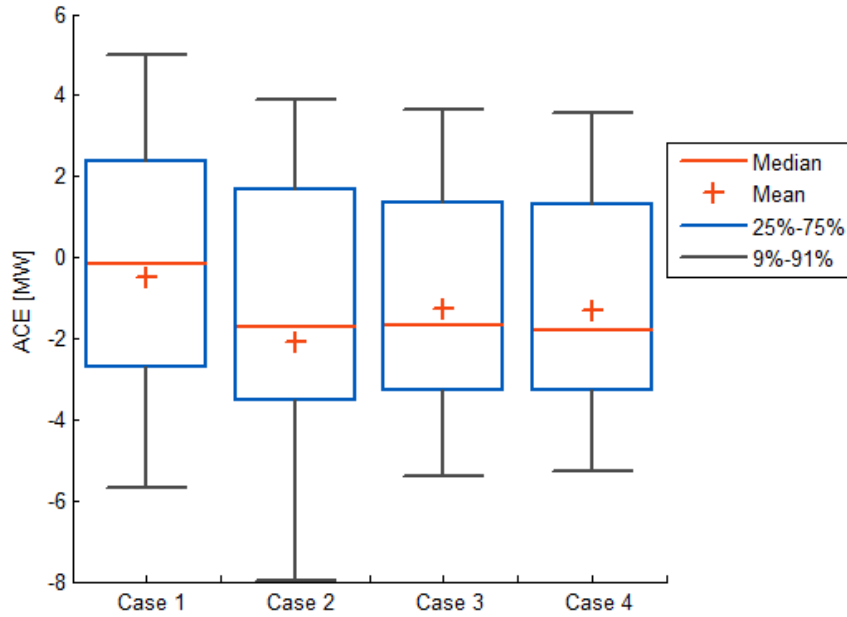


Figure 16 - Distribution of ACE across all cases in April

Including the reserves in the stochastic formulation tightens the distribution. Similar trends can be found in the other months as well. This was due to the extra flexibility in the system from the additional thermal capacity afforded by the additional thermal generators being turned on (see Figure 15). Another interesting result is the stochastic formulations result with a negative bias in the net ACE (mean and median value are more negative than the fully deterministic case). This has to do with the nature of the stochastic formulation and how the optimization handle the load peaks. Due to computational limitations and the methodology of the optimizations, the stochastic solutions do not arrive to the same optimal solution, but rather a solution that is good enough, i.e. near optimal, that minimizes the difference between scenarios. With a set of imperfectly forecasted scenarios, the final dispatch solution will most likely vary from the realized load and wind profiles. In addition to this, under peak conditions, the system is typically experiencing the most operational stress, e.g. generators are ramping at their

capacities and transmission lines are carrying near limit flows. As a result, AGC is not able to fully make up this difference and sometimes results with intervals that experience under-generation at peak loads. For example, the simulation of the week in July experienced noticeable under-generation for three out of the seven load peaks with minor under-generation occurring on another peak.

It is also worthwhile to compare cases 1 and 2. For convenience, Case 1 is the fully deterministic model and Case 2 is the fully stochastic model that does not include a reserve obligation. In general, the system production cost is unaffected (the difference of a few percentage points from a total of over \$22M is deemed negligible). However, the AACEE metric noticeably increases in the stochastic model without reserves. The stochastic model is unable to capture the full uncertainty spectrum of the load and wind profiles and sometimes fails to prepare the system for ramps in the net-load. Figure 17 shows one instance where the deterministic case was better able to track an upward ramp in the net-load profile (solid, blue trace) with the online thermal assets (dashed, black trace). The plot on the left is case 1, the fully deterministic case; the plot on the right is case 2, the stochastic case without a reserve requirement. Similar behavior can be observed throughout each simulation week.

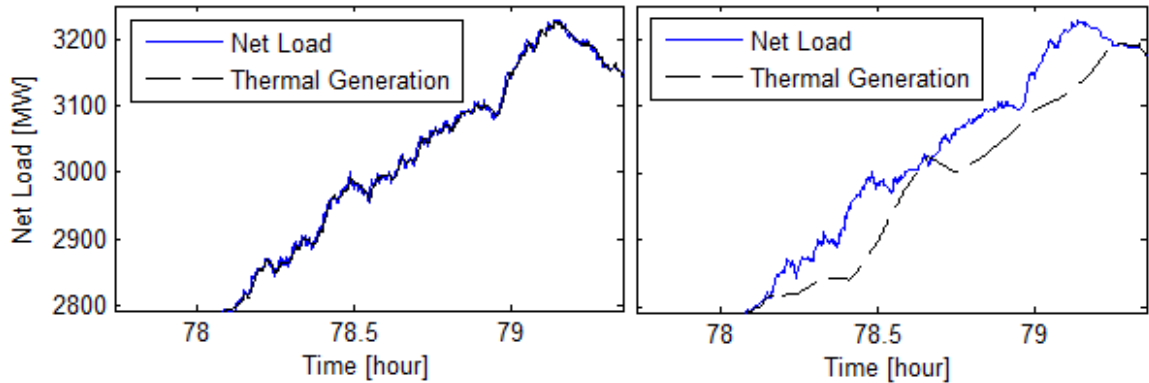


Figure 17 - Comparison of net-load ramp tracking in Case 1 and Case 2

Comparing cases 3 and 4 shows that in terms of reliability, it is better to include a reserve requirement and a stochastic requirement offers more benefit to the system than a deterministic requirement.

It is during the economic dispatch stage of the scheduling process that decisions on reserve schedules are made. Therefore, in order to study the impacts of reserves in a stochastic model, the following sensitivities were also studied. All sensitivities only include the reserve requirement in the economic dispatch stage of the simulation and the unit commitment stages do not have any such requirement. Case 5 implements a type 2 scenario set for the reserve requirement. Case 6 implements a type 1 scenario set. Case 7 includes a deterministic requirement in the first interval and no reserve requirement in the future intervals, i.e. all cases have the same reserve requirement in the first interval and no requirement in the future intervals. Case 8 includes a stochastic requirement in the first interval and no reserve requirement in the future intervals, i.e. each scenario has a different requirement in the first interval and no requirement in the future intervals.

	First Interval	Look-ahead Intervals
Case 5	Deterministic	Stochastic
Case 6	Stochastic	Stochastic
Case 7	Deterministic	None
Case 8	Stochastic	None

Table 13 – Summary of sensitivity scenario reserve requirements

The motivation behind cases 8 and 9 is that the uncertainty is more significant in the look-ahead timeframes. As a result, the reserve requirement can be used to address the uncertainty in the next five minutes while the stochastic model itself can be used to address the uncertainty happening an hour from now.

Since the decision on reserve schedules is made in the real-time economic dispatch stage, several sensitivities we run in order to explore the impacts of reserves in a stochastic modeling framework, namely cases 5-8. Table 14 summarizes the costs and reliability ACE metric results from these cases.

Cost	Δ Cost	AACEE	Δ AACEE
------	---------------	-------	----------------

		[\$M]	[%]	[MWh]	[%]
January	Case 5	16.70	+1.2	924.1	-18.0
	Case 6	16.89		757.9	
	Case 7	17.79	-0.2	965.0	+37.1
	Case 8	16.75		1323.1	
April	Case 5	13.38	+3.1	859.9	+22.2
	Case 6	13.79		1050.3	
	Case 7	13.61	+0.1	856.1	+24.2
	Case 8	13.63		1063.3	
July	Case 5	24.02	+5.7	4868.7	-2.6
	Case 6	25.39		4740.3	
	Case 7	24.59	-3.4	4807.2	+4.3
	Case 8	23.77		5012.5	
October	Case 5	14.54	+0.5	1023.7	+3.0
	Case 6	14.61		1054.6	
	Case 7	14.58	+0.2	1029.2	-0.0
	Case 8	14.60		1029.1	

Table 14 – Summary of stochastic sensitivity scenario results

Cases 5 and 6 essentially compare the impact of scheduling reserves to address the uncertainty in the binding interval. Stochastically generated scenarios are used to address the uncertainty in future time intervals. The uncertainty in the binding interval is addressed via a deterministic requirement in case 5 and a stochastic requirement in case 6. It is more expensive to use a stochastic requirement in the binding interval. The reliability metrics relate to the amount of renewable energy in the system. In the April and October weeks, where there are intervals with instantaneous VG penetration of more than 78%, there are less thermal generators committed which results in less operational flexibility. With less flexibility in the system, it is better to minimize risk in the scheduling problem by reducing the considered uncertainty, i.e. deterministic requirements in the binding interval.

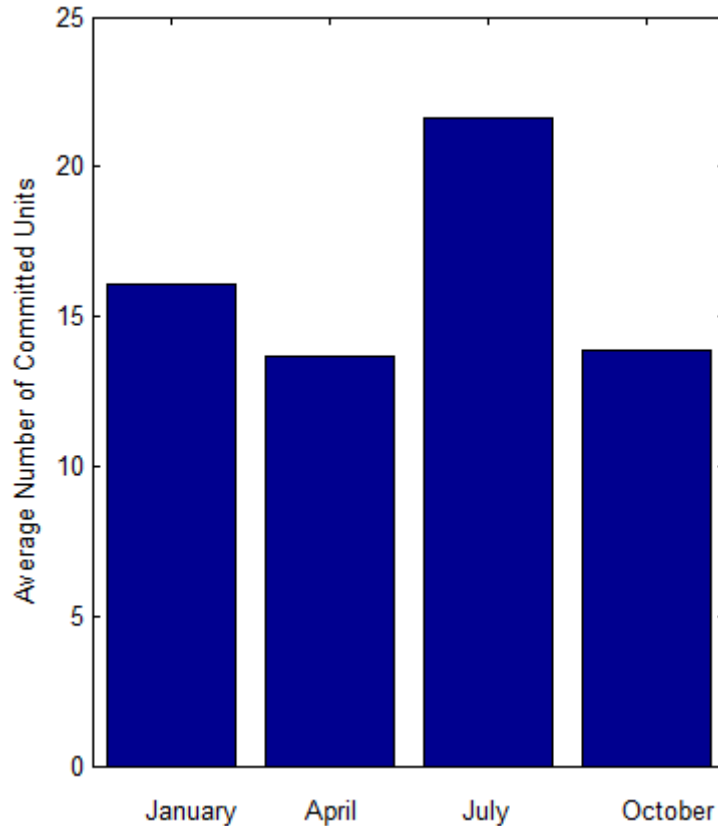


Figure 18 – Number of committed thermal units in each simulated month

Comparing cases 7 and 8 shows that without explicitly addressing the uncertainty in future intervals, a deterministic reserve requirement performs better than a stochastic reserve requirement. Since the system is not reserving capacity, generators are dispatched only to meet the expected net-load in the next five minutes. In the stochastic scenario, a singular dispatch cannot meet all expected net-load forecasts and as a result, the system is susceptible to load shedding. Figure 19 shows the sign of the accumulated ACE in the system in October. Clearly, the use of the stochastic requirement increases the amount of ACE accrued in the negative direction, i.e. under generation.

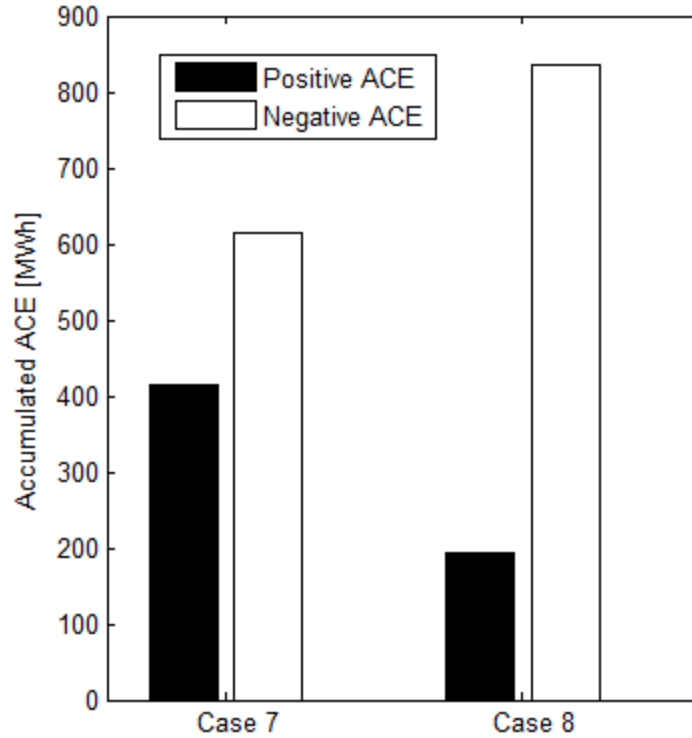


Figure 19 – Direction of accumulated ACE for cases 7 and 8 in October

While Figure 19 only shows the ACE results for the October simulation, similar trends are visible in all of the other cases as well.

4.4 Three-Stage Stochastic Modifiers

Based on the previous analysis, the three stage stochastic modification process is designed to speed up solution time while maintaining solution integrity. This process is empirically designed based on observations of system operations in a stochastic model. The modification process is outlined below.

Step 1: Define the net-load as follows:

$$\mu(t) = L(t) - P_w(t) \quad (31)$$

Step 2: Calculate the first modifier based on the net-load penetration level as follows:

$$\rho = \frac{\mu - \bar{\mu}}{\underline{\mu} - \bar{\mu}} \cdot 100 \quad (32)$$

Step 3: If modifier ρ is greater than 80, then bind all requirements in the first interval across all scenarios.

Step 4: Calculate the second modifier as follows:

$$\delta = \text{round}(\rho) \cdot S_{max} \quad (33)$$

Step 5: Set the number of scenarios equal to modifier δ .

Step 6: Calculate the third modifier based on the standard deviation of the load and wind power as follows:

$$\varepsilon = \frac{\sigma(X(t))}{\max(X(t))} \quad \forall t \in [t - T, t] \quad (34)$$

Step 7: Set the standard deviation of the ARMA forecasts equal to modifier ε .

In (31), L is the electrical demand and P_w is the expected wind power. In (32), the bars indicate the forecasted maximum (upper-bar) and minimum (lower-bar) net-load profile values. These values can be adjusted to control the modification process to best serve the system being studied. T represents the amount of time to consider in determining the standard deviation of the wind and load profiles. This variable also serves as a tuning parameter that can be adjusted on a case-by-case basis. In (33), S_{max} is the maximum number of scenarios to consider for the current simulation. This number can also be tuned throughout the simulation. In (34), X stands for either the load or wind data.

The basic motivation for this process lies in the implicit intention of using stochastic modeling to begin with, how to best address future uncertainty. When the

power system is under the most strain, there is less flexibility in the system. As a result, it is beneficial to minimize the uncertainty in the optimization. This is achieved in the first stage by binding the uncertain variables in the first interval, i.e. the first interval becomes a deterministic problem. Conversely, when the system is not under duress, e.g. during the valleys of the net-load profile, the system typically has excess energy and ramping capacity available. Also, since the use of stochastic modeling is highly motivated by the presence of variable renewable generation, there is less need for fully stochastic optimizations during these times. As a result, the second stage helps reduce the stochastic problem during these time periods by reducing the number of scenarios being considered. Since the goal of utilizing the scenario-based stochastic modeling approach is to address the uncertainty in load and renewable generation data, the third stage updates the standard deviation of the scenarios to match the standard deviation realized in the load and wind in real-time based on actual data. The simulation workflow is adjusted to accommodate the 3-stage modifiers. The new workflow is shown in Figure 20.

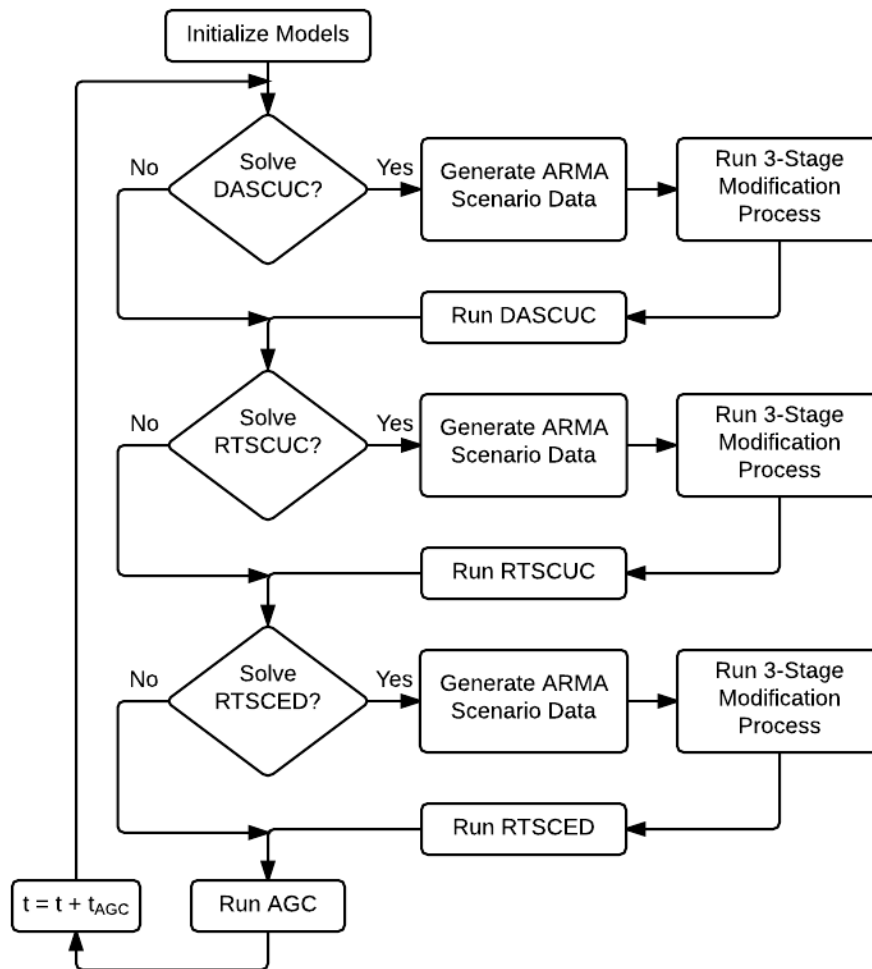


Figure 20 – Stochastic simulation workflow with modification stage

Three scenarios were simulated to study the benefit of the three stage stochastic modifiers. Scenario 1 is fully deterministic formulation. This scenario serves as a sort of baseline scenario. Scenario 2 is a normal stochastic formulation that utilizes the model described in Section 4.2. Scenario 3 is a stochastic formulation that utilizes the three-stage modification process. Table 15 summaries the simulation results. With the exception of January, stochastic modeling was able to reduce the production costs. The

three-stage modifiers were able to even further reduce these costs. Even in January, the costs increased a nonsignificant amount (less than 2% increase). Across all cases, the stochastic model was able to improve the AACEE metrics. The three stage modifiers were able to even further improve these metrics as well, although the benefit is less pronounced than the benefit afforded to costs.

		Cost [\$M]	AACEE [MWh]
Jan.	Deterministic	2.385	76.6
	Regular Stochastic	2.427	73.4
	Modified Stochastic	2.430	71.7
Apr.	Deterministic	1.864	130.3
	Regular Stochastic	1.756	116.9
	Modified Stochastic	1.763	116.7
Jul.	Deterministic	3.015	98.5
	Regular Stochastic	2.679	88.5
	Modified Stochastic	2.658	83.4
Oct.	Deterministic	2.261	122.1
	Regular Stochastic	1.982	83.2
	Modified Stochastic	1.981	81.0

Table 15 – Three stage stochastic modifier simulation results

The greatest benefit of the three-stage stochastic modifiers is the reduction in computation time. Figure 21 compares the solution time for all cases.

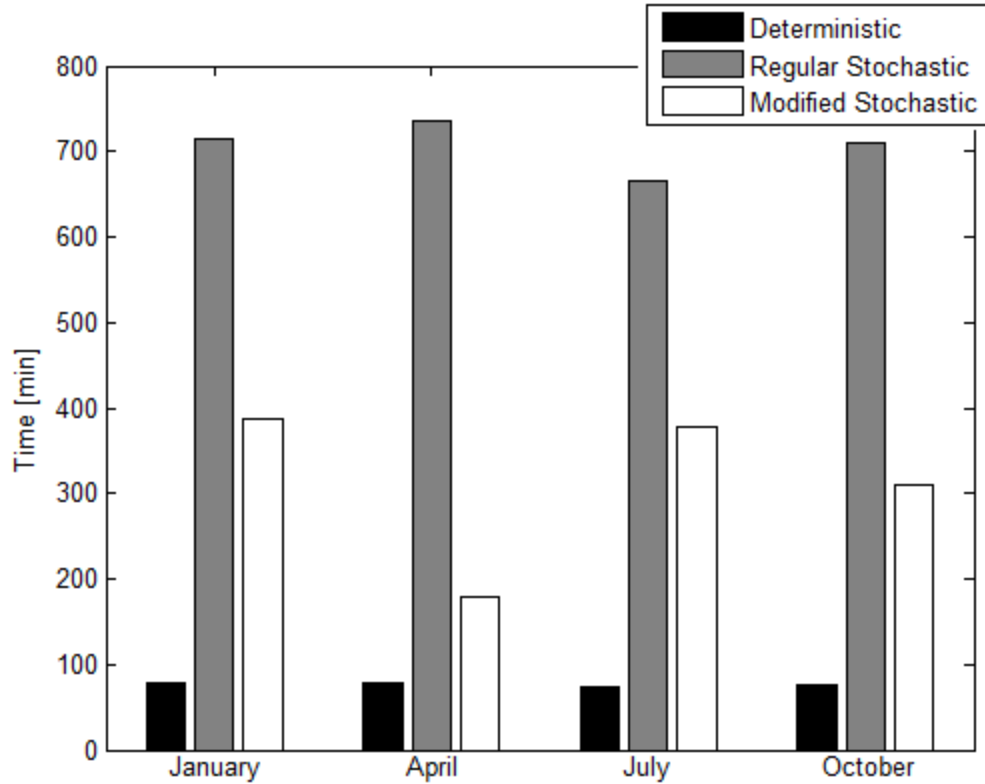


Figure 21 – Computation time (in minutes) across all cases

As expected, the stochastic model significantly increases the computation time compared to the case that uses a fully deterministic formulation. There is up to four times reduction in solution time. This is because there is a significant computational burden in attempting to solve multiple scenarios to a single optimal solution. However, using the three-stage stochastic modifiers is able to significantly reduce the computation time by simplifying the design of the scenarios. For example, it is computationally more efficient to reduce the number of scenarios being simulated during times of low wind and solar generation output. This could be achieved during stage 2 of the modification process. Figure 22 shows the distribution of ACE for the three cases simulated in April.

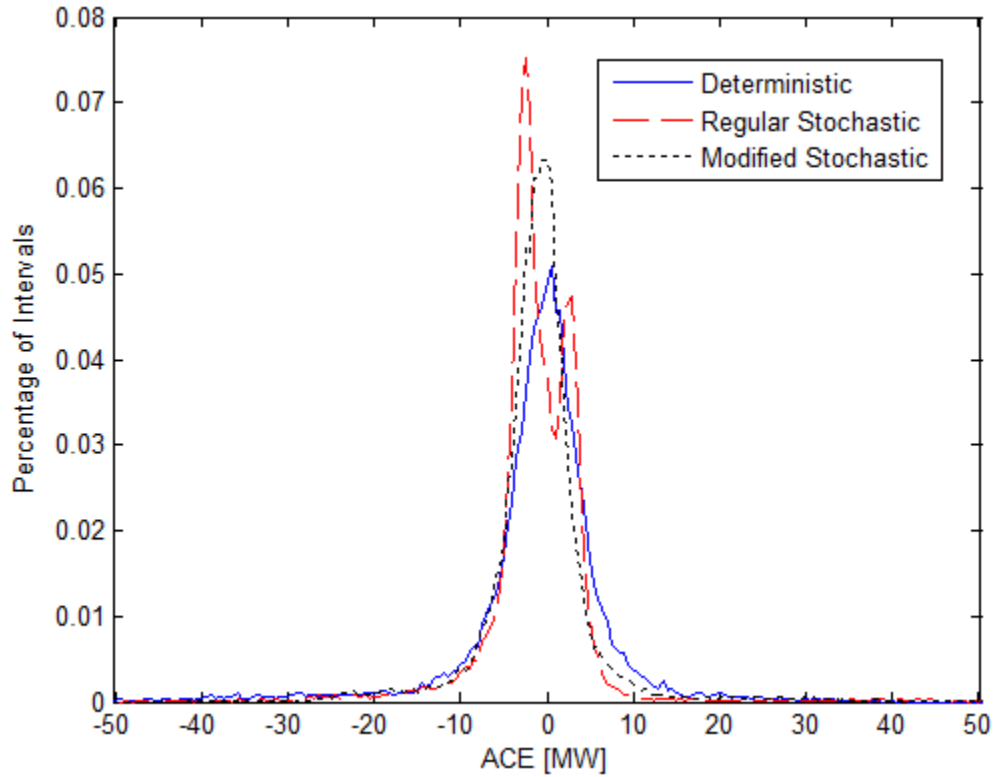


Figure 22 – Distribution of ACE in April

The characteristic stochastic model has a noticeable negative bias in the ACE distribution. This is because the stochastic model is susceptible to under-generation during times of peak load as discussed earlier. The three-stage modification process is able to mitigate this impact and help move the distribution closer around zero. Similar trends can be observed in the other simulations as well. During the rest of the simulation, the stochastic modifiers help better situate the system in terms of available thermal ramping capacity. Figure 23 shows the average unused ramping capacity across all cases.

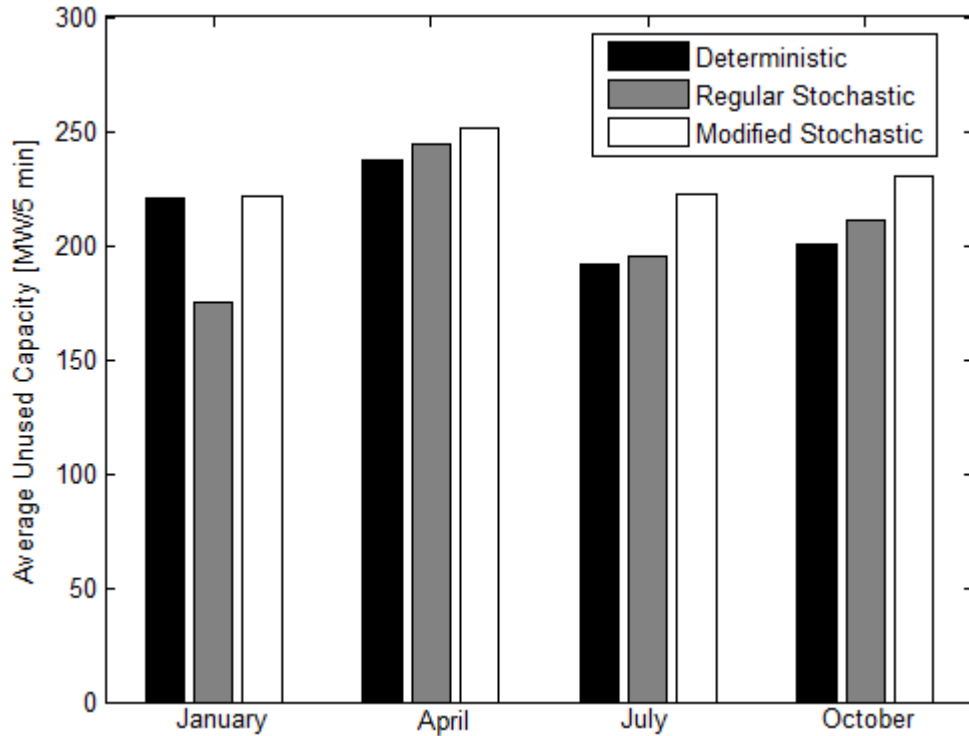


Figure 23 – Average unused thermal ramping capacity

This excess ramping capacity correlates with the number of generators online. In general, the stochastic models commit more thermal generation than the deterministic case. The three-stage modifiers can even help during peak times by providing a clearer picture of what is happening in the system at this time. This can be seen in Figure 24 which shows the number of thermal generators committed throughout the simulation in January. Notice that during the peak times, the three-stage modifiers commit more thermal generators than any of the other scenarios.

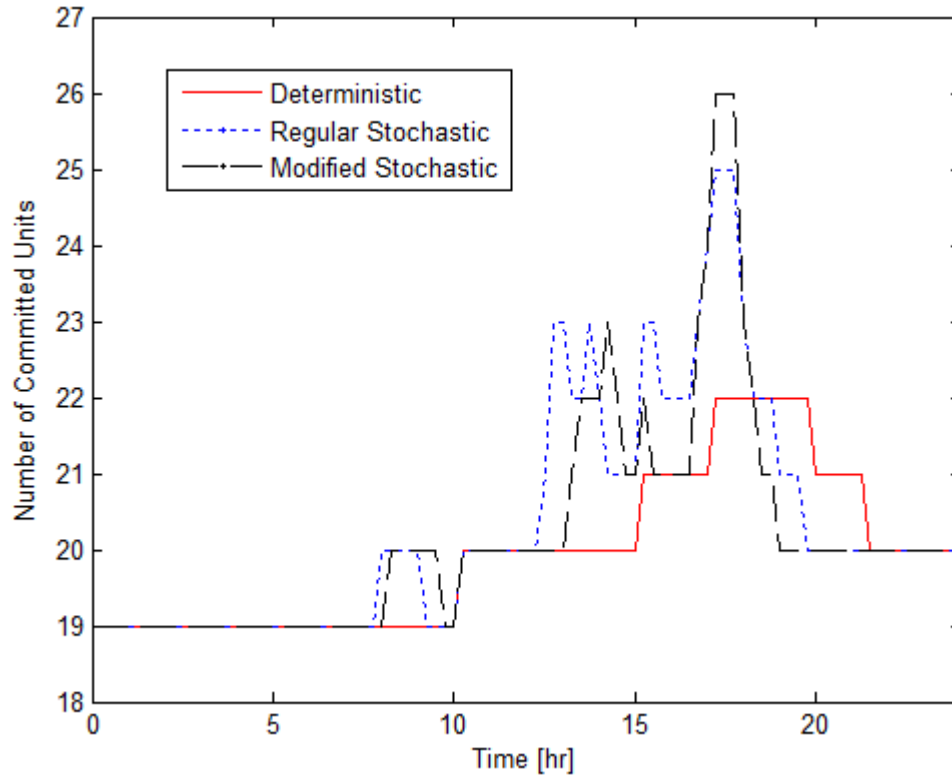


Figure 24 – Number of committed thermal generators in January

This extra flexibility helps facilitate the integration of renewable energy in the system.

Table III shows the amount of curtailed wind energy in the system for all cases. Using the three-stage stochastic modifiers is able to reduce the amount of curtailed wind energy in the system.

	Case	Curtailed Wind [GWh]
Jan	Regular Stochastic	4.81
	Modified Stochastic	4.59
Apr	Regular Stochastic	10.9
	Modified Stochastic	10.8
Jul	Regular Stochastic	7.56
	Modified Stochastic	7.32
Oct	Regular Stochastic	5.69
	Modified Stochastic	5.51

Table 16 – Summary of curtailed wind with stochastic modifiers

As renewable energy generators become larger players in power systems, operators will have to find new ways to accommodate them. The uncertainty in power systems is typically handled via operating reserves. New research is being performed in advanced modeling techniques that can perhaps supplant traditional operating schemes. One such technique is known as stochastic modeling. Stochastic modeling is quickly becoming a more and more viable solution to the problem of best integrating variable renewable energy generation. Due to computational limitations, it is beneficial to combine both approaches, namely including a stochastic operating reserve requirement in a stochastic modeling formulation. However, there are significant technical issues that must be addressed first. Perhaps the biggest concern is the long computation times for solutions. This report presented a three-stage stochastic modification process that can be used to reduce the computation time significantly while maintaining solution integrity.

Chapter 5: Future Roles of Emerging Technologies in Grid Operations

5.1 Utilizing PHEVs for Reserve Scheduling

The future of electric power systems will vary greatly from the power systems we know today. Emerging technologies, such as energy storage systems (ESS) and electric vehicles (EV), will become more common throughout the network. It will be important to handle these new components of the power system in the most efficient way possible so as to maximize the benefits they offer. This will entail finding ancillary applications for these technologies that can serve the system operator while also benefiting the technology owner. The additional loading these technologies will have on the distribution system will stagnate their adoption. By finding ways they can benefit the system, hopefully this stagnation can be turned into motivation. While pure EVs have high potential, there is still social hesitation that is hindering their widespread adoption. One of the major concerns of consumers is the limited driving range today's battery packs can provide. Thus plug-in hybrid electric vehicles (PHEV) are being seen at the transitional stepping stone to an electrified personal transportation future. These vehicles have both an internal combustion engine as well as an electric machine and battery pack. They also consist of a physical connection to the main grid. This opens the doors for many potential

power system applications for PHEVs. Typically daily commutes only exercise a small fraction of total battery capacities. Theoretically, this means that PHEV owners could be providing ancillary services to the power system for the rest of the day.

Since PHEV battery packs typically have high cost per kWh of energy, they should focus on providing high value, short term ancillary services. This will help maximize the economic compensation PHEV owners receive while mitigating potential impacts on battery life. It also makes sense for PHEV owners to participate in spinning contingency reserves since system operators typically pay providers of this ancillary service an availability payment, thus owners can be paid to be plugged in. This is especially attractive since there is no guarantee that the PHEV owner will be called on to actually deploy these reserves but will be compensated for their availability regardless. Consequently, this report will propose allowing PHEVs to participate in the scheduling of spinning contingency reserves and the potential benefits and implications this type of control will have on system operations and the PHEV owner.

While the amount of energy available in a single PHEV battery pack is not sufficient to provide meaningful assistance to the power system operator, it is not an unfounded assumption that load aggregators will begin to aggregate PHEVs in a similar fashion as they become more ubiquitous. By aggregating PHEVs in a single area, the available energy from their onboard battery packs can be harnessed and used by the system operator in a meaningful way. In smaller microgrids, it might not even be necessary to aggregate PHEVs, depending on the size of the system. In order to capture the operational implications of PHEVs providing spinning contingency reserves, the

energy available in the aggregated PHEV fleet needed to be modeled. The following equations based on [47] are used to model the PHEVs within the DASCUC.

$$I_{CH,t} \cdot P_{CH,min} \leq P_{CH,t} \leq I_{CH,t} \cdot P_{CH,max} \cdot N \quad (35)$$

$$I_{DCH,t} \cdot P_{DCH,min} \leq P_{DCH,t} \leq I_{DCH,t} \cdot P_{DCH,max} \cdot N \quad (36)$$

$$E_{NET,t} = E_{DCH,t} - \eta \cdot E_{CH,t-1} \quad (37)$$

$$P_{EV,t} = P_{DCH,t} - P_{CH,t-1} \quad (38)$$

$$E_t = E_{t-1} - E_{NET,t} \quad (39)$$

$$I_{CH,t} + I_{DCH,t} \leq 1 \quad (40)$$

$$E_{min} \cdot N \leq E_t \leq E_{max} \cdot N \quad (41)$$

$$E_{24} = E_{max} \cdot N \cdot SOC_{24} \quad (42)$$

$$P_{EV,t} + \sum_i R_{i,t} \geq R_{TOT,t} \quad (43)$$

In the above equations, I_{CH} and I_{DCH} are the status of charging and discharging variables respectively, P_{CH} and P_{DCH} are the charging and discharging powers respectively, E_{CH} and E_{DCH} are the charging and discharging energies respectively. E_{NET} is the net energy exchanged with the battery, η is the charging efficiency of the battery, N is the number of PHEVs being considered, P_{EV} is the amount of power available in the battery, and E is the amount of energy available in the battery. Equations (35) and (36) set the limits on the battery charging and discharging powers. Equation (37) describes the net exchange of energy with the batteries. Equation (38) describes the amount of power available in the battery during the current time interval based on the actions in the previous interval. Equation (39) describes how much energy is in the batteries at time t . Equation (40) ensures the battery is not charging and discharging at the same time. Equation (41) enforces the energy limits on the batteries. Equation (42) enforces a minimum state of charge at the end of the optimization horizon. Equation (43) incorporates the PHEVs into the reserve scheduling constraint.

The PHEV operational data used in the optimization model is shown in Table 17. The first three rows correspond to the quadratic coefficients of the cost function. The remaining rows characterize the operating behavior of the PHEV battery packs.

	Value per PHEV
A (\$/kW ²)	0.41
B (\$/kW)	8.21
C (\$/h)	0
Max Charge (kW)	7.29
Min Charge (W)	7.3
Max Discharge (kW)	6.2
Min Discharge (W)	6.2
Max Capacity (kWh)	27.4
Min Capacity (kWh)	5.48

Table 17 – PHEV operational data used in simulations

A small microgrid was simulated based on the IEEE 9-bus test system taken from MATPOWER [48]. Transmission and generator data used in this study are shown in Table 18 and Table 19.

From Bus	To Bus	X (pu)	Max (kW)
1	4	0.0576	250
4	5	0.092	250
5	6	0.17	150
3	6	0.0586	300
6	7	0.1008	150
7	8	0.072	250
8	2	0.0625	250
8	9	0.161	250
9	4	0.085	250

Table 18 – Nine bus system line data

	Unit 1	Unit 2	Unit 3
a (\$/h)	1000	700	450
b (\$/kWh)	16.19	16.6	19.7
c (\$/kW ² h)	0.00048	0.002	0.00398

P_{\min} (kw)	80	20	25
P_{\max} (Kw)	455	130	162
Ramp Up Rate (kW/h)	100	80	50
Ramp Down Rate (kW/h)	60	30	40
Minimum On Time (h)	8	5	6
Minimum Off Time (h)	8	5	6
Start Up Cost (\$)	4500	550	900

Table 19 – Nine bus system generator data

As discussed in [4] and mentioned in chapter 2, there is no industry-wide standard for determining the amount of reserves that need to be scheduled. NERC standard BAL-002 says that a balancing area (BA) needs to withhold enough capacity to withstand the single, largest contingency. According to WECC, an operator must schedule the maximum of the most severe single contingency or 5% of total hydro generation plus 7% of total thermal generation. The Union for Coordination of Transmission of Electricity in Europe requires enough reserve to cover the maximum instantaneous power deviation. To this end, three different spinning contingency reserve requirements are used in this analysis. Scenario 1 considers the largest, single contingency, in this case the outage of the largest generator. Scenario 2 requires enough reserve to meet the peak load demand. Scenario 3 requires enough reserve to cover 7% of total thermal generation. In order to extract the implications of PHEVs providing this spinning contingency reserve, each scenario is simulated both with and without the PHEVs to obtain this effect. Table 20 summarizes the total system-wide production cost for each scenario.

Scenario	Production Cost	Penalty Cost
----------	-----------------	--------------

50% Reserve with 20 PHEVs														Cost: \$130,332.38									
1	1	1	1	1	1	1	1	1	1	1	1	1	1	0	0	0	0	0	0	0	0	0	0
0	0	0	0	0	0	0	0	0	0	1	1	1	1	1	1	1	1	1	1	1	1	1	1
0	0	0	0	0	0	0	0	0	0	1	1	1	1	1	1	1	1	1	1	1	1	1	1

Table 21 – Generator commitment schedules impact by PHEV scheduling

The inclusion of PHEVs also has an interesting effect on the system LMPs. Figure 25 shows the system LMPs for 24 hours. Notice that there is no congestion occurring in the system since all buses share the same LMP. While the effect is small in this case, there are times where the PHEVs were able to reduce the LMPs.

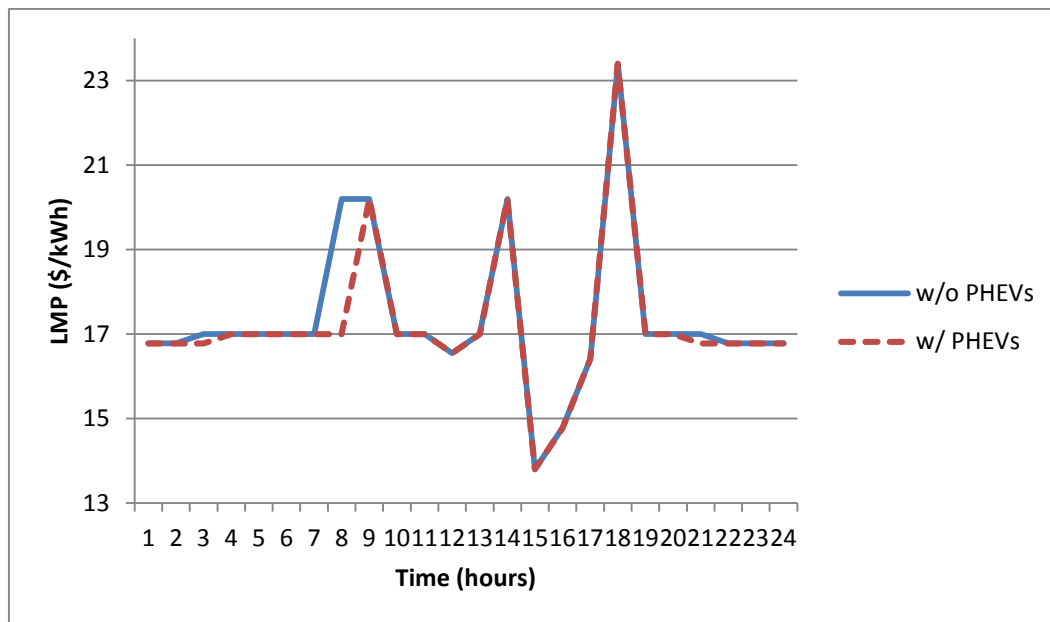


Figure 25 – System LMPs with and without PHEVs providing energy and ancillary services

Utilizing the batteries onboard PHEVs will undoubtedly impact the lifetime of the battery. This comes as a result of increasing the depth of discharge (DOD) of the battery pack. Rapidly charging and discharging the battery as well as increasing the depth of discharge negatively affect the battery’s expected lifetime. Figure 26 shows the

relationship between the number of PHEVs participating and the depth of discharge of the collective battery pack.

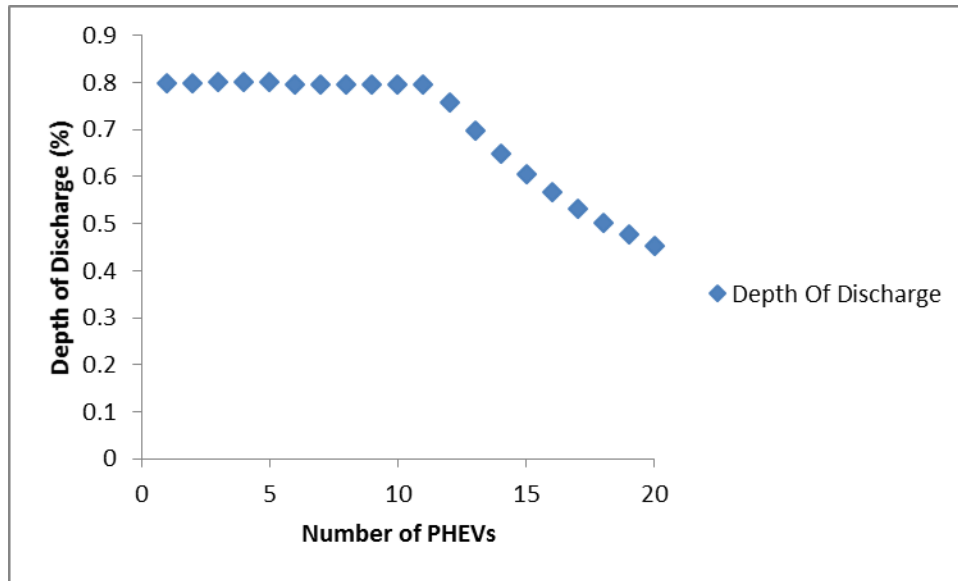


Figure 26 – Relationship between the number of PHEVs and depth of discharge

Figure 26 shows that the benefits that PHEVs can provide severely affect the DOD of the aggregated battery capacity. Until a certain number of PHEVs are connected, the microgrid will almost completely utilize all available energy in each battery pack. The break point in this graph can be referred to as the critical number of PHEVs, in this case, 11 PHEVs. This is the minimum number of PHEVs required such that each individual PHEV's schedulable energy is not completely exhausted. The further the number of PHEV's increasing beyond this point, the more the effect of scheduling on the DOD is mitigated.

PHEVs will be players in future energy markets and how they are controlled will directly impact the amount of benefit they can afford operators. While individually they might not impact system operations significantly, aggregating them will provide

operators considerable flexibility. PHEVs can help reduce the system total production costs by displacing expensive thermal generation and potentially avoiding penalty costs resulting from insufficient scheduling capacity. They can also help compress system LMPs. There is a critical number of PHEVs that are necessary to begin to mitigate the DOD issues of making the energy in PHEVs available to system operators.

It should be noted that the analysis in this report does not include the cost incurred by market operators to properly incentivize PHEV owner to participate in ancillary services and assumes that owners will be willing to support grid operations. The issue of reporting revenues is quite sensitive and heavily reliant on the accuracy of cost information provided. Since real-world cost, revenue, and incentive data was unavailable during the writing of this report, these costs were ignored. However, before this type of control strategy can be implemented by system operators, they need to be addressed.

5.2 Optimizing BESS for Ancillary Services in Microgrids

Improvements in BESS technologies and reductions in costs will make them significant players in the future power system. These technologies provide superior performance from an operational point of view because they are controlled and interfaced via power electronics. This means that they provide system operators with fast, accurate generation that can be available almost instantaneously. Their ability to charge and discharge, thus behaving as both generation and load, also provides the operator with valuable flexibility. This is especially valuable during times where the system operator is tasked with balancing highly variable wind and solar generation. Their size and

portability make them ideal components for use in a microgrid that typically lacks the generation resources larger power systems have at their disposal for balancing electrical supply and demand. Thus it is important to design a control algorithm that will maximize the benefits these resources offer. In order to accomplish this task, a BESS model is added to the previously discussed unit commitment and economic dispatch formulations. While the BESS shares many similar constraints with traditional thermal generation, e.g. maximum/minimum capacity limits, charge/discharge ramp rates, minimum charge/discharge times, etc., there are some operational differences that need to be accounted for. The following equations detail the unique constraints of the BESS.

$$\sigma_{i,t} = \sigma_{i,t-1} - [P_{i,t} \cdot \eta_{dis,i} + PS_{i,t} \cdot \eta_{chg,i}] \quad (44)$$

In (44), σ represents the storage level, i represents the index of the BESS unit, t represent the current time index, $P_{i,t}$ is the current generation schedule of unit i at time t , $PS_{i,t}$ is the current charging schedule of unit i at time t , and $\eta_{dis,i}$ and $\eta_{chg,i}$ are the discharging and charging efficiency of the BESS unit respectively. This equation is used to model the current level of the BESS based on the previous level and current action of the BESS unit. Note that either $P_{i,t}$ or $PS_{i,t}$ or both must be zero because the battery cannot charge and discharge simultaneously.

The following constraint is used to ensure that the storage level does not exceed its maximum capacity at the end of each optimization.

$$\sigma_{i,t} \leq \sigma_{max,i} + \sigma_{wasted} \quad (45)$$

In (45), $\sigma_{i,t}$ is the storage level of unit i at time t , $\sigma_{max,i}$ is the maximum storage

level of unit i , and σ_{wasted} is any wasted storage capacity (i.e. energy that is trying to be stored beyond the capacity limit that is ultimately wasted).

The following constraint is used to model the startup trajectory of the battery when starting to store energy modeled after [49].

$$PS_{i,t} - \sum_{\substack{\Gamma= \\ \text{Up Reserves}}} R_{i,t,\Gamma} \geq \alpha + \beta - \gamma \quad (46)$$

where

$$\alpha = PS_{min,i} \cdot \left(IP_{i,t} - \sum_{H=t}^{t+PDP-1} zp_{i,H} - \sum_{H=t-PUP+1}^t yp_{i,H} \right) \quad (47)$$

$$\beta = PS_{min,i} \left(\sum_{H=t-PUP+1}^t (H-t+1)yp_{i,t} \right) \min \left(1, \frac{1}{tp_{start}} \right) \quad (48)$$

$$\gamma = P_{max,i} \cdot I_{i,t} \quad (49)$$

In the previous equations, $PS_{i,t}$ is the charging schedule of unit i at time t , PUP is the number of intervals a unit has been storing energy during startup, PDP is the number of intervals a unit has been storing energy during shutdown, $R_{i,t}$ is the reserve schedule of unit i at time t , yp is the charging startup indicator, tp_{start} is the time it takes for a unit to reach charging status, $P_{max,i}$ is the maximum discharge level of the unit, and $I_{i,t}$ is the generation commitment variable. Equation (47) is required to ensure that a unit is storing above the minimum required storage level if a unit is neither starting up nor shutting down. Equation (48) is used to set the trajectory limit of a unit during startup. The trajectory is assumed to be a linear trajectory over the amount of time it takes a unit to

reach its minimum storage level. Equation (49) is required to relax the constraint if the unit is generating rather than storing energy.

The microgrid system simulated is a modified version of the IEEE single area reliability test system intended to reflect a microgrid that might serve large industrial/commercial customers or even small towns. The modifications were motivated by the Perfect Power microgrid at the Illinois Institute of Technology [50]. Distributed wind and solar generation in addition to the BESS are spread throughout the microgrid. The underlying data used in this analysis is from available data from NREL for northern California [41]. A one-line diagram of the new system is shown in Figure 27.

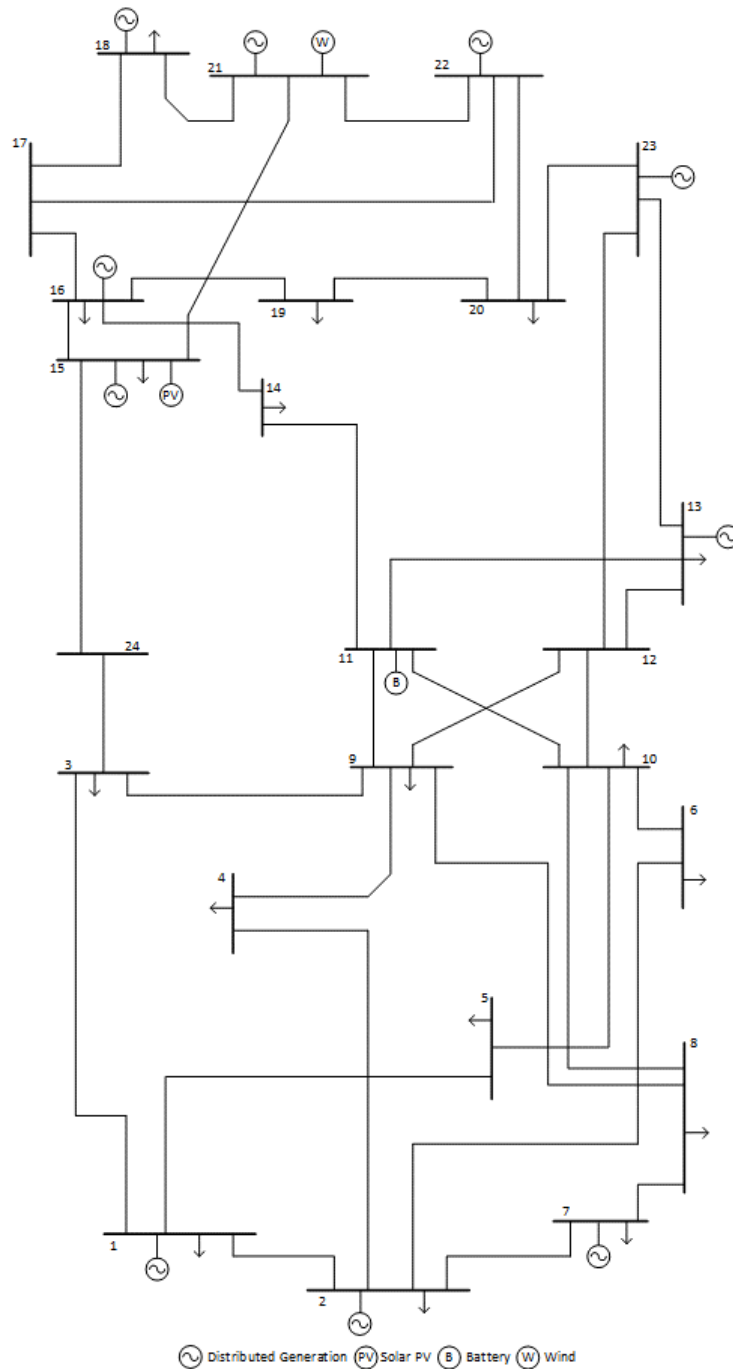


Figure 27 – Modified IEEE single-area reliability test system for microgrid applications

The location of the wind and solar generators are selected to maximize access to transmission. The system is simulated for four weeks (the third week in January, April, July, and October) in order to capture the seasonal behavior of wind and solar. Three

cases are simulated to capture the benefits of the BESS. Case 1 does not include any BESS. Case 2 includes BESS participating in both energy and ancillary service provisions. Case 3 only allows the BESS to provide ancillary services. Numerical results from this analysis is shown in Table 22.

		Case 1	Case 2	Case 3
Jan	Cost [\$M]	1.638	1.610	1.608
	AACEE [kWh]	597	632	479
	Sigma ACE [kW]	5.01	5.46	4.11
	MAACE [kW]	3.55	3.76	2.85
	VG Curtailment [kW]	314	169	243
Apr	Cost [\$M]	1.336	1.303	1.289
	AACEE [kWh]	711	772	588
	Sigma ACE [kW]	6.35	6.72	5.37
	MAACE [kW]	4.24	4.59	3.50
	VG Curtailment [kW]	875	300	395
Jul	Cost [\$M]	1.987	1.961	1.934
	AACEE [kWh]	422	488	368
	Sigma ACE [kW]	3.60	4.31	3.04
	MAACE [kW]	2.52	2.90	2.19
	VG Curtailment [kW]	435	73	221
Oct	Cost [\$M]	1.451	1.485	1.468
	AACEE [kWh]	713	711	502
	Sigma ACE [kW]	6.13	6.35	4.31
	MAACE [kW]	4.24	4.23	2.99
	VG Curtailment [kW]	225	666	613

Table 22 – Numerical results from BESS analysis

As expected, the inclusion of the BESS reduces the system production cost due to the displacement of thermal generation. What was not expected, was the BESS increased the ACE metrics. This was due to reducing the number of online generators and thus loading the remaining online generators even more. The reduced headroom resulted in less flexibility for the microgrid because it did not have sufficient thermal flexibility to make up for this loss. However, Case 3 shows that by controlling the BESS in such a way that they focus strictly on providing regulation services, it can actually improve reliability

metrics significantly. The AACEE, standard deviation of the ACE, and the mean-absolute ACE (MAACE) all improve by allowing the BESS to focus on providing regulation only.

Figure 28 shows the distribution of ACE across all three cases considered.

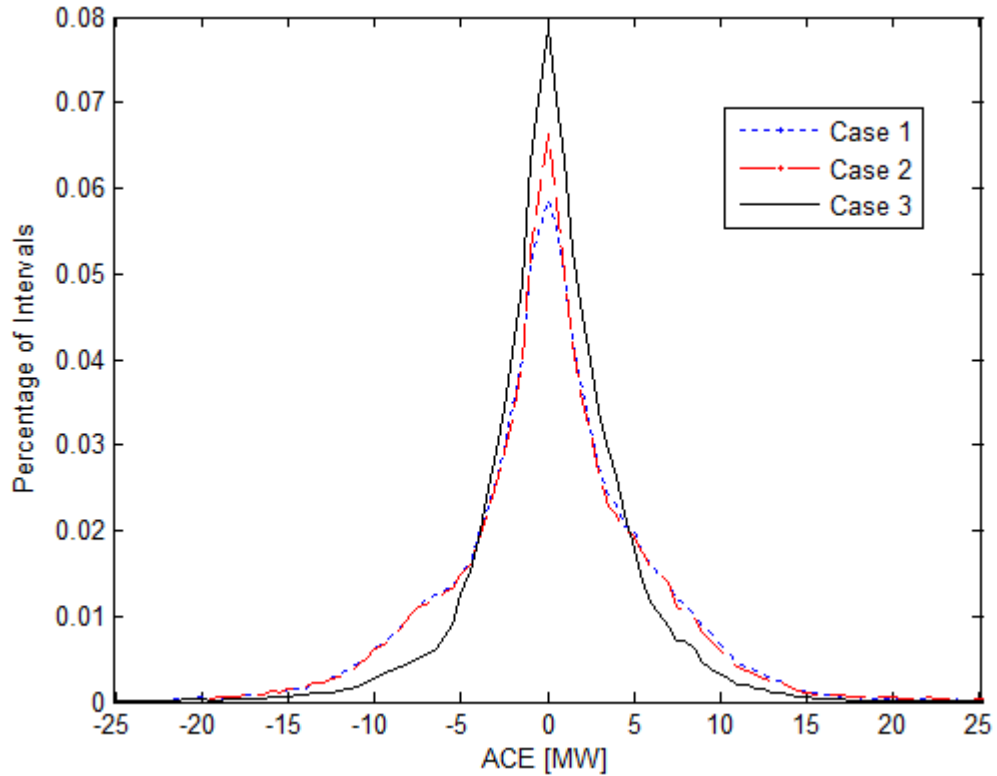


Figure 28 – Distribution of ACE in October for all microgrid operating scenarios

Notice that the distributions get tighter around zero by adding the BESS and even tighter by allowing the BESS to focus on regulation reserves. Allowing the BESS to focus on regulation reserves provides another operational benefit. Figure 29 shows the state of charge (SOC) of the battery for cases 2 and 3.

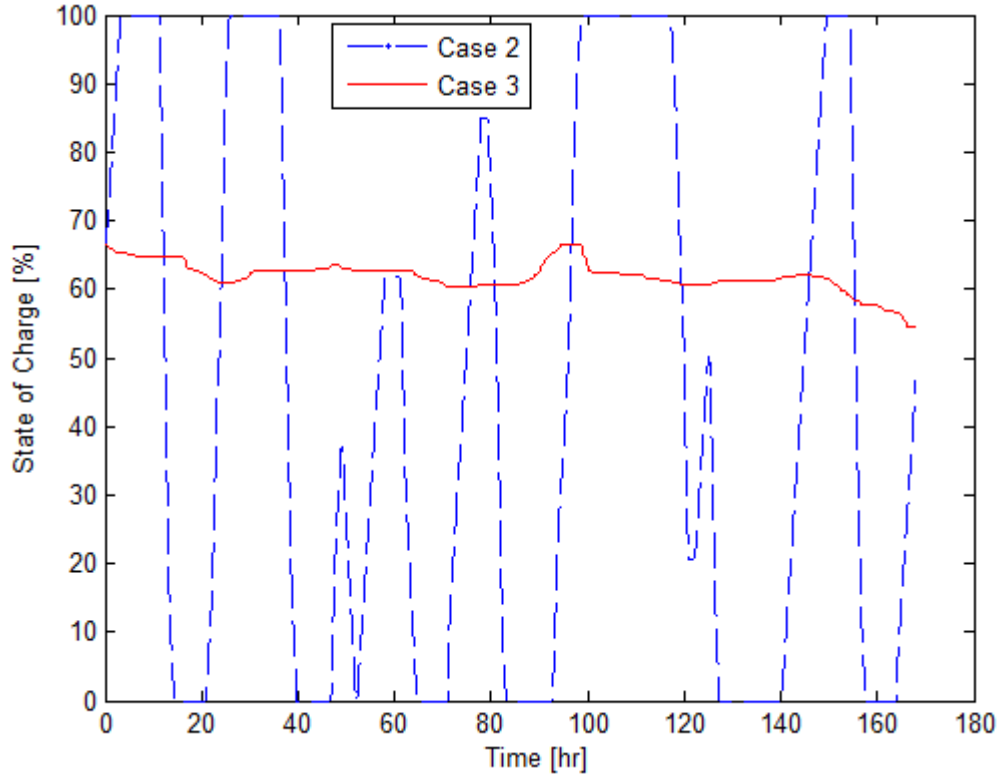


Figure 29 – SOC of the battery providing energy and regulation and regulation only

For these simulations, it was assumed that the battery starts with a 66% SOC. Notice that if the BESS is providing both energy and reserves, the microgrid controller will try to maximize the output from the battery and completely cycle the energy within it. By allowing the battery to focus on providing regulation only, the BESS energy profile is flat, thus protecting the BESS from behavior that will shorten its operational lifetime.

The impact of energy storage systems providing contingency spin/nonspin contingency reserves is also examined. In order to perform this analysis, several contingency events were simulated both with and without the energy storage system to extract the impact of energy storage systems on contingency response. In order to capture the benefit of energy storage systems providing contingency response, several different contingency events were simulated, at different times during the day, and throughout

different weeks of the year. The first contingency considered is the loss of a large thermal generator at 8 a.m. in October. This was chosen to capture the impact of losing a large thermal generator under medium loading conditions in the morning as the load profile is typically ramping up. The second contingency considered is the loss of solar generation at 11 a.m. in January. This was chosen to capture the effect of losing solar generation at around its peak output during high penetration levels, around 12% instantaneous penetration during this time period. The third contingency considered is the loss of a medium thermal generation unit at 1 p.m. in July. This was chosen to capture the impact of losing a potential peaking generation unit as peak load approaches. The fourth contingency considered is the loss of wind generation at 7 p.m in April. This was chosen to investigate the loss of highly variable, zero cost generation during local peaks in the load profile. A summary of these results is shown in Table 23.

		Without ESS	With ESS
Scenario 1	Cost [\$k]	224	228
	AACEE [kWh]	198	177
	Sigma ACE [kW]	28.6	25.6
	MAACE [kW]	8.3	7.4
	Lost Load [kWh]	63	35
Scenario 2	Cost [\$k]	218	221
	AACEE [kWh]	82	66
	Sigma ACE [kW]	10.3	5.7
	MAACE [kW]	3.4	2.7
	Lost Load [kWh]	13	0
Scenario 3	Cost [\$k]	216	224
	AACEE [kWh]	64	50
	Sigma ACE [kW]	6.6	8.9
	MAACE [kW]	2.7	2.1
	Lost Load [kWh]	0.15	0
Scenario 4	Cost [\$k]	172	245
	AACEE [kWh]	128	93
	Sigma ACE [kW]	12.3	12.1
	MAACE [kW]	5.3	3.9
	Lost Load [kWh]	20	5

Table 23 – Numerical results from contingency scenarios

The cost of operating this system remains relatively unchanged, increasing only slightly. There is a significant increase in scenario 4 because the BESS caused an additional thermal generator to be committed to support it during charging mode and thus resulted in increased production costs. The AACEE and MAACE are improved by including the BESS because it can quickly respond to generator outages and provide emergency energy very quickly. The standard deviation for scenario 3 actually increases when the BESS is included. This is because the loss of the small peaking generator that was used for regulation reduces the regulation response of the system. Since the BESS is mostly providing energy to replace the outage, the regulation burden goes unserved and the variability of the ACE increases. Another important result is the significant reduction

in lost load due to generator outages. Since the BESS can respond almost instantaneously, the amount of demand that is unserved can be minimized. This immediate response had an additional benefit in that it can quickly help arrest frequency deviations in the microgrid. For a microgrid operating in islanding mode, the frequency can be approximated by equation 32.

$$f = f_n + \frac{ACE}{-10B} \quad (50)$$

In (50), f_n is the nominal frequency, 60 Hertz in this case, ACE is the area control error, and B is the frequency bias of the system. Figure 30 shows the system imbalance during the four contingency scenarios.

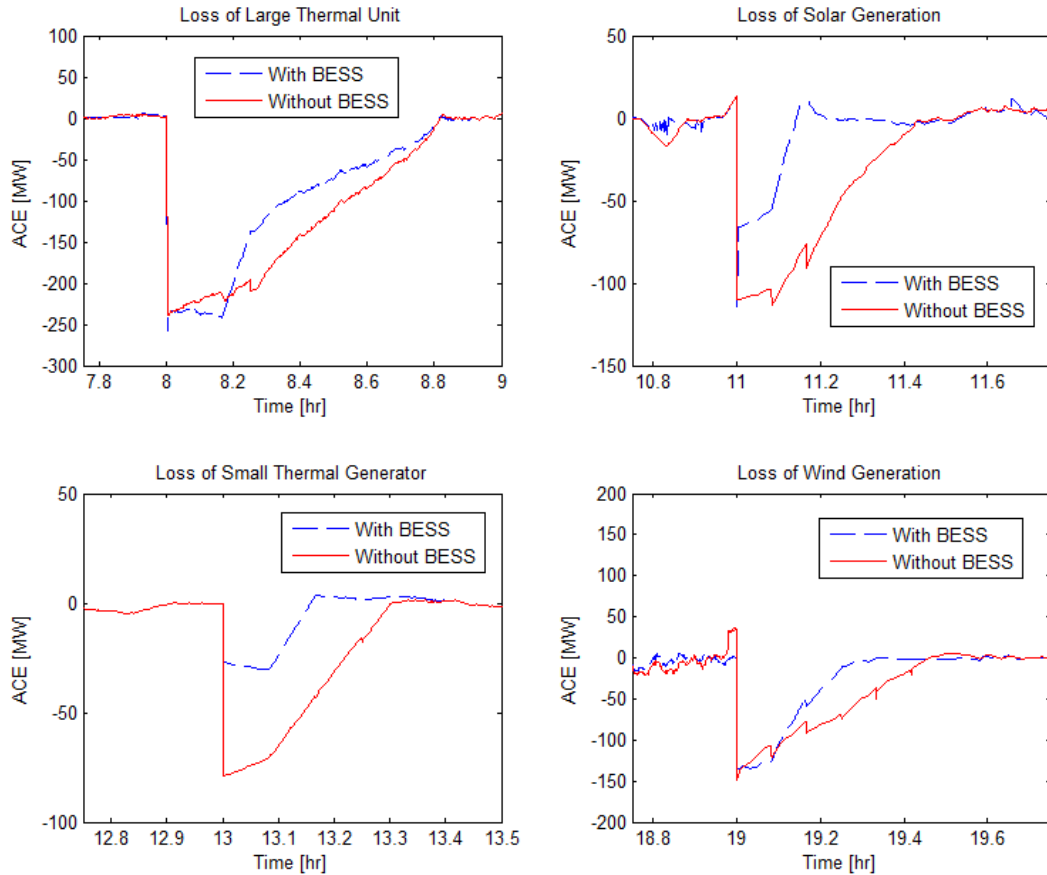


Figure 30 – Amount of load lost to multiple contingencies with and without the BESS

There is some overshoot immediately after the outage event while the BESS is transitioning into providing more energy, but overall, the load lost is brought back to near zero quicker than the scenarios without the BESS. This is expected since the BESS has much faster charge and discharge rates than similarly sized thermal generators. This allows the BESS to quickly respond to contingency events and quickly resume service to electrical loads.

Battery energy storage systems provide many benefits, especially for smaller microgrids. These BESS can help improve microgrid reliability during islanded operation. They can help with real-time balancing of electrical supply and demand. They can also provide valuable response to generator outages to help replace lost energy and arrest frequency deviation. In order to maximize benefits of BESS, it is important to allow them to provide ancillary services. Allowing the battery energy storage system to focus on strictly providing ancillary services can still provide reliability improvements while minimizing the impact on the battery operational lifetime. This is possible by mitigating the amount of energy charged and discharged over short periods of time.

Chapter 6: Conclusion

6.1 Final Remarks

The landscape of power systems is evolving. The traditional makeup of power systems is evolving. Renewable generation resources are becoming a more viable option to system operators and are consequently being installed all over the world. Emerging technologies, such as batteries and electric cars, are becoming more cost effective and desirable by consumers. Microgrids are being considered as potential solutions for customers that need increased reliability or would like to arbitrage energy as distributed energy technologies become more cost effective. As these scenarios become more prevalent, traditional operating techniques need to be revisited to account for their contributions to the net load.

This report proposed several potential operating changes that can help mitigate the impact of these technologies and maximize the benefit they afford operators. Flexibility reserves are designed to account for the additional uncertainty introduced by increased VG resource penetrations. This report proposed a three-stage, reliability-based reserve modification process to improve these flexibility reserves by explicitly taking into account the actual variability introduced by VG resources. This three-stage process was

shown to minimally impact the total system production cost while improving reliability and real time electricity market outcomes.

One of the potential mechanisms to be used in the future to address the uncertainty of wind and solar generation is the use of stochastic programming to model the scheduling problem in power systems. Due to computational and hardware limitations, stochastic models typically run a reduced set of “most-likely” scenarios in order to obtain an optimal solution in a practical amount of time. Reducing the number of scenarios increases the amount of uncertainty unaddressed in the system. This paper explored using an explicit operating reserve requirement in a stochastic formulation to help address this issue. In addition to this analysis, this report also presented a three-stage stochastic modification process that can be used to help reduce the solution time while minimally impacting the solution. Results show that the three-stage stochastic modification process can reduce system production costs while maintaining, and even slightly improving, reliability metrics.

Plugin Hybrid Electric Vehicles are being seen as the stepping stone to a completely electrified transportation sector and have recently gained popularity. This report proposed a control scheme to utilize the aggregated energy capacity of these vehicles in order to help provide contingency spinning reserves. It was shown that this control scheme helps reduce the system operating costs, especially if it helps avoid expensive alternatives for procuring the required spinning capacity, such as importing the required capacity.

As battery technology improves and manufacturing costs come down, batteries are being utilized more in power system applications, namely microgrid applications. This report proposed a control technique for a microgrid to utilize batteries for providing regulation and contingency spinning reserves. This type of control scheme helps reduce the total system production cost while minimizing the imbalance observed in the microgrid. It also helps minimize the impact on the battery's operational lifetime by minimizing the depth of discharge. It also provides superior contingency support and is able to arrest frequency deviation and quickly restore it to nominal.

While the research presented in this report provides insight and potential solutions for power system operators, there is still opportunity for improvement. Wind and solar generation profiles are inherently stochastic. Meteorologists are still improving the ways wind speed and solar irradiation are forecasted. In order to fully investigate the implications of flexibility reserves and to improve upon the flexibility reserve requirement methodology, the interaction between flexibility reserves and other reserve products should be extensively studied. There is potential of double counting megawatts between reserve products and the total reserve requirement should be optimized across all products.

The uncertainty of wind and solar generation naturally lends itself to stochastic modeling. However, there are still major hurdles that need to be addressed before stochastic modeling can become a realistic solution. The first hurdle, and perhaps the largest, is the long solution times necessary before reaching the optimal solution of a stochastic model. There are many factors that impact this, particularly the structure of the

scenarios and solution search method. There is also the concern of having to find a reduced number of scenarios that can adequately capture the amount of uncertainty in the system all while considering the solution time. A too steep reduction in scenarios opens the system to additional uncertainty at the cost of solution time. Considering too many scenarios will unnecessarily increase the solution time, perhaps to infeasible times. To this end, there should be a more efficient way to combine stochastic modeling and reserve requirements. This paper presents a three-stage stochastic modification framework that can help solve this problem, but more extensive testing should be done on more realistic data sets to confirm performance.

One of the main benefits of microgrids is their inherent customization for their specific applications. As such, there may be no overall best way to design and operate a microgrid. There is incentive to propose overall best-practice guidelines. Microgrids must be able to satisfy their own electrical demands while operating in islanding mode. This often implies some form of redundancy in the design of the microgrid to ensure reliability. One way to achieve this reliability is through the scheduling of operating reserves to satisfy these requirements. Consequently, there may be opportunity with emerging technologies, such as distributed VG resources and battery systems, to improve the way operators handle this requirement of maintaining reliability. It may be possible to emulate the scheduling of these operating reserves by intelligently controlling these technologies and foregoing the explicit scheduling of the operating reserves.

There will undoubtedly be many issues facing power system operators in the future. Addressing some of the issues discussed in this report will help shed light on a

few of these concerns, and will hopefully prepare power system engineers to handle what will certainly be a dynamic, intelligent power system in the future.

6.2 List of Publications

1. **I. Krad**, and W. Gao, "Impact of PHEV on reserve scheduling: A MILP-SCUC method," North American Power Symposium (NAPS) 2013, pp.1-6, 22-24 Sept. 2013.
2. E. Ibanez, **I. Krad**, and E. Ela, "A systematic comparison of operating reserve methodologies," IEEE PES General Meeting Conference & Exposition 2014, pp.1-5, 27-31 July 2014.
3. **I. Krad**, E. Ibanez, and E. Ela, "Quantifying the Potential Impacts of Flexibility Reserve on Power System Operations," IEEE Seventh Annual Green Technologies Conference (GreenTech), pp.66-73, 15-17 April 2015.
4. **I. Krad**, E. Ibanez, E. Ela, and W. Gao, "Operational Impacts of Operating Reserve Demand Curves on Production Cost and Reliability," 14th Annual Wind Integration Workshop. Brussels, Belgium. Oct 2015.
5. **I. Krad**, E. Ibanez, and W. Gao, "A Comprehensive Comparison of Current Operating Reserve Methodologies." IEEE Transmission and Distribution Conference and Exposition. Dallas, TX. May 2016.
6. **I. Krad** and W. Gao, "Utilizing Energy Storage Systems to Provide Operating Reserves in a Microgrid." Renewable Energy Journal. [Under Review].
7. **I. Krad**, E. Ibanez, E. Ela, and W. Gao, "Three Stage Reserve Modification for High Renewable Energy Penetration Scenarios." El Sevier Electric Power Systems Research Journal. [Under Review].

8. **I. Krad** and W. Gao, “Three-Stage Stochastic Modeling Modifiers for Improved Performance Under High Renewable Penetration Scenarios.” North American Power Symposium 2016, Denver, CO.
9. **I. Krad**, W. Gao, and H. Wu, “An Assessment of Flexibility Reserves in Stochastic Modeling at Multiple Timescales.” IEEE Transactions on Sustainable Energy. [Under Review].
10. **I. Krad**, W. Gao, E. Ela, E. Ibanez, and H. Wu, “Analysis of Operating Reserve Demand Curves in Power System Operation in the Presence of Variable Generation.” IET Renewable Power Generation Journal. 2016. [Under Review].

References

- [1] Sharkawi, Mohamed A. *Electric Energy: An Introduction*. 2nd ed. Boca Raton, Fla.: CRC, 2005. Print.
- [2] "Renewable Portfolio Standard Policies." Database of State Incentives for Renewables and Efficiency. September 2014. < <http://ncsolarcenterprod.s3.amazonaws.com/wp-content/uploads/2015/11/Renewable-Portfolio-Standards.pdf> >.
- [3] Saadat, Hadi. *Power System Analysis*. 3rd ed. Boston: WCB/McGraw-Hill, 1999. Print.
- [4] E. Ela, M. Milligan, and B. Kirby, "Operating reserves and variable generation: A comprehensive review of current strategies, studies, and fundamental research on the impact that increased penetration of variable renewable generation has on power system operating reserves," NREL, Golden, CO, Tech. Rep., NREL/TP-5500-51978, 2011.
- [5] I. Krad, E. Ibanez, and E. Ela, "Quantifying the Potential Impacts of Flexibility Reserve on Power System Operations," in 2015 Seventh Annual IEEE Green Technologies Conference (GreenTech), pp.66-73, 15-17 April 2015.
- [6] D. Lew, G. Brinkman, E. Ibanez, A. Florita, M. Heaney, B.-M. Hodge, M. Hummon, G. Stark, J. King, S.A. Lefton, N. Kumar, D. Agan, G. Jordan, and S. Venkataraman, "Western Wind and Solar Integration Study Phase 2," NREL, Golden, CO, NREL/TP-5500-55588, 2013.

- [7] E. Ibanez, G. Brinkman, M. Hummon, and D. Lew, "Solar Reserve Methodology for Renewable Energy Integration Studies Based on Sub-Hourly Variability Analysis." Presented at 2nd Annual International Workshop on Integration of Solar Power into Power Systems Conference. Lisbon, Portugal: 12-13 November 2012. <<http://www.osti.gov/scitech/servlets/purl/1051953>>.
- [8] R. Doherty and M. O'Malley, "A new approach to quantify reserve demand in systems with significant installed wind capacity," *Power Systems, IEEE Transactions on* , vol.20, no.2, pp.587,595, May 2005.
- M.A. Matos and R.J. Bessa, "Setting the Operating Reserve Using Probabilistic Wind Power Forecasts," *Power Systems, IEEE Transactions on* , vol.26, no.2, pp.594,603, May 2011.
- [9] M.A. Matos and R.J. Bessa, "Setting the Operating Reserve Using Probabilistic Wind Power Forecasts," *Power Systems, IEEE Transactions on* , vol.26, no.2, pp.594,603, May 2011.
- [10] J. Wang, X. Wang, and Y. Wu, "Operating reserve model in the power market," *Power Systems, IEEE Transactions on* , vol.20, no.1, pp.223,229, Feb. 2005.
- [11] GE Energy (2010). Western Wind and Solar Integration Study. NREL/SR-550-47434. Golden, CO: NREL. Accessed January 2015. <<http://www.nrel.gov/docs/fy10osti/47434.pdf>>.

- [12] “Matrix of Assumptions – 2011 TEPPC Study Program.” Western Electricity Coordinating Council: Transmission Expansion Planning Policy Committee. 2011.
- [13] M.A. Ortega-Vazquez and D.S. Kirschen, "Estimating the Spinning Reserve Requirements in Systems With Significant Wind Power Generation Penetration," Power Systems, IEEE Transactions on , vol.24, no.1, pp.114,124, Feb. 2009.
- [14] “ERCOT Methodologies for Determining Ancillary Service Requirements.” April 01, 2013.
<http://www.ercot.com/content/meetings/ros/keydocs/2013/1114/05._ERCOT_Methodologies_for_Determining_Ancillary_Service_Re.doc>.
- [15] L. Xu and D. Tretheway, “Flexible Ramping Products: Incorporating FMM and EIM.” Draft Final Proposal. California Independent System Operator. December 4, 2014.
<http://www.caiso.com/Documents/DraftFinalProposal_FlexibleRampingProduct_includingFMM-EIM.pdf>.

- [16] N. Navid and G. Rosenwald. "Ramp Capability Product Design for MISO Markets." Market Development and Analysis. Midcontinent Independent System Operator. July 10, 2013. <<https://www.misoenergy.org/Library/Repository/Communication%20Material/Key%20Presentations%20and%20Whitepapers/Ramp%20Product%20Conceptual%20Design%20Whitepaper.pdf>>.
- [17] K.H. Abdul-Rahman, H. Alarian, M. Rothleder, P. Ristanovic, B. Vesovic, and L. Bo Lu, "Enhanced system reliability using flexible ramp constraint in CAISO market," in *IEEE 2012 PES GM Proc.*, vol., no., July 22–26, 2012, pp. 1, 6.
- [18] N. Navid and G. Rosenwald, "Market solutions for managing ramp flexibility with high penetration of renewable resource," *IEEE Trans. Sustainable Energy*, vol. 3, no. 4, pp. 784, 790, Oct. 2012.
- [19] L. Wu, M. Shahidehpour, and T. Li, "Stochastic Security-Constrained Unit Commitment," *Power Systems, IEEE Transactions on*, vol.22, no.2, pp.800,811, May 2007.
- [20] Q.P. Zheng, J. Wang, P.M. Pardalos, and Y. Guan, "A decomposition approach to the two-stage stochastic unit commitment problem," *Ann. Oper. Res.*, vol. 61, no.3, pp. 387-410, 2013.
- [21] Y. Huang, Q. P. Zheng, and J. Wang, "Two-stage stochastic unit commitment model including non-generation resources with conditional value-at-risk constraints," *Electr. Power Syst.*, vol. 116, pp. 427-438, Nov. 2014.

- [22] Q. Wang, J. Wang, and Y. Guan, "Stochastic Unit Commitment With Uncertain Demand Response," *Power Systems, IEEE Transactions on*, vol.28, no.1, pp.562,563, Feb. 2013.
- [23] C. Zhao and Y. Guan, "Unified Stochastic and Robust Unit Commitment," *Power Systems, IEEE Transactions on*, vol.28, no.3, pp.3353-3361, Aug. 2013.
- [24] Q.P. Zheng, J. Wang, and A.L. Liu, "Stochastic Optimization for Unit Commitment—A Review," Accepted into *IEEE Transactions on Power Systems*.
- [25] Watson J-P, Woodruff D (2011) Progressive hedging innovations for a class of stochastic mixed-integer resource allocation problems. *Comput. Management Sci.* 8(4):355–370.
- [26] Ryan, S.M.; Wets, R.J.-B.; Woodruff, D.L.; Silva-Monroy, C.; Watson, J.-P., "Toward scalable, parallel progressive hedging for stochastic unit commitment," *Power and Energy Society General Meeting (PES), 2013 IEEE*, vol., no., pp.1,5, 21-25 July 2013.
- [27] B. Wang and B.F. Hobbs, "A flexible ramping product: Can it help real-time dispatch markets approach the stochastic dispatch ideal?" *Electric Power Systems Research*, vol. 109, pp. 128–140, April 2014.
- [28] C. Lowery and M.O. Malley, "Reserves in Stochastic Unit Commitment: An Irish System Case Study," *IEEE Transactions on Sustainable Energy*, in Press.

- [29] Papavasiliou, S.S. Oren, and R.P. O'Neill, "Reserve Requirements for Wind Power Integration: A Scenario-Based Stochastic Programming Framework," *Power Systems, IEEE Transactions on* , vol.26, no.4, pp.2197,2206, Nov. 2011.
- [30] R. Mudumbai and S. Dasgupta, "Distributed control for the smart grid: The case of economic dispatch," *Information Theory and Applications Workshop (ITA)*, 2014 , vol., no., pp.1,6, 9-14 Feb. 2014.
- [31] A.M. Zein Alabedin, E.F. El-Saadany, and M.M.A. Salama, "Generation scheduling in Microgrids under uncertainties in power generation," *Electrical Power and Energy Conference (EPEC)*, 2012 IEEE , vol., no., pp.133,138, 10-12 Oct. 2012.
- [32] Seon-Ju Ahn, Soon-Ryul Nam, Joon-Ho Choi, and Seung-II Moon, "Power Scheduling of Distributed Generators for Economic and Stable Operation of a Microgrid," *Smart Grid, IEEE Transactions on* , vol.4, no.1, pp.398,405, March 2013.
- [33] A. Zakariazadeh, and S. Jadid, "Energy and reserve scheduling of microgrid using multi-objective optimization," *Electricity Distribution (CIRED 2013)*, 22nd International Conference and Exhibition on , vol., no., pp.1,4, 10-13 June 21.
- [34] Quanyuan Jiang, Meidong Xue, and Guangchao Geng, "Energy Management of Microgrid in Grid-Connected and Stand-Alone Modes," *Power Systems, IEEE Transactions on* , vol.28, no.3, pp.3380,3389, Aug. 2013.

- [35] M.E. Khodayar, M. Barati, and M. Shahidehpour, "Integration of High Reliability Distribution System in Microgrid Operation," *Smart Grid, IEEE Transactions on* , vol.3, no.4, pp.1997,2006, Dec. 2012.
- [36] O. Hafez and K. Bhattacharya. "Optimal planning and design of a renewable energy based supply system for microgrids." *Renewable Energy: An International Journal*, vol 45, pp. 7–15. 2012.
- [37] L.D. Watson, and J.W. Kimball, "Frequency regulation of a microgrid using solar power," *Applied Power Electronics Conference and Exposition (APEC), 2011 Twenty-Sixth Annual IEEE* , vol., no., pp.321,326, 6-11 March 2011.
- [38] B. Kirby, M. Milligan, and E. Ela, "Providing Minute-to-Minute Regulation from Wind Plants." Ackerman, T., ed. *Proceedings of the 9th International Workshop on Large-Scale Integration of Wind Power into Power Systems as well as on Transmission Networks for Offshore Wind Power Plants*, 18-19 October 2010, Quebec, Canada. Langen, Germany: Energynautics GmbH 8 pp.; NREL Report No. CP-5500-54610.
- [39] CPLEX Optimizer: High-performance mathematical programming solver for linear programming, mixed integer programming, and quadratic programming <
<http://www-01.ibm.com/software/commerce/optimization/cplex-optimizer/>>.
- [40] G. Stark, "A Systematic Approach to Better Understanding Integration Costs." NREL Technical Report. NREL Report No. TP-5D00-64502. 2015.

- [41] D. Lew, G. Brinkman, E. Ibanez, A. Florita, M. Heaney, B. M. Hodge, M. Hummon, G. Stark, J. King, S. A. Lefton, N. Kumar, D. Agan, G. Jordan, and S. Venkataraman, "Western Wind and Solar Integration Study Phase 2," National Renewable Energy Laboratory, Golden, CO. NREL Report No. TP-5500-55588.
- [42] C. L. Williams, "Introduction to System Operations." Western Electricity Coordinating Council. June 24, 2015.
- [43] H. Wu, Q. Zhai, X. Guan, F. Gao, and H. Ye, "Security-Constrained Unit Commitment Based on a Realizable Energy Delivery Formulation," *Math Probl. Eng.*, 2012.
- [44] J. P. Watson and D. L. Woodruff, "Progressive hedging innovations for a class of stochastic mixed-integer resource allocation problems," *Comput. Manage. Sci.* vol. 8, pp. 355-370, Nov. 2011.
- [45] H. Wu, M. Shaidehpour, A. Alabdulwahab and A. Abusorrah, "Thermal Generation Flexibility With Ramping Costs and Hourly Demand Response in Stochastic Security-Constrained Scheduling of Variable Energy Resources," *IEEE Transactions on Power Systems*, vol. 30, no. 6, pp. 2955-2964, Nov. 2015.
- [46] A. Boone, "Simulation of short-term wind speed forecast errors using a multivariate ARMA (1,1) time-series model," Master Thesis, KTH, 2005.
- [47] Khodayar, M.E.; Lei Wu; Shahidehpour, M., "Hourly Coordination of Electric Vehicle Operation and Volatile Wind Power Generation in SCUC," *Smart Grid, IEEE Transactions on* , vol.3, no.3, pp.1271,1279, Sept. 2012.

- [48] R. D. Zimmerman, C. E. Murillo-Sánchez, and R. J. Thomas, "MATPOWER: Steady-State Operations, Planning and Analysis Tools for Power Systems Research and Education," *Power Systems, IEEE Transactions on*, vol. 26, no. 1, pp. 12-19, Feb. 2011
- [49] Jose M. Arroyo and Antonio J. Conejo, "Modeling of start-up and shut-down power trajectories of thermal units," *IEEE Transactions on Power Systems*, vol. 19, no. 3, pp. 1562-1568, Aug. 2004.
- [50] Perfect Power at the Illinois Institute of Technology. <
<http://www.iitmicrogrid.net/microgrid.aspx>>.

Appendix A: Additional Model Details

List of Symbols

SCALARS

VOIR – Value of Insufficient Reserve

VOLL – Value of Lost Load

VOIE – Value of Insufficient Energy

SETS

i : Generator index

t : Time interval index

b: Bus index

0 : Initial value index

type: Type of reserve product

k : Block associated with the piecewise linear cost curve of generators

VG : Set of wind and solar resources

CSG: Set of conventional storage generation

G: Set of all generators

L: Set of all demand

VARIABLES

QSC : Quick start capability of a generator

MT_{off} : Maximum possible down town of a generator

H : Optimization horizon

X_{off} : Time generator has been off initially

I : Commitment status of a generator

I_{DAC} : Optimization resolution

IP : Commitment status of a storage unit

P : Power output of a generator

CPS: Power output of a storage unit

B : B matrix

θ : Branch angles

Y : Admittance matrix

D : Electrical demand

d : Load distribution factor

PL : Power flow on a transmission line

R_{TOT} : Total scheduled reserve

RT: Reserve time requirement per reserve product

R : Generators' reserve schedules

R_{level} : Total reserve requirement

LL : Lost load

PX : Generation per block of the piecewise linear cost curve approximation of generator costs
 IF : Cost per block of the piecewise linear cost curve approximation of generator costs
 RR : Ramp rate per generator
 PRR: Charging ramp rate of ESS
 y : start-up indicator
 z : shut-down indicator
 yp : storage unit has started charging indicator
 zp : storage unit has stopped charging indicator
 SDP : Number of intervals required to shut down
 SUP : Number of intervals required to start up
 PUP: Number of intervals required to begin charging
 ISA : How many intervals ago the start-up process began
 IPSA: How many intervals ago the charging process began
 ISUP : Indicator implying a generator has recently begun the start-up process
 IPUP: Indicator implying an ESS has recently begun the charging process
 T_{ON} : Unit minimum run time
 T_{OFF} : Unit minimum off time
 TP_{ON} : Storage unit minimum charging time
 TP_{OFF} : Storage unit minimum down time
 IR: Online reserve indicator
 λ : Shift factor
 ST: Amount of energy stored in the ESS at the end of the optimization
 SV: Value of stored energy at the end of the optimization
 SL: Storage level
 C: General cost function
 η : Efficiency (either charging or discharging)
 IR: Binary variable where a value of 1 means the unit must be online to provide that reserve
 RAGC: Binary variable where a value of 1 means that the reserve requires AGC
 IAGC: Binary variable where a value of 1 means that the unit is capable of AGC
 G: Binary variable where a value of 1 means the unit requires a governor to provide reserve
 UR: Upward regulation schedule
 DR: Downward regulation schedule

Unit Commitment Formulation

The objective function to be optimized is given below:

$$\begin{aligned}
 PRODCOST = & \sum_t \left\{ \sum_i \left[\sum_k (IF_{i,k} \cdot PX_{i,k}) + I_{i,t} \cdot C_{NL,i} \right. \right. \\
 & \left. \left. + C_{SU,i,t} \sum_{\substack{\text{reserve} \\ \text{types}}} (R_{i,t,type} \cdot C_{RES,i,type}) \right] + LL_t \cdot VOLL \right. \\
 & \left. + \sum_{\substack{\text{reserve} \\ \text{types}}} (R_{INS,t,type} \cdot VOIR) \right\} + \sum_{i \in \{\text{Storage}\}} (-SV_{STO} \cdot ST_{i,H_{DAC}})
 \end{aligned}$$

Load balance:

$$\sum_t \sum_i P_{i,t} = \sum_t \sum_b D_{t,b} + LL_t$$

DC Load Flow representation:

$$P_{inj,n,t} = \sum_i (P_{i,t} - CPS_{i,t}) - d_n(D_t) \quad i \in \{\text{units at bus } n\}$$

$$PL_{j,t} = \sum_n \lambda_{j,n} \cdot P_{inj,n,t}$$

$$|PL_{j,t}| \leq PL_{max,j}$$

Modeling system reserve requirements:

$$\sum_t \sum_i R_{i,t,\tau} \geq \Gamma_{t,\tau}$$

$$P_{i,t} + R_{i,t,\tau} \leq P_{max,i} \cdot I_{i,t}$$

$$P_{i,t} - R_{i,t,\tau} \geq P_{min,i} \cdot I_{i,t}$$

$$R_{i,t,\tau} \leq P_{max,i} \cdot (1 - y_{i,t} - z_{i,t})$$

$$R_{i,t,\tau} \leq I_{i,t} \cdot RR_i \cdot RT_\tau + (1 - I_{i,t}) \cdot QSC_i$$

A generator's output is modeled as follows:

$$P_{i,t} = \sum_k PX_{i,k,t}$$

$$PX_{i,k,t} \leq PX_{i,1,t} \text{ for } k = 1$$

$$PX_{i,k,t} \leq PX_{i,k,t} - PX_{i,k-1,t} \text{ for } k \neq 1$$

$$P_{i,t} \leq P_{max,i} \cdot I_{i,t}$$

$$P_{i,t} + \sum_{\substack{\text{upward} \\ \text{reserves}}} R_{i,t,type} \leq I_{i,t} \cdot P_{max,i} + IP_{i,t} \cdot CPS_{max,i}$$

$$P_{i,t} \geq P_{min,i} \cdot I_{i,t} - IP_{i,t} \cdot CPS_{max,i}$$

$$P_{i,t} - \sum_{\substack{\text{downward} \\ \text{reserves}}} R_{i,t,type} \geq P_{min,i} \cdot I_{i,t} - IP_{i,t} \cdot CPS_{max,i}$$

The unit ramp up and ramp down constraints for units with limited ramping capabilities are enforced as follows:

$$\begin{aligned} \text{for } t = 1 \quad & P_{i,t} - P_{i0} \leq 60 \cdot I_{DAC} \cdot RR_i \cdot (1 - y_{i,t}) + P_{min,i} \cdot y_{i,t} \\ \text{for } t > 1 \quad & P_{i,t} - P_{i,t-1} \leq 60 \cdot I_{DAC} \cdot RR_i \cdot (1 - y_{i,t}) + P_{min,i} \cdot y_{i,t} \end{aligned}$$

$$\begin{aligned} \text{for } t > 1 \quad & P_{i,t} - P_{i,t-1} \geq -60 \cdot I_{DAC} \cdot RR_i \cdot (1 - z_{i,t}) - P_{min,i} \cdot z_{i,t} \\ \text{for } t = 1 \quad & P_{i,t} - P_{i0} \geq -60 \cdot I_{DAC} \cdot RR_i \cdot (1 - z_{i,t}) - P_{min,i} \cdot z_{i,t} \end{aligned}$$

Generator start-up trajectories are modeled via the following constraints:

If $t \leq H_{DAC} - SDP_i$ & $t \geq SUP_i - 1$:

$$P_{i,t} - \sum_{\substack{\text{down} \\ \text{reserves}}} R_{i,t,type} \geq P_{min,i} \left[I_{i,t} - \sum_{H=t}^{t+SDP_i-1} z_{i,H} - \sum_{H=t-SUP_i+1}^t y_{i,H} \right] + \left[\sum_{H=t-SUP_i+1}^t \{(t-H+1) \cdot y_{i,H}\} \right] \cdot P_{min,i} \cdot 1/t_{startup} - IP_{i,t} \cdot CPS_{max,i}$$

If $t < SUP_i - ISA_i - 1$:

$$P_{i,t} - \sum_{\substack{\text{down} \\ \text{reserves}}} R_{i,t,type} \geq P_{min,i} \left[I_{i,t} - \sum_{H=t}^{t+SDP_i-1} z_{i,H} - ISUP_i - \sum_{H=1}^t y_{iH} \right] + ISUP_i \cdot [ISA_i + t] \cdot P_{min,i} \cdot 1/t_{startup} \\ + \left[\sum_{H=1}^t \{(t-H+1) \cdot y_{iH}\} \right] \cdot P_{min,i} \cdot 1/t_{startup} - IP_{i,t} \cdot CPS_{max,i}$$

If $t > H_{DAC} - SDP_i$:

$$P_{i,t} - \sum_{\substack{\text{down} \\ \text{reserves}}} R_{i,t,type} \geq P_{min,i} \left[I_{i,t} - \sum_{H=t}^{H_{DAC}} z_{i,H} - \sum_{H=t-SDP_i+1}^t y_{iH} \right] + \left[\sum_{H=t-SDP_i+1}^t \{(t-H+1) \cdot y_{iH}\} \right] \cdot P_{min,i} \cdot 1/t_{startup} - IP_{i,t} \\ \cdot CPS_{max,i}$$

Determine maximum possible down time of a generator:

$$MT_{off,i} = H_{DAC} + X_{off,i}(1 - I_{i0})$$

The output of a variable generator shouldn't exceed its forecasted value. This is enforced as follows:

$$P_{i,t} \leq P_{i,t,forecast} \quad \forall i \in \{VG\}$$

If a variable generator is going to provide reserves, then its total scheduled output must be below its forecasted output. This is enforced as follows:

$$P_{i,t} + \sum_{\substack{\text{up or both} \\ \text{types of reserves}}} R_{i,t,type} \leq P_{i,t,forecast} \quad \forall i \in \{VG\}$$

If the optimization period is more than the minimum run time required of unit i away from the end of the optimization horizon, then the minimum run time requirement of the unit is enforced as follows:

$$\sum_t^{t+T_{ON,i}/I_{DAC}-1} I_{i,t} \geq T_{ON,i} \cdot y_{i,t} \cdot \frac{1}{I_{DAC}} \cdot (1 - FO_{i,t})$$

However, if the optimization period is within the minimum run time required of the optimization horizon, the minimum run time requirement is enforced as:

$$\sum_t^{H_{DAC}} I_{i,t} \geq (H_{DAC} - t + 1) \cdot y_{i,t}$$

Similarly, if the optimization period is more than the minimum down time required of unit i away from the end of the optimization horizon, then the minimum down time requirement of the unit is enforced as follows:

$$\sum_t^{t+T_{OFF,i}/I_{DAC}-1} (I_{i,t} + IP_{i,t}) \leq T_{OFF,i} \cdot \frac{1}{I_{DAC}} \cdot (1 - z_{i,t} - zp_{i,t})$$

However, if the optimization period is within the minimum down time required of the optimization horizon, the minimum down time requirement is enforced as:

$$\sum_t^{H_{DAC}} (I_{i,t} + IP_{i,t}) \leq (H_{DAC} - t + 1) \cdot (1 - z_{i,t} - zp_{i,t})$$

The definitions of the start-up and shut-down indicators are modeled below:

$$\begin{aligned} y_{i,t} - z_{i,t} &= I_{i,t} - I_{i,t-1} \quad \text{for } t > 1 \\ y_{i,t} - z_{i,t} &= I_{i,t} - I_{i0} \quad \text{for } t = 1 \\ y_{i,t} + z_{i,t} &\leq 1 \end{aligned}$$

The reserve capability of a unit is modeled as:

$$\begin{aligned} R_{i,t,type} &\leq (I_{i,t} + IP_{i,t}) \cdot IR \cdot RR_i \cdot t_{reserve} \cdot RAGC \cdot IAGC \cdot (1 - G) \\ &\quad + (I_{i,t} + IP_{i,t}) \cdot IR \cdot RR_i \cdot t_{reserve} \cdot (1 - RAGC) \cdot (1 - G) \\ &\quad + (1 - I_{i,t} - IP_{i,t}) \cdot (1 - IR) \cdot P_{QSC,i,type} \cdot (1 - G) \end{aligned}$$

If the line outages are considered, then the following contingency constraints are added to the optimization problem.

If a line is under contingency, then its power flow is forced to zero:

$$PL_{j,t}^{(C)} = 0$$

The voltage angle at the slack bus is forced to remain zero under contingency:

$$\Delta\theta_{slack}^{(C)} = 0$$

The change in bus angle voltages is then solved from:

$$\mathbf{P}_{inj,t}^{(C)} = \mathbf{B}^{(C)} \cdot \Delta\boldsymbol{\theta}_t^{(C)}$$

The DC line flows under contingency are then calculated as:

$$PL_{j,t}^{(C)} = \sum_j Y_j (\Delta\theta_{n,t}^{(C)} - \Delta\theta_{m,t}^{(C)} - PSA_{j,t}^{(C)})$$

To ensure that line security is not compromised, the following constraints are enforced:

$$\begin{aligned} PL_{j,t}^{(C)} &\leq PL_{max,j}^{(C)} \\ PL_{j,t}^{(C)} &\geq -PL_{max,j}^{(C)} \end{aligned}$$

The minimum charging time is enforced with the following constraint if the current optimization period is more than the minimum pump time requirement away from the end of the optimization horizon:

$$\sum_t^{t+TP_{on,i}/I_{DAC}-1} IP_{i,t} \geq TP_{on,i} \cdot \frac{yp_{i,t}}{I_{DAC}} \cdot (1 - FO_{i,t}) \quad \forall i \in \{CSG\}$$

If the current optimization period is within the minimum on time requirement of the end of the optimization horizon, the following constraint is enforced instead of the previous one:

$$\sum_t^{H_{DAC}} IP_{i,t} \geq (H_{DAC} - t + 1) \cdot yp_{i,t}$$

The following constraints enforce the charging ramp rates:

$$\begin{aligned} CPS_{i,1} - CPS_{i,0} &\leq 60 \cdot I_{DAC} \cdot PRR_i \cdot (1 - yp_{i,1}) + CPS_{min,i} \cdot yp_{i,1} & t = 1, \forall i \in \{CSG\} \\ CPS_{i,t} - CPS_{i,t-1} &\leq 60 \cdot I_{DAC} \cdot PRR_i \cdot (1 - yp_{i,t}) + CPS_{min,i} \cdot yp_{i,t} & t > 1, \forall i \in \{CSG\} \\ CPS_{i,1} - CPS_{i,0} &\geq -60 \cdot I_{DAC} \cdot PRR_i \cdot (1 - zp_{i,1}) + CPS_{min,i} \cdot zp_{i,1} & t = 1, \forall i \in \{CSG\} \\ CPS_{i,t} - CPS_{i,t-1} &\geq -60 \cdot I_{DAC} \cdot PRR_i \cdot (1 - zp_{i,t}) + CPS_{min,i} \cdot zp_{i,t} & t > 1, \forall i \in \{CSG\} \end{aligned}$$

Charging mode trajectory constraints:

If $t > PUP_i$ & $t > 1$:

$$CPS_{i,t} - CPS_{i,t-1} \leq PRR_i \cdot \left(IP_{i,t} - \sum_{H=t-PUP_i}^t yp_{i,t} \right) + \frac{CPS_{min,i}}{t_{pstartup}} \cdot \sum_{H=t-PUP_i}^t yp_{i,t}$$

If $t < PUP_i - IPSA_i$ & $t > 1$:

$$CPS_{i,t} - CPS_{i,t-1} \leq PRR_i \cdot \left(IP_{i,t} - IPUP_i - \sum_{H=1}^t yp_{i,t} \right) + \frac{CPS_{min,i}}{t_{pstartup}} \cdot \left(IPUP_i + \sum_{H=1}^t yp_{i,t} \right)$$

If $t = 1$:

$$CPS_{i,t} - CPS_{i,0} \leq PRR_i \cdot (IP_{i,t} - IPUP_i - yp_{i,t}) + \frac{CPS_{min,i}}{t_{pstartup}} \cdot (IPUP_i + yp_{i,t})$$

The pumping up and down indicators are modeled similarly to the start-up and shut down indicators as follows:

$$\begin{aligned} yp_{i,t} - zp_{i,t} &= IP_{i,t} - IP_{i,t-1} \quad \text{for } t > 1 \\ yp_{i,t} - zp_{i,t} &= IP_{i,t} - IP_{i0} \quad \text{for } t = 1 \\ yp_{i,t} + zp_{i,t} &\leq 1 \end{aligned}$$

The following constraint is used to determine the start-up cost:

$$C_{SU,i,t} = C_{SU,i} \cdot y_{i,t}$$

Economic Dispatch Formulation

The objective function of the RTSCED problem is as follows:

$$\begin{aligned}
 PRODCOST = & \sum_t \left\{ \sum_i \left[\sum_k (IF_{i,k} \cdot PX_{i,k} \cdot \frac{5}{60} \cdot S_{base}) + I_{i,t} \cdot \frac{5}{60} \cdot C_{NL,i} + C_{SU,i,t} \cdot y_{i,t} \right. \right. \\
 & + \sum_{\substack{reserve \\ types}} (R_{i,t,type} \cdot C_{RES,i,type} \cdot \frac{5}{60} \cdot S_{base}) + S_{wasted,i,t} \cdot VOLL \cdot \frac{5}{60} \\
 & \left. \left. \cdot S_{base} \right] + LL_t \cdot VOLL \cdot \frac{5}{60} \cdot S_{base} \right. \\
 & \left. + \sum_{\substack{reserve \\ types}} (R_{INS,t,type} \cdot VOIR \cdot \frac{5}{60} \cdot S_{base}) \right\} \\
 & + \sum_{i \in \{Storage\}} (-C_{STO} \cdot S_{i,HRTD} \cdot S_{base})
 \end{aligned}$$

Load balance:

$$\sum_t \sum_i P_{i,t} = \sum_t \sum_b D_{t,b} + LL_t$$

Unit generation limits are enforced as follows:

$$P_{i,t} \geq P_{min,i} \cdot [I_{i,t} - y_{i,t} - z_{i,t}]$$

The generation limit including reserves is enforced as follows:

$$P_{i,t} - \sum_{\substack{down \\ reserves}} R_{i,t,type} \geq P_{min,i} \cdot [I_{i,t} - y_{i,t} - z_{i,t}] - IP_{i,t} \cdot CPS_{max,i}$$

The ramping constraints after the first time period are enforced as follows:

$$P_{i,t} - P_{i,t-1} \leq IM_t \cdot RR_i \cdot [I_{i,t} - y_{i,t}] + P_{min,i} \cdot \min\left(1, \frac{IM_t}{60t_{startup,i}}\right) \cdot y_{i,t}$$

$$P_{i,t} - P_{i,t-1} \geq -IM_t \cdot RR_i \cdot [I_{i,t-1} - z_{i,t}] - P_{min,i} \cdot \min\left(1, \frac{IM_t}{15}\right) \cdot z_{i,t}$$

To limit the amount of reserves that can be committed due to the status of the unit, the following constraint is enforced:

$$R_{i,t,type} \leq P_{max,i} \cdot (1 - y_{i,t} - z_{i,t})$$

To determine the storage level at the beginning of the optimization period, the following constraint is included:

$$SL_{i,t} = SL_{i,t-1} - P_{i,t} \cdot \frac{5}{60} + CPS_{i,t} \cdot \frac{5}{60} \cdot \eta_{sto}$$

The limits of the pumping schedule including reserves are determined as follows:

$$CPS_{i,t} - \sum_{\substack{up \\ reserves}} R_{i,t,type} \geq CPS_{min,i} \cdot [IP_{i,t} - yp_{i,t} - zp_{i,t}] - I_{i,t} \cdot P_{max,i}$$

$$CPS_{i,t} + \sum_{\substack{down \\ reserves}} R_{i,t,type} \leq P_{max,i}$$

The pumping ramping constraints after the first time period are enforced as follows:

$$CPS_{i,t} - CPS_{i,t-1} \leq 5 \cdot PRR_i \cdot [IP_{i,t} - yp_{i,t}] + CPS_{min,i} \cdot \frac{5}{60t_{pstartup,i}} \cdot yp_{i,t}$$

$$CPS_{i,t} - CPS_{i,t-1} \geq -5 \cdot PRR_i \cdot [IP_{i,t-1} - zp_{i,t}] - CPS_{min,i} \cdot \frac{5}{60t_{pshutdown,i}} \cdot zp_{i,t}$$

To limit the amount of reserves that can be committed due to the charging status of the unit, the following constraint is enforced:

$$R_{i,t,type} \leq CPS_{max,i} \cdot (1 - yp_{i,t} - zp_{i,t})$$

Modeling system reserve requirements:

$$\sum_t \sum_i R_{i,t,\tau} \geq \Gamma_{t,\tau}$$

$$P_{i,t} + R_{i,t,\tau} \leq P_{max,i} \cdot I_{i,t}$$

$$P_{i,t} - R_{i,t,\tau} \geq P_{min,i} \cdot I_{i,t}$$

$$R_{i,t,\tau} \leq P_{max,i} \cdot (1 - y_{i,t} - z_{i,t})$$

$$R_{i,t,\tau} \leq I_{i,t} \cdot RR_i \cdot RT_\tau + (1 - I_{i,t}) \cdot QSC_i$$

Automatic Generation Control Algorithm

This is a rule based module whose main purpose is not to optimize dispatch, but rather to eliminate area control error (ACE). As a result, this module is only concerned with units that are available and have the ramping capability to help correct the ACE. The basic operating principle of this module is to check if a unit has a regulation schedule. If it does not, then the unit should follow RTSCED dispatch schedule. If it does, then the unit should utilize this regulation capacity to proportionally correct the ACE.

The AGC algorithm quantifies the possible ramping ability of units through the following definitions:

<i>If unit is turning on:</i>	$Ramp_i = P_{min} / (60 \cdot t_{startup})$
<i>If unit is turning off:</i>	$Ramp_i = P_{min} / t_{shutdown}$
<i>If unit has begun charging:</i>	$Ramp_i = CPS_{min} / (60 \cdot t_{pstartup})$
<i>If unit has just shut down pumping:</i>	$Ramp_i = CPS_{min} / t_{pshutdown}$
<i>If unit is charging:</i>	$Ramp_i = PRR$
<i>Otherwise:</i>	$Ramp_i = RR$

The amount ramping capacity available for AGC action is defined as follows:

$$AGCRampUpAvail = \sum_{\substack{\text{units with} \\ \text{up regulation}}} Ramp_i$$

$$AGCRampDownAvail = \sum_{\substack{\text{units with} \\ \text{down regulation}}} Ramp_i$$

The ACE signal is calculated as:

$$ACE(t) = \sum_i P_i(t) - \sum_j D_j(t) \quad \forall i \in \{G\}, \forall j \in \{L\}$$

$$SACE = K_1 \cdot ACE(t) + \frac{1}{K_2} \int ACE(\tau) d\tau$$

The amount of energy available for positive AGC action is defined as:

$$AGCUpEnergyAvail = \sum_{\substack{\text{units with} \\ \text{up regulation}}} UR_i$$

$$AGCDownEnergyAvail = \sum_{\substack{\text{units with} \\ \text{down regulation}}} DR_i$$

The individual limits of units to provide regulation is defined as:

$$\max reg_i = \text{next generation RTSCED schedule}_i + UR_i$$

$$\min reg_i = \text{next generation RTSCED schedule}_i - DR_i$$

The actual AGC algorithm is as follows:

```

If ACE < 0
  If UR < ε
    If IP = 1 or zp = 1
      If current pumping schedule < next RTSCED pumping schedule
        AGCramp = min[Ramp,abs{(next-current)/(60(5 +
tagc/60))}]
        AGCbasepoint = max[0,current+AGCramp*(tagc/60)]
      Elseif current pump schedule > next RTSCED pump schedule
        AGCramp = min[Ramp,abs{(current-next)/(60(5 +
tagc/60))}]
        AGCbasepoint = max[0,current-AGCramp*(tagc/60)]
      Else
        AGCbasepoint = max[0,current]
    Else
      If current gen schedule < next gen schedule from RTSCED
        AGCramp = min[Ramp,abs{(next-current)/(60(5 +
tagc/60))}]

```

```

AGCbasepoint = max[0,current+AGCramp*(tagc/60)]
Elseif current gen schedule > next gen schedule from RTSCED
AGCramp = min[Ramp,abs{(current-next)/(60(5 +
tagc/60))}]
AGCbasepoint = max[0,current-AGCramp*(tagc/60)]
Else
AGCbasepoint = max[0,current]
End
Else
If IP = 1 or zp = 1
AGCramp = min[ramp(tagc/60),abs(UR,AGCUpEnergyAvail*ACE)]
AGCbasepoint = min[currentp,max(max reg, currentp-
AGCramp)]
End
AGCbasepoint = max[currentg,min(max reg, currentg-AGCramp)]
End
Else
If DR < ε
If IP = 1 or zp = 1
If current pumping schedule < next RTSCED pumping schedule
AGCramp = min[Ramp,abs{(next-current)/(60(5 +
tagc/60))}]
AGCbasepoint = max[0,current+AGCramp*(tagc/60)]
Elseif current pump schedule > next RTSCED pump schedule
AGCramp = min[Ramp,abs{(current-next)/(60(5 +
tagc/60))}]
AGCbasepoint = max[0,current-AGCramp*(tagc/60)]
Else
AGCbasepoint = max[0,current]
End
Else
If current gen schedule < next gen schedule from RTSCED
AGCramp = min[Ramp,abs{(next-current)/(60(5 +
tagc/60))}]
AGCbasepoint = max[0,current+AGCramp*(tagc/60)]
Elseif current gen schedule > next gen schedule from RTSCED
AGCramp = min[Ramp,abs{(current-next)/(60(5 +
tagc/60))}]
AGCbasepoint = max[0,current-AGCramp*(tagc/60)]
Else
AGCbasepoint = max[0,current]
End
Else
If IP = 1 or zp = 1

```

```
AGCramp =  
min[ramp(tagc/60),abs(DR,AGCDownEnergyAvail*ACE)]  
AGCbasepoint = min[currentg,max(min reg, currentg-  
AGCramp)]  
End  
End  
End
```

Appendix B: Extensive form of Stochastic RTS CED

Objective Function

Minimize:

$$\sum_{s \in S} \left(\sum_{t \in T} \left\{ \sum_{i \in G} [\alpha + \beta] + \gamma + \delta \right\} \right)$$

Where

$$\alpha = \sum_{k \in K_i} (IC_{i,k}^s \cdot Pk_{i,k,t}^s)$$

$$\beta = \sum_{rtype \in RTYPE} (RS_{i,t,rtype}^s \cdot C_{RES,i,rtype}^s)$$

$$\gamma = LL_t^s \cdot VOLL$$

$$\delta = \sum_{rtype \in R} (IR_{t,rtype}^s \cdot VOIR)$$

Subject to the Following Constraints:

Power Balance

$$\sum_{i \in G} DF_i^s \cdot Pg_{i,t}^s = \sum_{n \in N} DF_n^s \cdot (D_t^s - LL_t^s)$$

Reserve Balance

$$\sum_{i \in G} RS_{i,t,rtype}^s + IR_{t,rtype}^s \geq RD_{level,t,type}^s$$

Net Injection

$$NI_{n,t}^s = K_{i,n}^s \cdot Pg_{i,t}^s - LD_n^s (D_t^s - LL_t^s + AL_t^s)$$

Power Flow

$$LF_{l,t}^s = \sum_{n \in N} PTDF_{l,n} \cdot NI_{n,t}^s$$

Branch Limits

$$LF_{j,t}^s \leq \overline{LF}_l^s$$

$$LF_{j,t}^s \geq -\underline{LF}_l^s$$

Generator Maximum Capacity Limits

$$\sum_{k \in K} Pk_{i,k,t}^s = Pg_{i,t}^s$$

$$Pk_{i,k,t}^s \leq \overline{Pk}_{i,k}^s$$

$$Pg_{i,t}^s + \sum_{rtype \in R_{up}} RS_{i,t,rtype}^s \leq \overline{Pg}_i^s \cdot uu_{i,t}^s$$

Generator Minimum Capacity Limits

$$Pg_{i,t}^s - \sum_{rtype \in R_{down}} RS_{i,t,rtype}^s \geq \underline{Pg}_i^s \cdot uu_{i,t}^s$$

Generator Ramp Constraints

$$Pg_{i,t-1}^s - Pg_{i,t}^s \geq RR_i^s \cdot Int_t^s \cdot (u_{i,t-1}^s - yy_{i,t}^s) + yy_{i,t}^s \cdot \left(\underline{Pg}_i^s \cdot \frac{Int_t^s}{SDT_i^s} + RR_i^s \cdot (Int_t^s - SDT_i^s) \right)$$

$$Pg_{i,t-1}^s - Pg_{i,t}^s \leq -RR_i^s \cdot Int_t^s \cdot (uu_{i,t}^s - zz_{i,t}^s) - zz_{i,t}^s \cdot \left(\underline{Pg}_i^s \cdot \frac{Int_t^s}{SUT_i^s} + RR_i^s \cdot (Int_t^s - SUT_i^s) \right)$$

Reserve Capability Constraints:

$$RS_{i,t,rtype}^s \leq uu_{i,t}^s \cdot RON_{rtype}^s \cdot RR_i^s \cdot RTIME_{rtype}^s \cdot RAGC_{rtype}^s \cdot IAGC_i^s + uu_{i,t}^s \cdot RON_{rtype}^s \cdot RR_i^s \cdot RTIME_{rtype}^s \cdot (1 - RAGC_{rtype}^s) + (1 - uu_{i,t}^s) \cdot (1 - RON_{rtype}^s) \cdot QSC_{i,rtype}^s$$

$$\sum_{rtype} RON_{rtype}^s \cdot \frac{RS_{i,t,rtype}^s}{RTIME_{rtype}^s} \leq uu_{i,t}^s \cdot RR_i^s$$

Reserve Limitations when in start-up or shut-down mode

$$RS_{i,t,rtype}^s \leq \overline{Pg}_i^s \cdot [1 - zz_{i,t}^s - yy_{i,t}^s]$$

Non-anticipativity Constraints:

$$Pg_{i,t}^s = Pg_{i,bind} \quad , t = \text{Binding Interval}$$

$$RS_{i,t,rtype}^s = RS_{i,rtype,bind} \quad , t = \text{Binding Interval}$$